Diptych varieties and Mori flips

Gavin Brown and Miles Reid

Abstract

We present a new class of affine Gorenstein 6-folds obtained by smoothing the 1-dimensional singular locus of a reducible affine toric surface; their existence is established using explicit methods in toric geometry and serial use of Kustin–Miller Gorenstein unprojection. As an application, we use these varieties to give an explicit description of the canonical $\mathbb{G}_m$ cover of Mori flips of Type A.

Overview

Part I introduces a large class of remarkable 6-folds called *diptych varieties*; each is an affine 6-fold V_{ABLM} constructed starting from two toric 4-fold panels $V_{AB} \cup V_{LM}$ hinged along a reducible toric surface $T = V_{AB} \cap V_{LM}$ (compare the Wilton diptych [W]). The construction depends on discrete toric data called a *diptych of long rectangles*, describing the Newton polygon of monomials of the two toric panels V_{AB} and V_{LM}. It is equivariant under a big torus[1] $\mathbb{T} = (\mathbb{G}_m)^4 = (\mathbb{C}^\times)^4$. Apart from easy initial cases, diptych ft!one varieties are indexed by 3 natural numbers d, e, k, or by a 2-step recurrent continued fraction $[d, e, d, \dots, (d \text{ or } e)]$ (to k terms). We make a further case division into four families to handle the cases when d or $e = 1$.

The worked example 1.1 is an extended introduction in colloquial style, illustrating almost all the main features of our construction; see also [Ki], Section 11. The general introduction to Part I continues in 1.2.

Diptych 6-folds V_{ABLM} serve as ambient spaces or *key varieties* for Mori flips of Type A, and our work is motivated by this application. Part II

[1] Schizophrenic footnote: We write $\mathbb{A}^n$ for affine space $\mathbb{C}^n$ and $\mathbb{G}_m$ for the multiplicative group $\mathbb{C}^\times$. Our main interest is in varieties over $\mathbb{C}$, so it would also be natural to write $\mathbb{A}^n = \mathbb{C}^n$, $\mathbb{G}_m = \mathbb{C}^\times$ and $\mathbb{T} = (\mathbb{C}^\times)^4$ throughout. Our varieties mostly occur as schemes defined over $\mathbb{Z}$, for example an affine toric scheme $\operatorname{Spec} \mathbb{Z}[\sigma \cap M]$.

reinterprets Mori's classification of extremal neighbourhoods of Type A [M3], describing the canonical $\mathbb{G}_m$ cover of the flip as a specialisation of a diptych 6-fold (a regular pullback). Example 7.1 gives the first explicit instance. We expect diptych varieties also to appear as key varieties in other constructions of interest, in the same way as toric varieties.

Although Part I is self-contained and explicit (in fact rather elementary), the application in Part II to the explicit classification of Mori 3-fold flips is the driving force behind our study, and predicts many features of Part I that would otherwise seem mysterious or arbitrary choices. This applies especially to the level of generality adopted: why diptych? why long rectangles? We take up these points briefly in 1.3. The separate introduction to Part II discusses in more detail the background from explicit Mori theory and what our theory contributes to it.

Contents

Part I
Diptych varieties

1 Introduction to Part I

1.1 Extended example

ex!intr

1.1.1 Background and notation

As usual, for $r > 0$ and a coprime to r, we write $\frac{1}{r}(1,a)$ for the action of $\mathbb{Z}/r$ on $\mathbb{A}^2$ given by $(u,v) \mapsto (\varepsilon u, \varepsilon^a v)$ where $\varepsilon = \exp \frac{2\pi i}{r} \in \mathbb{C}$ is a chosen primitive rth root of 1. We use the same notation[2] for the cyclic quotient singularity $\mathbb{A}^2/(\mathbb{Z}/r) = \operatorname{Spec} \mathbb{C}[u,v]^{\mathbb{Z}/r}$. See [More] for elementary tutorial material on this construction. We focus here on concrete cases, starting with $\frac{1}{7}(1,2)$; the ring of invariants $\mathbb{C}[u,v]^{\mathbb{Z}/7}$ is generated by the monomials

$$y_0 = u^7, \quad y_1 = u^5 v, \quad y_2 = u^3 v^2, \quad y_3 = uv^3, \quad y_4 = v^7, \tag{1.1}$$

with relations between them determined by the *tag equations* eq!tag72

$$y_0 y_2 = y_1^2, \quad y_1 y_3 = y_2^2, \quad y_2 y_4 = y_3^3. \tag{1.2}$$

These are of the general form $v_{i-1}v_{i+1} = v_i^{a_i}$ for any 3 consecutive monomials v_{i-1}, v_i, v_{i+1} on the Newton boundary. The exponents or *tags* a_i are the entries in the Jung–Hirzebruch continued fraction expansion of $\frac{r}{r-a}$; here $\frac{7}{7-2} = 2 - \frac{1}{2-\frac{1}{3}} = [2,2,3]$. The quotient $\mathbb{A}^2 \to S \subset \mathbb{A}^5_{\langle y_{0\dots 4}\rangle}$ is thus the morphism $(u,v) \mapsto (y_{0\dots 4})$, and the image S is uniquely determined by (1.2): the complete intersection (1.2) consists of S plus the (y_0, y_4)-plane with a "fat" nonreduced structure. To see actual generators of the ideal I_S we also need the "long equations" $y_0 y_3 = y_1 y_2$, $y_1 y_4 = y_2 y_3^2$ and $y_0 y_4 = y_1 y_3^2$, that derive from (1.2) using easy syzygy manipulations. In what follows, we write $S = S_3$ for the quotient $\frac{1}{7}(1,2)$.

In the same way, the quotient singularity $\frac{1}{7}(1,3)$ is eq!tag73

$$S_1 \subset \mathbb{A}^4_{\langle x_0,x_1,x_2,x_3\rangle} \quad \text{given by} \quad x_0 x_2 = x_1^2, \quad x_1 x_3 = x_2^4 \tag{1.3}$$

with $[2,4] = 2 - \frac{1}{4} = \frac{7}{4}$.

[2] Or (continuing the footnote of p. 1) $\frac{1}{r}(1,a)$ denotes the action of the multiplicative group μ_r on $\mathbb{A}^2$ given by $(u,v) \mapsto (\varepsilon u, \varepsilon^a v)$ for $\varepsilon \in \mu_r$.

1.1.2 The tent T

The starting point for our example is the reducible affine surface or *tent* of Figure 1.1 (with $k = 3$, $l = 4$ and $k + l + 2 = 9$ in our case). It consists of a f!T

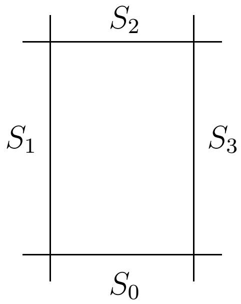

Figure 1.1: The tent $T = S_0 \cup S_1 \cup S_2 \cup S_3 \subset \mathbb{A}^{k+l+2}_{\langle x_{0\dots k}, y_{0\dots l}\rangle}$ is obtained by glueing $S_0 \cup S_1$ transversally along the x_0-axis, $S_1 \cup S_2$ along the x_k-axis, $S_2 \cup S_3$ along the y_l-axis, and $S_3 \cup S_0$ along the y_0-axis

cycle of 4 components, with vertical sides the surface quotient singularities $S_1 \subset \mathbb{A}^4_{\langle x_{0\dots k}\rangle}$ and $S_3 \subset \mathbb{A}^5_{\langle y_{0\dots l}\rangle}$ of types $\frac{1}{7}(1,3)$ and $\frac{1}{7}(1,2)$ as just described, and top and bottom the coordinate planes $S_2 = \mathbb{A}^2_{\langle x_k, y_l\rangle}$ and $S_0 = \mathbb{A}^2_{\langle x_0, y_0\rangle}$. In equations, $T \subset \mathbb{A}^9$ is the reducible variety defined by eq!T

$$I_{S_1}, I_{S_3} \quad \text{and} \quad x_i y_j = 0 \quad \text{for all } i, j \text{ with } (i,j) \neq (0,0), (k,l). \qquad (1.4)$$

1.1.3 First toric extension $T \subset V_{AB}$

We now seek to embed T into a toric variety V (irreducible and normal) so that T is both a regular section of V and a union of its toric strata; the main purpose of this paper is to analyse the several different ways of doing this, and the compatibilities between them.

One solution is the affine toric 4-fold V_{AB} with monomial cone schematically represented in Figure 1.2, our first *long rectangle*. It is a schematic f!lrAB representation of a cone $\sigma(V_{AB})$, the Newton polygon of V_{AB} in the monomial lattice $M = \mathbb{Z}^4$ (see Figure 2.3 for another perspective, with A, B in their position in the 4-dimensional lattice $\mathbb{M}$.) We read $\sigma(V_{AB})$ and the toric variety V_{AB} automatically from the figure as follows: the dots around the boundary (clockwise from bottom left) are the generators $x_{0\dots k}$, $y_{l\dots 0}$; the two remaining generators A, B are shown as *annotations* at the top corners. It is

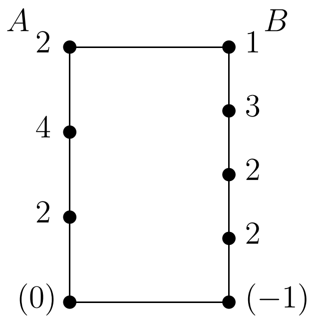

Figure 1.2: The long rectangle for V_{AB}

awkward and not very enlightening to draw them in their correct geometric position in the 4-dimensional lattice $\mathbb{M}$ (compare Figure 2.3). The relations (1.2) and (1.3) continue to hold, as represented by the tags down the long sides. These constrain $x_{0\ldots k}$ to a plane face of $\sigma(V_{AB})$, and in that plane they generate the Newton boundary of $\frac{1}{7}(1,4)$; ditto $y_{0\ldots l}$. The new ingredients are the tags and annotations ${}^A2, 1^B$ at the top corners, that say how we intend to deform the reducible equations $x_2y_4 = 0$ and $x_3y_3 = 0$ for T appearing in (1.4) to usual binomial equations of toric geometry: eq!AB

$$x_2y_4 = x_3^2A, \quad x_3y_3 = y_4B. \tag{1.5}$$

We view A and B as deformation parameters, and interpret (1.5) as smoothing the reducible double locus along the x_3- and y_4-axes, the top corners $S_1 \cap S_2$ and $S_2 \cap S_3$ of Figure 1.1.

On the other hand, equations (1.5) and the original tag equations (1.2–1.3) now completely determine the cone $\sigma(V_{AB})$ in a monomial lattice $M = \mathbb{Z}^4$. Indeed, x_3, y_4, A, B is a $\mathbb{Z}$-basis of $\mathbb{M}$, and the remaining generators $x_2, \ldots, x_0$, $y_3, \ldots, y_0$ are Laurent monomials in this basis, obtained by *continued division* from (1.5) together with (1.2–1.3): eq!Laur

$$\begin{array}{ll} x_2 = x_3^2(Ay_4^{-1}), & y_3 = y_4(Bx_3^{-1}), \\ x_1 = x_3^7(Ay_4^{-1})^4, & y_2 = y_4^2(Bx_3^{-1})^3, \\ x_0 = x_3^{12}(Ay_4^{-1})^7, & y_1 = y_4^3(Bx_3^{-1})^5, \\ & y_0 = y_4^4(Bx_3^{-1})^7. \end{array} \tag{1.6}$$

A rational, polyhedral cone σ in the monomial lattice $\mathbb{M}$ defines a (irreducible, normal) toric variety $V_{\mathbb{M},\sigma} = \operatorname{Spec}\mathbb{C}[\mathbb{M} \cap \sigma]$. We claim more: our monomials $x_{0\ldots 3}, y_{0\ldots 4}, A, B$ in $\mathbb{M}$ generate $\mathbb{M} \cap \sigma_{AB}$, and the resulting toric variety $V_{AB} = \operatorname{Spec}\mathbb{C}[\mathbb{M} \cap \sigma_{AB}]$ is a flat deformation of T. When we say deformation, we mean the total space of the deformation; in fact A, B define a flat morphism $V_{AB} \to \mathbb{A}^2_{\langle A,B\rangle}$ with fibre $T : (A = B = 0)$ over 0, although the morphism does not figure prominently in our considerations.

The relations satisfied by our monomials come implicitly from their inclusion in $\mathbb{M}$. We are usually not interested in writing them all out, but we want to find enough equations to justify our claim. By substituting from (1.6), we find the relation eq!tag0

$$x_1 y_0 = A^4 B^7 \tag{1.7}$$

that deforms the original equation $x_1 y_0 = 0$ in T; this is the *corner tag* (0) of Figure 1.2, indicating a tag equation at x_0, with tag 0 derived from the other tags (the annotation A^4B^7 is left implicit). We view it as a partial smoothing of the reducible double locus of T along the x_0-axis – the hypersurface in $\mathbb{A}^4_{\langle x_1,y_0,A,B\rangle}$ defined by (1.7) is of course normal.

Now, how does the relation $x_0 y_1 = 0$ deform? From (1.6) we write out $x_0 y_1 = x_3^7 y_4^{-4} A^7 B^5$, hence eq!tag-1

$$x_0 y_1 = y_0^{-1} A^7 B^{12} \quad \text{or} \quad x_0 y_1 = x_1 A^3 B^5. \tag{1.8}$$

The first equality is a tag equation for y_0, with negative tag -1; this is the (-1) at the bottom right of Figure 1.2. Along the y_0-axis of T, where $y_0 \neq 0$, (1.8) ensures that the A, B deformation is also a partial smoothing of the singularity, making it irreducible and normal. However, (1.8) with its negative tag is anomalous in that it is not a polynomial equation, so we are not really allowed to use it as a generator of the ideal of the affine variety V_{AB}. We thus replace it by the second expression, which in view of (1.7) is equivalent to it where $y_0 \neq 0$. The relation $x_0 y_1 = x_1 A^3 B^5$ is also anomalous as a tag equation for y_0, since it involves the "opposite" generator x_1 in place of y_0. Now the equations of V_{AB} include (1.7–1.8); these define an irreducible normal complete intersection in $\mathbb{A}^6_{\langle x_0,x_1,y_0,y_1,A,B\rangle}$.

Since V_{AB} is a toric 4-fold, it is Cohen–Macaulay; we see in Lemma 2.4 that it is also Gorenstein. (Exercise: check from the above description that the semigroup ideal of interior monomials of $\sigma(V_{AB})$ is generated by AB; compare Section 2.3 and Figure 2.3.) One checks that the locus $(A = B = 0)$ inside V_{AB} equals T at the general point of each component, and in particular each component is 2-dimensional. Therefore A, B is a regular sequence and $T \subset V_{AB}$ is a flat deformation.

1.1.4 Conclusion

In this example we found the A, B deformation $T \subset V_{AB}$ in a more-or-less inevitable way starting from the new tag equations $x_2y_4 = x_3^2A$ and $x_3y_3 = y_4B$, that naturally smooth the double locus of T along the x_3- and y_4-axes. After a monomial calculation that is birationally forced, our rectangle closed up neatly to give the tag equations (1.7–1.8), so that this deformation also leads to partial smoothings of the x_0 and y_0-axes, giving an irreducible and normal variety V_{AB} such that $A = B = 0$ contains S_0 as a reduced component. Corollary 2.9 explains that this miracle works precisely because the concatenation $[4, 2, 1, 3, 2, 2]$ is a *continued fraction expansion of* 0. These numbers are the tags at x_2, x_3, $y_4, \ldots, y_1$; the asymmetry (x_1 omitted but y_1 included) is significant, and relates to the anomalous tag equations (1.8).

1.1.5 Second toric extension $T \subset V_{LM}$

As hinted above, T has more than one deformation to a toric 4-fold. We now write down the second long rectangle Figure 1.3 and the resulting deformation $T \subset V_{LM}$. The calculations are just as for V_{AB}, except that we start from the f!lrLM

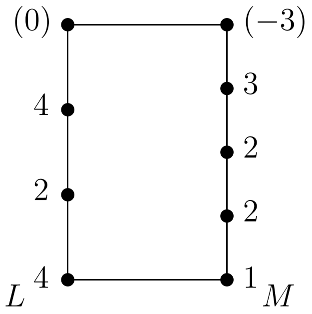

Figure 1.3: The long rectangle for V_{LM}

bottom and work up. Hindsight based on Corollary 2.9 and $[3, 2, 2, 1, 4, 2] = 0$ tells us that this will work. The new tag equations that smooth out the x_0- and y_0-axes of T are represented by the ${}_L4, 1_M$ at the bottom: eq!LM

$$x_1y_0 = x_0^4L, \quad x_0y_1 = y_0M. \tag{1.9}$$

This time x_0, y_0, L, M base the monomial lattice and (1.9) together with (1.2–1.3) give the remaining variables as Laurent monomials:

$$\begin{aligned} x_1 &= x_0^4(Ly_0^{-1}), & y_1 &= y_0(Mx_0^{-1}), \\ x_2 &= x_0^7(Ly_0^{-1})^2, & y_2 &= y_0(Mx_0^{-1})^2, \\ x_3 &= x_0^{24}(Ly_0^{-1})^7, & y_3 &= y_0(Mx_0^{-1})^3, \\ & & y_4 &= y_0^2(Mx_0^{-1})^7. \end{aligned} \tag{1.10}$$

As before, we deduce the tag equations for x_3 and y_4: eq!tLM

$$x_2y_4 = L^2M^7, \quad x_3y_3 = y_4^{-3}L^7M^{27} = x_2^3LM^3. \tag{1.11}$$

The latter is anomalous as before: the partial smoothing along the y_4-axis is specified either by the Laurent monomial y_4^{-3} or by a polynomial equation x_2^3 in the "opposite" variable x_2.

1.1.6 The 6-fold V_{ABLM}

ss!2xt

We now have two deformations $T \subset V_{AB}$ and $T \subset V_{LM}$ of our tent T to toric 4-folds. They are quite different: indeed, V_{AB} is smooth along the x_3- and y_4-axes by (1.5), but has hypersurface singularities along the x_0- and y_0-axes of transverse type $x_1y_0 = A^4B^7$ and $x_0y_1 = y_0^{-1}A^7B^{12}$ by (1.7) and (1.8). In contrast, V_{LM} smooths the x_0- and y_0-axes by (1.9), but leaves the x_3- and y_4-axes with the transverse hypersurface singularities $x_2y_4 = L^2M^7$ and $x_3y_3 = y_4^{-3}L^7M^{27}$ of (1.11).

Main Theorem 1.2.3 now asserts that these two toric panels fit together in a 4-parameter deformation $T \subset V_{ABLM}$: eq!dip

$$\begin{array}{ccc} T & \subset & V_{AB} \\ \cap & & \cap \\ V_{LM} & \subset & V_{ABLM} \end{array} \tag{1.12}$$

More precisely, we build an affine 6-fold V_{ABLM} with a regular sequence A, B, L, M such that the section $L = M = 0$ is V_{AB} and $A = B = 0$ is V_{LM}. The idea is amazingly naive: starting at the top, we simply merge the tag equations (1.5) and (1.11) for x_3 and y_4 from V_{AB} and V_{LM}, obtaining eq!mix

$W \subset \mathbb{A}^8_{\langle x_2,x_3,y_4,y_3,A,B,L,M\rangle}$ defined by

$$x_2y_4 = x_3^2A + L^2M^7, \quad x_3y_3 = y_4B + x_2^3LM^3. \tag{1.13}$$

It is a codimension 2 complete intersection, A, B, L, M is a regular sequence for W, and the section $L = M = 0$ is birational to V_{AB} by the Laurent monomial argument of (1.6).

The plan is now to adjoin x_1, x_0, y_2, y_1, y_0 as rational functions on W, so V_{ABLM} will be birational to W. In commutative algebra terms, the coordinate ring of V_{ABLM} is constructed from the complete intersection (1.13) by *serial unprojection*. We run through the construction as a pleasant narrative; the reasons it all works include some detailed tricks that we explain later when we treat the material more formally. Suffice it to say that we add the new variables x_1, x_0, y_2, y_1, y_0 one at a time, *and in that order*. Adding them in a different order does not work.

1.1.7 First pentagram

We construct x_1 as a rational function on W (1.13) with divisor of poles the codimension 3 complete intersection eq!D

$$D : (x_3 = y_4 = LM^3 = 0) \subset W, \tag{1.14}$$

where LM^3 is the hcf of the two terms L^2M^7 and $x_2^3LM^3$ in (1.13). The new variable x_1 appears in three equations eq!x1un

$$x_1x_3 = \cdots, \quad x_1y_4 = \cdots, \quad x_1LM^3 = \cdots, \tag{1.15}$$

that express the rational function x_1 as a homomorphism $\mathcal{I}_D \to \mathcal{O}_W$. More intrinsically, x_1 is an *unprojection variable* $x_1 \in \mathcal{H}om(\mathcal{I}_D, \omega_W)$ with Poincaré residue a basis of $\omega_D \cong \mathcal{O}_D$; see [PR] and [Ki] for the theory and practice of unprojection. In our calculation we take as input the equations (1.13) and (1.14) of W and D, and use them to fix up a 5×5 skew matrix $A = \{a_{ij}\}$ whose five 4×4 Pfaffians are the two input equations (1.13) and the three new unprojection equations (1.15) for x_1. This calculation is repeated serially in what follows, and we make it systematic with *magic pentagrams*: penta!1

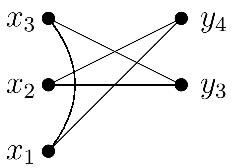

$$\begin{pmatrix} y_3 & x_2^3 & -B & -x_1 \\ & y_4 & LM^3 & -x_3A \\ & & x_3 & LM^4 \\ & & & x_2 \end{pmatrix} \tag{1.16}$$

23.45 $x_2y_4 = x_3^2A + L^2M^7$,
12.34 $x_3y_3 = y_4B + x_2^3LM^3$,

12.35 $x_1y_4 = x_2^3x_3A + y_3LM^4$,
13.45 $x_1x_3 = x_2^4 + BLM^4$,
12.45 $x_2y_3 = x_3AB + x_1LM^3$.

The array is a skew 5×5 matrix $A = \{a_{ij}\}$; we only write the 10 upper-triangular entries $a_{12} = y_3, \dots, a_{15} = -x_1$, etc. Its 4×4 Pfaffians are

$$\mathrm{Pf}_{ij.kl} = a_{ij}a_{kl} - a_{ik}a_{jl} + a_{il}a_{jk} \quad \text{for any distinct } i, j, k, l \tag{1.17}$$

(as with minors and cofactors, with an overall choice of ± 1; in long calculations we abbreviate $\mathrm{Pf}_{ij.kl}$ to $ij.kl$). In (1.16), viewing y_3, y_4, x_3, x_2 and the two equations $x_2y_4 = \cdots$, $x_3y_3 = \cdots$ as given, we seek to add x_1 and three new equations $x_1x_3 = \cdots$, $x_1y_4 = \cdots$ and $x_2y_3 = \cdots + x_1LM^3$. These trinomial equations play a role for V_{ABLM} similar to the binomial tag equations $v_{i-1}v_{i+1} = v_i^{a_i}$ for the cyclic quotient singularities S_i and the tent T. The array is written out automatically from the pentagram and the given equations (1.13): we write the given variables y_3, y_4, x_3, x_2 down the superdiagonal, the new unprojection variable x_1 in the top right, and the given $LM^3 = \mathrm{hcf}(L^2M^7, x_2^3LM^3)$ as the entry a_{24}. Requiring $\mathrm{Pf}_{12.34}$ and $\mathrm{Pf}_{23.45}$ to give (1.13) determines the remaining entries. The output is the three equations involving x_1 as the three remaining Pfaffians in (1.16).

1.1.8 Serial pentagrams

s!ser

The remaining variables x_0, y_2, y_1, y_0 are adjoined likewise to give the codimension 7 variety V_{ABLM} (see Chapter 5 for a formal treatment). We write out the calculations without further comment for your delight.

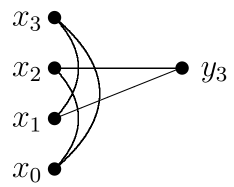

$$\begin{pmatrix} y_3 & x_1 & -AB & -x_0 \\ & x_3 & LM^3 & -x_2^3 \\ & & x_2 & BM \\ & & & x_1 \end{pmatrix}$$

23.45 $\quad x_1x_3 = x_2^4 + BLM^4$,
12.34 $\quad x_2y_3 = ABx_3 + LM^3x_1$,

12.35 $\quad x_0x_3 = x_1x_2^3 + BMy_3$,
13.45 $\quad x_0x_2 = x_1^2 + AB^2M$,
12.45 $\quad x_1y_3 = ABx_2^3 + LM^3x_0$.

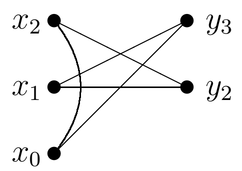

$$\begin{pmatrix} y_3 & LM^2x_0 & -ABx_2^2 & -y_2 \\ & x_2 & M & -x_1 \\ & & x_1 & AB^2 \\ & & & x_0 \end{pmatrix}$$

23.45 $\quad x_0x_2 = x_1^2 + AB^2M$,
12.34 $\quad x_1y_3 = ABx_2^3 + LM^3x_0$,

12.35 $\quad x_2y_2 = AB^2y_3 + LM^2x_0x_1$,
13.45 $\quad x_1y_2 = A^2B^3x_2^2 + LM^2x_0^2$,
12.45 $\quad x_0y_3 = ABx_1x_2^2 + My_2$.

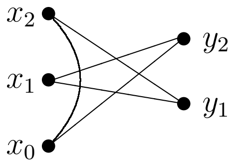

$$\begin{pmatrix} y_2 & LMx_0^2 & -A^2B^3x_2 & -y_1 \\ & x_2 & M & -x_1 \\ & & x_1 & AB^2 \\ & & & x_0 \end{pmatrix}$$

$$\begin{array}{ll} 23.45 & x_0x_2 = x_1^2 + AB^2M, \\ 12.34 & x_1y_2 = A^2B^3x_2^2 + LM^2x_0^2, \end{array}$$

$$\begin{array}{ll} 12.35 & x_2y_1 = AB^2y_2 + LMx_0^2x_1, \\ 13.45 & x_1y_1 = A^3B^5x_2 + LMx_0^3, \\ 12.45 & x_0y_2 = A^2B^3x_1x_2 + My_1. \end{array}$$

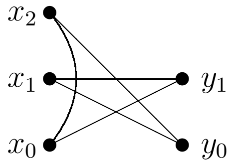

$$\begin{pmatrix} y_1 & Lx_0^3 & -A^3B^5 & -y_0 \\ & x_2 & M & -x_1 \\ & & x_1 & AB^2 \\ & & & x_0 \end{pmatrix}$$

$$\begin{array}{ll} 23.45 & x_0x_2 = x_1^2 + AB^2M, \\ 12.34 & x_1y_1 = A^3B^5x_2 + LMx_0^3, \end{array}$$

$$\begin{array}{ll} 12.35 & x_2y_0 = AB^2y_1 + Lx_0^3x_1, \\ 13.45 & x_1y_0 = A^4B^7 + Lx_0^4, \\ 12.45 & x_0y_1 = A^3B^5x_1 + My_0. \end{array}$$

The final two equations $x_1y_0 = \cdots$ and $x_0y_1 = \cdots$ merge the tag equations (1.7–1.8) and (1.9) for x_0 and y_0 at the bottom of the two long rectangles in exactly the same way as (1.13) merged the tag equations at the top. In other words, the whole calculation could have been done starting with these two equations and working up – if you liked the puzzle, you will enjoy turning it upside down and doing it all over again.

1.2 Introduction to Part I continued

intro!I

1.2.1 Tents and their toric extensions

A tent $T = S_0 \cup S_1 \cup S_2 \cup S_3$ is an affine Gorenstein surface as in Figure 1.1; its 4 irreducible components are $S_0, S_2 \cong \mathbb{A}^2$ and S_1, S_3 cyclic quotient singularities of type $\frac{1}{r}(\alpha, 1)$ and $\frac{1}{s}(\beta, 1)$ (where r, α are coprime natural numbers, and similarly for s, β). They glue transversally along their toric strata (= coordinate axes), giving T four singular axes of transverse ordinary double points; the two axes on S_2 are the *top* axes, and the two on S_0 the *bottom* axes. For details, see Definition 2.3.

Our first result is the easy toric Lemma 2.11: an extension $T \subset V_{AB}$ of a tent T to an (irreducible, normal) affine toric 4-fold V_{AB} that smooths the top axes is given by a matrix $\left(\begin{smallmatrix} r & a \\ b & s \end{smallmatrix}\right) \in \mathrm{SL}(2,\mathbb{Z})$ with $a, b \geq 0$ and $a \equiv \alpha \bmod r$, $b \equiv \beta \bmod s$; this exists if either α or β divides $rs - 1$. Corollary 2.9 gives an alternative treatment in terms of *continued fraction expansions of* 0, such as $[4, 2, 1, 3, 2, 2] = 0$ in our example. By Proposition 2.1.d, this is obtained by concatenating with a 1 the expansions of *complementary* fractions $\frac{r}{a}$ and $\frac{r}{r-a}$, and is thus easy to set up. This is standard material in toric geometry, and only the interpretation is new.[3]

1.2.2 Classification Theorems 3.5 and 3.9

The input to our Main Theorem 1.2.3 is a diptych of extensions $T \subset V_{AB}$ and $T \subset V_{LM}$ as above, smoothing respectively the top and bottom axes of T. Section 3.1 discusses the condition on T for two such smoothings to exist (see Lemma 3.2): we need a second matrix $\left(\begin{smallmatrix} r & g \\ h & s \end{smallmatrix}\right) \in \mathrm{SL}(2,\mathbb{Z})$ with $ag \equiv 1 \bmod r$ and $bh \equiv 1 \bmod s$. Theorem 3.5 classifies all solutions to this problem: with simple initial exceptions, each corresponds to a 2-step recurrent continued fraction $[d, e, d, \ldots, (d \text{ or } e)]$. We think of $d, e \geq 2$ as the *main case* or Type $\mathrm{I}(d, e, k)$, with Example 1.1 as $[2, 4, 2]$ or Type $\mathrm{I}(2, 4, 3)$; the more detailed Classification Theorem 3.9 separates off the cases with d or $e = 1$ into three further families II, III and IV.

1.2.3 Main Theorem

th!main

A diptych of 4*-fold toric panels* $T \subset V_{AB}$ *and* $T \subset V_{LM}$ *that smooth respectively the top and bottom axes of* T *extends to a* 6*-fold* V_{ABLM} *as in* (1.12). unique?

The diptych variety V_{ABLM} *is an affine variety with an action of the torus* $\mathbb{T} = (\mathbb{G}_m)^4$. *It has a regular sequence* A, B, L, M *consisting of eigenfunctions of the* $\mathbb{T}$*-action such that* V_{AB} *and* V_{LM} *are the sections given by* $L = M = 0$ *and* $A = B = 0$*, and* T *is their intersection* $A = B = L = M = 0$.

It follows that V_{ABLM} is a Gorenstein affine 6-fold and is a flat 4-parameter deformation of the tent T. The $\mathbb{T}$-action restricts to the big torus of both 4-fold panels V_{AB} and V_{LM}; the original tent T is a union of toric strata in each, with the $\mathbb{T}$-action inducing the natural $(\mathbb{G}_m)^2$ action on each of its four toric components.

[3]Although the extension $T \subset V_{AB}$ is a deformation, we treat it organically rather than infinitesimally (as Altmann [A]).

1.2.4 Indications of the proof

ss!inpf

We want to handle our diptych varieties V_{ABLM} as explicit objects, but, as with toric varieties, without necessarily writing down all the relations for their coordinate rings. Pfaffian equations arising from pentagrams as in (1.16) ffoll. of Example 1.1 are trinomials, analogous to the binomial equations of toric geometry (especially the tag equations of cyclic quotient singularities), and we hope to get away using only these.

Main Theorem 1.2.3 is proved by *serial unprojection*, supported by a mass of toric geometry. As described in Example 1.1, we start from two equations defining a codimension 2 complete intersection in $\mathbb{A}^8$, and adjoin the remaining variables one at a time using the Kustin–Miller unprojection theorem of [PR]; the serial use of this theorem provides most of what we need.

The order the variables are adjoined is already determined at the level of the toric panel V_{AB}, whose coordinate ring can also be analysed by serial projection. At each step of the induction we have to set up the new unprojection divisor $D_\nu \subset V_\nu$. The divisor D_ν itself is the product of a monomial curve $A^\alpha B^\beta = 0$ with affine space $\mathbb{A}^4$. This is where we make essential use of the relation between the combinatorics of the two panels V_{AB} and V_{LM}, the key point being to compare the order of variables in the projection sequences of V_{AB} and V_{LM} as in Corollary 5.4. The reader with extensive teaching and administrative obligations may wish to take most of this on trust.

1.3 Motivation from Mori flips

s!motiv

Part II applies diptych varieties to explicit Mori theory; the first genuine case is Example 7.1. We confine ourselves here to the motivation that Mori flips of Type A offer our treatment of diptych varieties. This discussion is intended partly to explain some of the objects and features that turn up, and to justify the level of generality we work at, and partly as a mnemonic aid.

1.3.1 Definition of Mori flip

ss!dFlp

A flipping extremal neighbourhood is a 3-fold morphism

$$C \subset X \xrightarrow{f} Y \ni P, \tag{1.18}$$

where $P \in Y$ is an isolated 3-fold singularity, f contracts a single curve $C \cong \mathbb{P}^1$ to P and is an isomorphism on the complements $(X \setminus C) \cong (Y \setminus P)$.

What category do we work in? $P \in Y$ is naturally an isolated singularity, that is, a germ of algebraic variety over $\mathbb{C}$ up to local analytic equivalence, and $X \to Y$ is a projective morphism, hence an analytic germ of neighbourhood of C. One can replace *analytic* by *formal* or *etale* according to taste. Our approach to these matters is pragmatic: we choose a model of Y as an affine variety over $\mathbb{C}$, treating changes of analytic model, category-switching, etc., by assuming whatever we need. In other words, we assume that the necessary localisation and analytic change of models have already taken place; this is implicit in the assumption that f contracts only one irreducible curve C, and in the following.

We assume that X has analytically $\mathbb{Q}$-factorial terminal singularities, and $-K_X$ is relatively ample. Moreover, the Weil divisor class group of X is cyclic: $\operatorname{Cl} X = \mathbb{Z}A$, with ample generator A. (One reduces to this case by passing if necessary to an Abelian cover ramified only at the singularities.) Write $-K_X = \delta A$, where $\delta \geq 1$ is the *Fano index* of X. Mori's famous flip theorem gives another small partial resolution

$$C^+ \subset X^+ \xrightarrow{f^+} Y \ni P \tag{1.19}$$

with $C^+ \cong \mathbb{P}^1$, where X^+ has terminal singularities and K_{X^+} is ample. See Mori [M1] for the original proof and Corti [Co02] for a recent update based on Shokurov's ideas.

1.3.2 The $\mathbb{G}_m$ cover of a flip

ss!Gmcv

We explain the ideology of the first part of Reid [Wf?], that views a flip as the Proj of a $\mathbb{Z}$-graded ring, or as variation of GIT quotient for a $\mathbb{G}_m$ action.

A flipping singularity Y has a $\mathbb{Z}$-graded algebra $\mathcal{R} = \bigoplus_{n\in\mathbb{Z}} \mathcal{O}_Y(nf_*A)$, where A is the ample generator of $\operatorname{Cl} X$; the finite generation of $\mathcal{R}$ as an $\mathcal{O}_Y$-algebra is equivalent to the flip theorem. Taking Spec defines an affine Gorenstein 4-fold $\operatorname{Spec}\mathcal{R} = \mathcal{A}$ (a finitely presented scheme over Y) that is a $\mathbb{G}_m$ cover $\mathcal{A} \to Y$ closely related to the total space of the canonical bundle K_Y (N.B.: this is not a $\mathbb{Q}$-line bundle over the flipping point $P \in Y$). On the other hand, taking only the homogeneous part of $\mathcal{R}$ of degree ≥ 0 gives the $\mathbb{N}$-graded finitely generated $\mathcal{O}_Y$-algebra

$$\mathcal{R}_+ = \bigoplus_{n\geq 0} \mathcal{O}_Y(nf_*A), \quad \text{with} \quad \operatorname{Proj}\mathcal{R}_+ = X.$$

This holds by definition, because A is an ample $\mathbb{Q}$-divisor on X. Doing the same with the homogeneous part of $\mathcal{R}$ of degree ≤ 0 gives X^+ in the same way. This means that X and X^+ can both be studied by graded ring methods. See Example 7.1 for an actual construction.

The grading of $\mathcal{R}$ defines an action of $\mathbb{G}_m$ on it and on $\mathcal{A} = \operatorname{Spec}\mathcal{R}$, and the three varieties in the flip diagram $X \to Y \leftarrow X^+$ are three different GIT quotients by this action. The categorical quotient is Spec of the ring of invariants, that is, $\operatorname{Spec}\mathcal{R}_0 = Y$. Taking $\operatorname{Proj}\mathcal{R}_+$ excludes the variety of the "irrelevant ideal" defined by the vanishing of all the graded elements of degree > 0. Thus taking $\operatorname{Proj}\mathcal{R}_+$ is the GIT procedure of taking the quotient of the set of semistable points V^{ss}; similarly for $\operatorname{Proj}\mathcal{R}_-$.

1.3.3 The general elephant

Write $S = S_Y \in |-K_Y|$ for the general elephant of Y and $S_X = f^{-1}(S) \subset X$ for its birational transform. It is known (see Kollár and Mori [KM], Section 2) that $P \in S$ is a Du Val surface singularity, and it follows from the adjunction formula that $f\colon S_X \to S$ is a crepant partial resolution; since the minimal resolution of a Du Val singularity dominates every crepant partial resolution, and f contracts just one irreducible curve, it follows that S_X is the surface obtained by extracting one exceptional curve of the minimal resolution. (Or to put it another way, start from the minimal resolution of S and contract back down all but one of the exceptional curves.)

Now the equation of $S \subset Y$ is a global section of $\mathcal{O}_Y(\delta A)$, and hence the $\mathbb{G}_m$ cover of S is a principal divisor or hyperplane section in $\mathcal{A}$. The $\mathbb{G}_m$ cover of Y can therefore be studied as a 1-parameter deformation of the $\mathbb{G}_m$ cover of S, which is determined by a Du Val singularity plus extra data.

This is the second ideological point of Reid [Wf?]. It says that a 3-fold flip can be seen as a 1-parameter deformation of a Du Val singularity with a suitable twisting by $\mathbb{G}_m$. The analogy is with the classification of terminal singularities, each of which can be viewed as an equivariant 1-parameter deformation of a cyclic cover of a Du Val singularity ([YPG], Theorem 6.1).

1.3.4 The Type A assumption

We now assume in addition that S is a Du Val singularity of Type A, that is, a cyclic quotient singularity of type $\frac{1}{r}(1,-1)$ for some r. Since the minimal resolution of S is a simple chain of $r-1$ exceptional curves, the partial resolution $S_X \to S$ is just a matter of extracting one link of the chain, that is, breaking the chain into two pieces of length $a-1$ and $r-a-1$ (just one if $a = 1$ or $r-1$); thus S_X is a neighbourhood of an exceptional $\mathbb{P}^1$ on a toric surface with two singularities of type $\frac{1}{a}(1,-1)$ and $\frac{1}{r-a}(1,-1)$. When we make a $\mathbb{G}_m$ cover of S or S_X, it is almost inevitable that the result will be a toric 3-fold.

1.3.5 The section

There is another way of reducing dimension, namely taking a general section through $P \in Y$. Kollár and Mori [KM], Theorem 1.8 use this as the basis of a classification of flips. In fact, Mori [M3], 2.1 proves the much easier statement that under the Type A assumption, the general hyperplane section through $P \in Y$ is also a cyclic quotient singularity. This is the basis for our diptych viewpoint: the $\mathbb{G}_m$ cover of a flip is a 4-fold having two quite different hyperplane sections, each isomorphic to a toric variety.

1.3.6 Long rectangles

ss!Mlr

The top and bottom are $C = \mathbb{P}^1$ and $C^+ = \mathbb{P}^1$. This is the reason that our long rectangles only have 2 monomials x_0, y_0 and x_k, y_l at the bottom and the top, whereas they have any number of monomials down the side. Do this

It would be nice to get this in a more precise form out of Mori's k2A or k1A assumptions. We want k1A to be a special case of k2A.

1.3.7 Unobstructed deformations

s!unob

A key point for us is that deformation problems concerning Mori flips are a priori unobstructed. That is, the obstruction space T^2 is zero for formal reasons. Indeed, X has isolated hyperquotient singularities (see [YPG], Theorem 3.2); thus if we arrange our deformations to take place within the hypersurface, the deformation problem has no local T^2, and has a finite dimensional T^1 at finitely many points. Moreover, f has relative dimension 1 over an affine (or Stein or formal) neighbourhood of a point.

1.3.8 Conclusion

In this section we have tried to convince you of the following points:

- The $\mathbb{G}_m$ cover of a Mori flip of Type A is an affine Gorenstein 4-fold $\mathcal{A}$ with two different Gorenstein toric 3-folds as regular sections. The two panels correspond to "elephant" and "section" of the flipping singularity $P \in X$.

- Each toric panel is a "long rectangle". The top and bottom of each panel corresponds to the exceptional curves of $X^- \to X$ and $X^+ \to X$; they only need two monomial generators, corresponding to the fact that both exceptional curves are weighted $\mathbb{P}^1$s.

- Moreover, the deformation problem from either of these 3-fold sections out to $\mathcal{A}$ can be treated in a way that is a priori unobstructed.

2 Toric geometry

ch!trc

This chapter centres around the combinatorics of Jung–Hirzebruch continued fractions. After recalling standard facts, we define a tent T, and, under appropriate assumptions, construct a toric extension $T \subset V_{AB}$ that smooths its top two axes. We particularly appreciate tents T that admit a second toric extension $T \subset V_{LM}$ smoothing also the bottom two axes as in 1.1.6. These pairs of extensions (1.12) are the input for Main Theorem 1.2.3, and our Theorem 3.5 classifies them in terms of 2-step recurrent continued fractions $[d, e, d, \dots]$.

We also prepare material for the proof of Main Theorem 1.2.3, especially the combinatorics of serial unprojection. The toric extension $T \subset V_{AB}$ can be treated in terms of a matrix $\left(\begin{smallmatrix} r & a \\ b & s \end{smallmatrix}\right) \in \mathrm{SL}(2, \mathbb{Z})$, or equivalently, in terms of a certain continued fraction expansion of 0. The latter treatment gives V_{AB} a sequence of Gorenstein projections.

2.1 Jung–Hirzebruch continued fractions

2.1.1 Formal properties

A *continued fraction expansion* is a formal expression ss!HJ

eq!HJ

$$\begin{aligned}[c_1, \dots, c_n] &= c_1 - 1/(c_2 - 1/(c_3 - \cdots - 1/c_n)) \\ &= c_1 - \cfrac{1}{c_2 - \frac{1}{\dots - \frac{1}{c_n}}} = c_1 - \frac{1}{[c_2, \dots, c_n]} \end{aligned} \tag{2.1}$$

The entries c_i are called *tags*. If $c_1, \dots c_n$ are integers, the righthand side is a rational number, provided that the expression makes sense (that is, division by zero does not occur).[4]

The next proposition discusses four aspects of continued fractions. We spell out this material, because we use it often and with large multiplicity in what follows: we invert continued fractions and pass to complementary fractions, we "top and tail" them by cutting off a tag at one end and adding one at the other, say:

$$[a_0, \dots, a_{k-1}] \mapsto [a_k, a_{k-1}, \dots, a_1], \quad \text{etc.,} \tag{2.2}$$

[4]For tutorial material and exercises, see Reid [More]. The notation is explained in Riemenschneider [R] §3, pp. 220–3, where complementary tags are calculated using the *Riemenschneider staircase.* Related material on concatenated continued fractions is used in Craw and Reid [CR], 2.2.

and we concatenate the resulting fractions.

Proposition 2.1 **(a) Factoring a matrix:** *The formal identity* prop!hj

eq!prod

$$\begin{pmatrix} 0 & 1 \\ -1 & c_1 \end{pmatrix} \begin{pmatrix} 0 & 1 \\ -1 & c_2 \end{pmatrix} \cdots \begin{pmatrix} 0 & 1 \\ -1 & c_n \end{pmatrix} = \begin{pmatrix} -q' & q \\ -p' & p \end{pmatrix}. \tag{2.3}$$

holds in indeterminates or variables $c_1, \dots, c_n$*, where* p, q, p', q' *are polynomials, the numerators and denominators of* $p/q = [c_1, \dots, c_n]$ *and* $p'/q' = [c_1, \dots, c_{n-1}]$*. (No cancellation occurs in the fraction* p/q*, whatever the nature or values of the quantities* c_i*, because* p *and* q *satisfy an* hcf *identity* $\alpha p + \beta q = 1$*.) The fraction* p'/q' *is the* first convergent *of* p/q*.*

(b) Blowdown: $[c_1, \dots, c_{n-1}, 1] = [c_1, \dots, c_{n-1} - 1]$ *and* eq!bld

$$[c_1, \dots, c_{i-1}, 1, c_{i+1}, \dots, c_n] = [c_1, \dots, c_{i-1} - 1, c_{i+1} - 1, \dots, c_n]. \tag{2.4}$$

This is just the identity $\left(\begin{smallmatrix} 0 & 1 \\ -1 & a \end{smallmatrix}\right)\left(\begin{smallmatrix} 0 & 1 \\ -1 & 1 \end{smallmatrix}\right)\left(\begin{smallmatrix} 0 & 1 \\ -1 & b \end{smallmatrix}\right) = \left(\begin{smallmatrix} 0 & 1 \\ -1 & a-1 \end{smallmatrix}\right)\left(\begin{smallmatrix} 0 & 1 \\ -1 & b-1 \end{smallmatrix}\right)$*.*

Two notions of "inverse" of a continued fraction play a role in our theory:

(c) Reciprocal: $[c_1, \dots, c_n] = p/q$ *and its* reciprocal *continued fraction*

$$[c_n, \dots, c_1] = p/q^* \tag{2.5}$$

share the same numerator p*, and their denominators are inverse modulo* p*. More precisely, there is a formal identity*

$$qq^* = N(c_2, \dots, c_{n-1}) \cdot p + 1, \tag{2.6}$$

where $N(c_2, \dots, c_{n-1})$ *is the numerator of* $[c_2, \dots, c_{n-1}]$*. In particular, if* $c_i \in \mathbb{Z}$ *and the expressions are meaningful then* $[c_n, \dots, c_1] = p/q^*$*, where* $qq^* \equiv 1 \bmod p$*. See* (2.11) *for what this means in our context.*

(d) Complement: *Let* $p/q = [c_1, \dots, c_n]$ *with* $c_i \in \mathbb{Z}$ *and* $c_i \geq 2$*. Then the* complementary *continued fraction is* $[b_1, \dots, b_m] = p/(p - q)$*, and satisfies*

$$[c_n, \dots, c_1, 1, b_1, \dots, b_m] = 0. \tag{2.7}$$

Moreover, serial blowdown reduces the expansion to $[1, 1] = [0] = 0$*; in particular,* $\sum(c_i - 1) = \sum(b_j - 1)$*, and one of* $b_1, c_1 \leq 2$*. For example,*

$$[4, \underline{2, 1, 3}, 2, 2] = [\underline{4, 1, 2}, 2, 2] = [\underline{3, 1, 2}, 2] = [\underline{2, 1, 2}] = [1, 1] = 0. \tag{2.8}$$

Remark 2.2 Traditionally, one uses Jung–Hirzebruch continued fractions to write a fraction $\frac{r}{a}$ with $r > a \geq 1$ and a, r coprime integers as rk!JHc

$$\frac{r}{a} = [b_1, \dots, b_{n-1}] = b_1 - \cfrac{1}{b_2 - \cdots}.$$

Then b_1 is the round-up $b_1 = \lceil \frac{r}{a} \rceil$, and is ≥ 2, because $\frac{r}{a} > 1$, and for the same reason all subsequent $b_i \geq 2$ (to the end of the algorithm). Here we do something slightly bigger, with $a \geq 1$, but $r \in \mathbb{Z}$ any integer coprime to a: for example, $\frac{-24}{7} = -3 - \frac{3}{7} = [-3, 3, 2, 2]$. This means that $b_1 = \lceil \frac{r}{a} \rceil \in \mathbb{Z}$; however, from the second step onwards and to the end of the algorithm, $1/(b_1 - \frac{r}{a}) > 1$ is a conventional fraction, so that $b_i \geq 2$ for each i with $2 \leq i \leq n-1$.

In traditional use, (2.3) identifies 3 types of data: a rational fraction $p/q > 1$, a continued fraction $[c_1, \dots, c_n]$ with all $c_i \geq 2$, and a matrix $\begin{pmatrix} -q' & q \\ -p' & p \end{pmatrix} \in \mathrm{SL}(2, \mathbb{Z})$ with $p > q > 0$. However, we relax these restrictions, considering things like $[5, 1, 3] = 5 - \frac{3}{2} = \frac{7}{2} = [4, 2]$ (a blowdown) or $[2, 0, 2] = 4$, with eq!202

$$\begin{pmatrix} 0 & 1 \\ -1 & 2 \end{pmatrix} \begin{pmatrix} 0 & 1 \\ -1 & 0 \end{pmatrix} \begin{pmatrix} 0 & 1 \\ -1 & 2 \end{pmatrix} = \begin{pmatrix} 0 & 1 \\ -1 & 2 \end{pmatrix} \begin{pmatrix} -1 & 2 \\ 0 & -1 \end{pmatrix} = \begin{pmatrix} 0 & -1 \\ 1 & -4 \end{pmatrix}. \tag{2.9}$$

The matrix product (2.3) is meaningful even when (2.1) involves division by zero. More generally, the sequence of integer tags $[c_1, \dots, c_n]$ contain more information than the matrix (2.3), which contains more information than the fraction $\frac{p}{q}$: while $\begin{pmatrix} -q' & q \\ -p' & p \end{pmatrix} \in \mathrm{SL}(2, \mathbb{Z})$, the fraction $\frac{p}{q}$ (when defined) is its image in the quotient group $\mathrm{PSL}(2, \mathbb{Z})$, whereas the expression $[c_1, \dots, c_n]$ is a lift to the "universal cover" of $\mathrm{SL}(2, \mathbb{Z})$ inside the universal cover of $\mathrm{SL}(2, \mathbb{R})$, keeping track of winding number. For example, $[0, 0, 0, 0]$ is the composite of 4 rotations by $\pi/2$, or $\begin{pmatrix} 0 & 1 \\ -1 & 0 \end{pmatrix}^4 = \mathrm{id}$. Running around one of our long rectangles always gives winding number 1.

2.1.2 Notation for the quotient $\frac{1}{r}(1, a)$

As in Example 1.1, for $r \geq 1$ and $0 < a \leq r$ coprime to r we write $\frac{1}{r}(1, a)$ for the $\mathbb{Z}/r$ action on $\mathbb{A}^2_{\langle u,v \rangle}$ given by $(u, v) \mapsto (\varepsilon u, \varepsilon^a v)$, and for the quotient $S = \mathbb{A}^2 / \frac{1}{r}(1, a)$ by this action. We allow $\mathbb{A}^2$ as the case $r = 1$, without worrying unduly about the value of a (of course, $a = 0$); it corresponds to the identity matrix or the empty continued fraction $[\emptyset]$. The lattice $\mathbb{M}$ of invariant Laurent monomials consists of u^iv^j with $i+aj\equiv 0 \bmod r$; it is a copy of $\mathbb{Z}^2$, but with no preferred basis. The coordinate ring of S, based by $\mathbb{Z}/r$-invariant monomials, is minimally generated by monomials on the Newton boundary of the positive quadrant $\sigma\subset M_{\mathbb{R}}$, with $x_0=u^r$, $x_1=u^{r-a}v$, etc. The continued fraction $\frac{r}{r-a}=[a_1,\dots,a_{k-1}]$ provides the generators $x_{0\dots k}$ and the *tag equations* holding between them: eq!tag

$$x_{i-1}x_{i+1}=x_i^{a_i}\quad \text{for } i=1,\dots,k-1. \tag{2.10}$$

These determine S completely: they express any x_j as a Laurent monomial in any two consecutive monomials x_i, x_{i+1}. The complete intersection in $\mathbb{A}^{k+1}_{\langle x_{0\dots k}\rangle}$ given by (2.10) is S plus $\mathbb{A}^2_{\langle x_0,x_k\rangle}$ (usually with a nonreduced structure). The other generators of I_S are "long equations" $x_ix_j=$ monomial for $|i-j|>2$, that can be deduced from (2.10) via syzygies.

When $ab\equiv 1 \bmod r$ the expressions $\frac{1}{r}(1,a)$ and $\frac{1}{r}(b,1)$ give the same group action (up to choosing the primitive root ε^a as the new basis of μ_r); the reciprocal continued fractions define the same invariant monomials, read in the opposite direction: eq!opp

$$\begin{aligned}\frac{r}{r-a}&=[a_1,\dots,a_{k-1}] &\mapsto\quad & x_0=u^r,\ x_1=u^{r-a}v,\ x_2=x_1^{a_1}x_0^{-1},\dots\\ \frac{r}{r-b}&=[a_{k-1},\dots,a_1] &\mapsto\quad & x_k=v^r,\ x_{k-1}=uv^{r-b},\dots.\end{aligned} \tag{2.11}$$

2.2 Tents and fans

2.2.1 The definition of tent

s!tnf

Definition 2.3 A *tent* $T=S_0\cup S_1\cup S_2\cup S_3\subset \mathbb{A}^{k+l+2}_{\langle x_{0\dots k},y_{0\dots l}\rangle}$ is the union of the four affine toric surfaces of Figure 1.1, with horizontal sides $S_0=\mathbb{A}^2_{\langle x_0,y_0\rangle}$ and $S_2=\mathbb{A}^2_{\langle x_k,y_l\rangle}$ and vertical sides the cyclic quotient singularities def!tnt

$S_1=\frac{1}{r}(1,\alpha)$ with coordinates $x_{0\dots k}$ from $\frac{r}{r-\alpha}=[a_1,\dots,a_{k-1}]$, and
$S_3=\frac{1}{s}(1,\beta)$ with coordinates $y_{0\dots l}$ from $\frac{s}{s-\beta}=[b_1,\dots,b_{l-1}]$

(where r,α are coprime natural numbers, and similarly for s,β). The coordinates $x_{0\dots k}, y_{0\dots l}$ of the ambient space $\mathbb{A}^{k+l+2}$ and the equations for T are shown schematically in Figure 2.1. The components glue transversally along

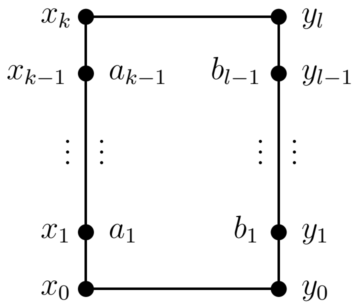

Figure 2.1: Coordinates and tags for T

their toric strata (= coordinate axes), giving T four singular axes of transverse ordinary double points; the two axes on S_2 are the *top* axes, and the two on S_0 the *bottom* axes. f!tnt

Our definition expresses T embedded in $\mathbb{A}^{k+l+2}$ by explicit coordinates; its ideal I_T is generated by I_{S_1}, I_{S_3}, determined by the tags down the sides as in Section 2.1, together with the cross-equations $x_i y_j = 0$ for all pairs $(i,j) \neq (0,0), (k,l)$.

However, T can be viewed abstractly as an identification scheme as studied more generally in Reid [dP]: write $\Gamma'_i \cup \Gamma''_i$ for the toric 1-strata of the S_i and $C = \bigsqcup_{i=1}^4 (\Gamma'_i \cup \Gamma''_i)$. Let D be the four axes $\mathbb{A}^1$ with coordinates x_0, x_k, y_l, y_0 glued transversally at a common origin (as coordinate axes in $\mathbb{A}^4$); write $\varphi\colon C \to D$ for the morphism given by x_0 on the x_0-axes of S_0 and S_1, and so on, to perform the identifications of Figure 1.1. Then

$$T = \big(S_0 \sqcup S_1 \sqcup S_2 \sqcup S_3\big)/\varphi. \tag{2.12}$$

There are no parameters or moduli in this glueing.

l!tnt

Lemma 2.4 *Let T be the tent of Definition 2.3. Then T is a Gorenstein scheme. Moreover, T has an action of $(\mathbb{G}_m)^4$ that restricts to the toric structure on each component.*

Proof We use elementary results of [dP], Section 2. T is Cohen–Macaulay because all the glueing happens in codimension 1 ([dP], 2.2). We prove it is Gorenstein using the criterion of [dP], Corollary 2.8.

Each component S_i is a toric surface; on each, choose a $\mathbb{Z}$-basis m_1, m_2 for the monomial lattice, oriented clockwise (e.g., on S_1, take x_0, x_1 or x_{k-1}, x_k;

on S_2, take x_k, y_l). The 2-form $s = \frac{\mathrm{d}\,m_1}{m_1} \wedge \frac{\mathrm{d}\,m_2}{m_2} \in \Omega^2_{\mathbb{T}}$ on the big torus is a basis for $\Omega^2_{\mathbb{T}}$, is defined over $\mathbb{Z}$, independent of the choice of oriented basis, and has log poles along each stratum of S, with residue along each stratum $\mathbb{A}^1$ equal to $\pm$ times the natural basis $\frac{\mathrm{d}\,m}{m}$ of $\Omega^1_{\mathbb{T}'}$. We take this basis element s on each component. Under the identification $\varphi\colon C \to D$ of the double locus, over the general point of each component of D, the residues from the two components are $\pm\frac{\mathrm{d}\,m}{m}$, and therefore cancel out; thus s satisfies the conditions of [dP], Corollary 2.8.ii and is a basis of the dualising sheaf ω_T.

Each component of T is a toric variety, so $(\mathbb{G}_m)^8$ acts on the disjoint union of the components. Each glueing imposes one linear condition on the action; we think of $\mathbb{T}_{S_0} = (\mathbb{G}_m)^2 = \{(\lambda_0, 1, 1, \lambda_3)\}$ as the big torus of S_0 and $\mathbb{T}_{S_1} = \{(\lambda_0, \lambda_1, 1, 1)\}$ that of S_1, etc. Q.E.D.

2.2.2 The fan $\Phi\left(\begin{smallmatrix} r & a \\ b & s \end{smallmatrix}\right)$ in the plane given by $\left(\begin{smallmatrix} r & a \\ b & s \end{smallmatrix}\right) \in \mathrm{SL}(2,\mathbb{Z})$ ss!fan

Jung–Hirzebruch continued fractions factor a base change in $\mathrm{SL}(2,\mathbb{Z})$ into elementary moves (Proposition 2.1.a); in our case, the base change goes from the monomials x_0, y_0 at the bottom of our long rectangle to x_k, y_l at the top (up to sign and orientation). Section 2.3 constructs the toric variety V_{AB} and the first extension $T \subset V_{AB}$ generalising (1.6), using a matrix in $\mathrm{SL}(2,\mathbb{Z})$ to generate the monomial cone σ_{AB} of Figure 2.3 in the 4-dimensional lattice $\mathbb{M} = \mathbb{Z}^4$.

We first analyse the combinatorics of this construction in a stripped-down 2-dimensional setting obtained by projecting $\mathbb{M}$ to $\overline{\mathbb{M}} = \mathbb{Z}^2$. Consider two oriented bases x_0, y_0 and η, ξ of $\mathbb{Z}^2$ related by inverse base changes eq!x0

$$x_0 = \eta^{-r}\xi^{a}, \quad y_0 = \eta^{b}\xi^{-s} \quad \text{and} \quad \eta = x_0^{-s}y_0^{-a}, \quad \xi = x_0^{-b}y_0^{-r}. \tag{2.13}$$

Here $r, s, a, b \geq 0$ are integers with $rs - ab = 1$, so eq!mats

$$\begin{pmatrix} r & a \\ b & s \end{pmatrix} \quad \text{and} \quad \begin{pmatrix} s & -a \\ -b & r \end{pmatrix} \in \mathrm{SL}(2,\mathbb{Z}) \tag{2.14}$$

are a pair of inverse elements.[5] (If a or $b = 0$ then $r = s = 1$, and one or two points in what follows may need minor restatement; 2.2.4 summarises the initial cases.)

[5] Exercise: Run through $\left(\begin{smallmatrix} r & a \\ b & s \end{smallmatrix}\right) = \left(\begin{smallmatrix} 7 & 24 \\ 2 & 7 \end{smallmatrix}\right)$ and $\left(\begin{smallmatrix} r & g \\ h & s \end{smallmatrix}\right) = \left(\begin{smallmatrix} 7 & 12 \\ 4 & 7 \end{smallmatrix}\right)$ as a sanity check, to recover the two long rectangles of Example 1.1.

The vectors x_0, y_0, η, ξ subdivide the plane $\overline{M}_{\mathbb{R}}$ into the fan $\Phi\left(\begin{smallmatrix} r & a \\ b & s \end{smallmatrix}\right)$ of Figure 2.2.a consisting of 4 cones $\langle x_0, y_0\rangle$, $\langle x_0, \xi\rangle$, $\langle \xi, \eta\rangle$, $\langle y_0, \eta\rangle$. It determines a tent T, with coordinate ring generated by the 4 monomial cones and related by $m_1 m_2 = 0$ if m_1, m_2 are not in a common cone (compare Definition 2.3). The next lemma studies the tent T corresponding to $\Phi\left(\begin{smallmatrix} r & a \\ b & s \end{smallmatrix}\right)$.

l!wT

Lemma 2.5 *Consider the cone $\langle x_0, \xi\rangle$ (marked S_1 in Figure 2.2.a). The lattice $\overline{M}$ is generated by the monomials x_0, ξ together with either of*

$$y_0^{-1} = (x_0^b \xi)^{1/r} \quad \text{or} \quad \eta = (x_0^{-1}\xi^a)^{1/r}.$$

Therefore $\langle x_0, \xi\rangle$ is the monomial cone $\frac{1}{r}(\alpha, 1)$ or $\frac{1}{r}(1, r-\gamma)$, where α is the least residue of a mod *r, and γ that of b (note that $rs - ab = 1$ implies α and $r - \gamma$ are inverse* mod *r).* f!Phi

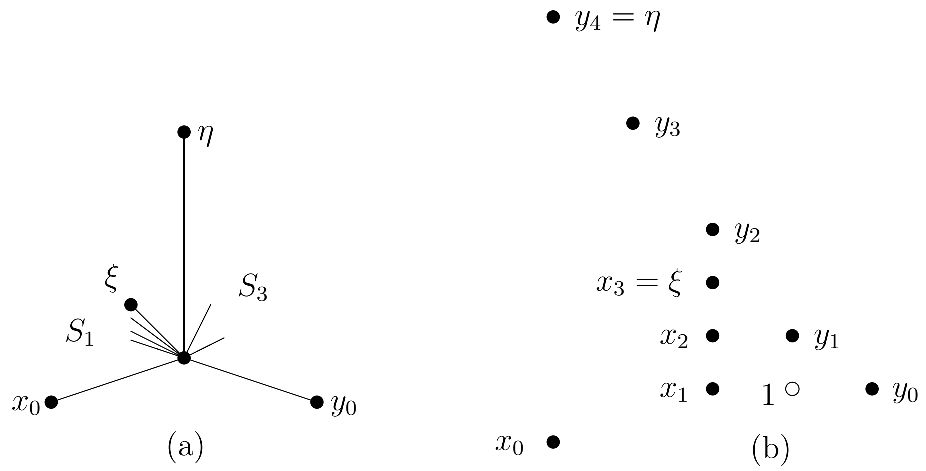

Figure 2.2: The fan $\Phi\left(\begin{smallmatrix} r & a \\ b & s \end{smallmatrix}\right) \in \mathrm{SL}(2, \mathbb{Z})$ defined by x_0, y_0, η, ξ

Write $x_0, x_1, \ldots, x_{k-1}, x_k = \xi$ for the successive monomials along the Newton boundary of $\langle x_0, \xi\rangle$. The number k and the monomials themselves come from factoring the base change (2.13) *into elementary moves:*

$$\begin{pmatrix} -r & a \\ b & -s \end{pmatrix} = \begin{pmatrix} 0 & 1 \\ -1 & a_0 \end{pmatrix} \begin{pmatrix} 0 & 1 \\ -1 & a_1 \end{pmatrix} \cdots \begin{pmatrix} 0 & 1 \\ -1 & a_{k-1} \end{pmatrix} \begin{pmatrix} 0 & 1 \\ -1 & a_k \end{pmatrix}. \qquad (2.15)$$

More concretely, they are given by the continued fraction expansions 2eq!b/s

$$[a_0, a_1, \ldots, a_{k-1}] = \frac{-b}{r} \quad \text{and} \quad [a_k, \ldots, a_1] = \frac{a}{r} \qquad (2.16)$$

by either of the following constructions:

(1) *From the bottom, x_0 is given, and $x_1 = (x_0^\gamma \xi)^{1/r}$, where γ is the least residue of b mod r. Thus $a_0 = \lceil \frac{-b}{r} \rceil = \frac{-b+\gamma}{r} \le 0$ and* eq!ctg

$$x_1 = (x_0^\gamma \xi)^{1/r} = y_0^{-1} x_0^{a_0}, \quad \text{that is,} \quad x_1 y_0 = x_0^{a_0}. \tag{2.17}$$

If $\gamma = 0$ then r divides b, whereas $rs - ab = 1$ implies that r, b are coprime; thus $r = 1$, so that $k = 1$ and $x_1 = \xi$. Otherwise $x_2, \dots, x_k$ are determined as usual by tag equations

$$x_{i-1} x_{i+1} = x_i^{a_i} \quad \text{for } i = 1, \dots, k-1,$$

where $[a_1, \dots, a_{k-1}] = \frac{r}{\gamma}$ (see Remark 2.2).

(2) *From the top, $x_k = \xi$ is given; if $r \mid a$ then, as before, $r = 1$ and the only monomials are $x_0, x_1 = \xi$. Otherwise, set $x_{k-1} = (x_0 \xi^{r-\alpha})^{1/r}$, where α is the least residue of a mod r. Then $r - \alpha = a_k r - a$ where $a_k = \lceil \frac{a}{r} \rceil \ge 1$, and*

$$x_{k-1} = \xi^{a_k} (x_0 \xi^{-a})^{1/r} = x_k^{a_k} \eta^{-1} \quad \text{that is,} \quad x_{k-1}\eta = x_k^{a_k}.$$

The remaining monomials are determined by

$$x_{i-1} x_{i+1} = x_i^{a_i}, \quad \text{where } [a_{k-1}, \dots, a_1] = \tfrac{r}{r-\alpha}.$$

In the same way, the sequence $[b_0, b_1, \dots, b_l]$ factors the inverse transformation of (2.13) *into elementary moves:*

$$\begin{pmatrix} -s & -a \\ -b & -r \end{pmatrix} = \begin{pmatrix} 0 & 1 \\ -1 & b_l \end{pmatrix} \begin{pmatrix} 0 & 1 \\ -1 & b_{l-1} \end{pmatrix} \cdots \begin{pmatrix} 0 & 1 \\ -1 & b_1 \end{pmatrix} \begin{pmatrix} 0 & 1 \\ -1 & b_0 \end{pmatrix}. \tag{2.18}$$

More concretely, $\langle y_0, \eta \rangle$ is the monomial cone $\frac{1}{s}(b, 1)$ or $\frac{1}{s}(1, -a)$, and the tags and monomials on the S_3 side are $b_0, \dots, b_l$ and $y_0, \dots, y_k$, given by

$$[b_0, b_1, \dots, b_{l-1}] = \frac{-a}{s} \quad \text{and} \quad [b_l, \dots, b_1] = \frac{b}{s} \tag{2.19}$$

and $y_1 = x_0^{-1} y^{b_0} = (y_0^\beta \eta)^{1/s}$ where β is the least residue of b mod s.

Not every tent $T = S_0 \cup S_1 \cup S_2 \cup S_3$ (Definition 2.3) is given by a fan as in 2.2.2. Which are? And in how many ways? What extra data does the fan know about beyond T? The tent T knows the 4 monomial cones up to $\mathrm{SL}(2, \mathbb{Z})$ isomorphism, but does does not know how they fit together in $\mathbb{Z}^2$; it knows the fractions $\frac{1}{r}(\alpha, 1)$ and $\frac{1}{s}(\beta, 1)$, but not the corner tags a_0, b_0, a_k, b_l.

Corollary 2.6 *The fan $\Phi(\begin{smallmatrix} r & a \\ b & s \end{smallmatrix})$ gives T with $S_1 = \frac{1}{r}(\alpha, 1)$, $S_3 = \frac{1}{s}(\beta, 1)$ by the construction of 2.2.2 if and only if $a \equiv \alpha \bmod r$ and $b \equiv \beta \bmod s$.*

For fixed T, except for initial cases with $r = s = 1$ (see 2.2.4), there are 0, 1 or 2 matrixes for which $\Phi(\begin{smallmatrix} r & a \\ b & s \end{smallmatrix})$ gives T:

- *if neither α nor β divides $rs - 1$, there are none;*
- *if α divides $rs - 1$ then $a = \alpha$, $b = (rs - 1)/\alpha$ provides a solution;*
- *similarly, if $\beta \mid (rs - 1)$ then $a = (rs - 1)/\beta$ and $b = \beta$ provides a solution.*

Remark 2.7 Whereas Figure 2.2.a just sketches the division of the plane into 4 cones $\langle x_0, y_0\rangle$, $\langle x_0, \xi\rangle$, $\langle \xi, \eta\rangle$, $\langle y_0, \eta\rangle$, (b) accurately plots the monomials in the case $(\begin{smallmatrix} r & a \\ b & s \end{smallmatrix}) = (\begin{smallmatrix} 7 & 24 \\ 2 & 7 \end{smallmatrix})$, with tags $[a_0, \dots, a_3] = [0, 4, 2, 4]$ at the x_i and $[b_0, \dots, b_4] = [-3, 3, 2, 2, 1]$ at the y_i. The comparison of the rich and messy reality of Figure 2.2.b with our square-cut projective pictures such as Figures 1.2–1.3 and 2.1 is enlightening, if somewhat startling.

Please check that you can see the effect of the tags in the picture:

$$\begin{aligned} a_0 = 0 \text{ at } x_0 &\implies x_1, 0, y_0 \text{ are in arithmetic progression;} \\ b_4 = 1 \text{ at } y_4 &\implies 0x_3y_4y_3 \text{ is a parallelogram;} \\ b_0 = -3 \text{ at } y_0 &\implies 1 \text{ is in the affine convex hull } 1 \in \langle x_0, y_1, y_0\rangle, \end{aligned}$$

and so on. The figure and its monomials have other convexity and collinearity properties to which we return later (compare the Scissors of Figure 4.2).

2.2.3 Big end, little end, and attitude of a long rectangle

ss!at

In the $\mathrm{SL}(2, \mathbb{Z})$ geometry of the plane, all basic cones are equivalent, so there is of course no notion of the *size* of an angle. Despite this, the bottom cone $\langle x_0, y_0\rangle$ is clearly the *big end* of Φ in Figure 2.2: if we view Φ as a pie chart, $\langle x_0, y_0\rangle$ occupies the lion's share of the plane, practically 50%. The issue is not size, but convexity. Our choice of signs in (2.13) is equivalent to eq!big

$$-\langle \xi, \eta\rangle \subseteq \langle x_0, y_0\rangle\,. \tag{2.20}$$

Even more holds: every monomial appearing as a minimal generator in the other cones has inverse in $\langle x_0, y_0\rangle$.

Our choices in Φ have already decided that the bottom $S_0 = \mathbb{A}^2_{\langle x_0, y_0 \rangle}$ is its big end and the top $S_2 = \mathbb{A}^2_{\langle \xi, \eta \rangle}$ its little end. (The two players swap ends for the second half of the game.) Once this choice is out of the way, there are still two dichotomies for the corner tags, forming a division into 4 cases, the *attitude* of the long retangle and of the panel V_{AB}. Treating this carefully here will save many headaches later.

cor!at

Corollary 2.8 *Except for initial cases with r or $s = 1$ (see 2.2.4) $r, s \neq a, b$ and*

$$r < a \iff b < s \quad \textit{and} \quad r < b \iff a < s.$$

The long rectangle σ_{AB} thus has attitude:

Top tags: *either $a_k \geq 2$ and $b_l = 1$ if $r < a$ and $b < s$; or*

$a_k = 1$ and $b_l \geq 2$ if $r > a$ and $b > s$; and

Bottom tags: *either $a_0 \leq -1$ and $b_0 = 0$ if $r < b$ and $a < s$; or*

$a_0 = 0$ and $b_0 \leq -1$ if $r > b$ and $a > s$.

cor!VAB

Corollary 2.9 *If $a_0 < 0$ and $b_0 = 0$ then $[a_2, \dots, a_k, b_l, \dots, b_2, b_1] = 0$. If $a_0 = 0$ and $b_0 < 0$ then $[a_1, \dots, a_k, b_l, \dots, b_2] = 0$.*

Conversely, given $\frac{1}{r}(1, \alpha)$ and $\frac{1}{s}(1, \beta)$ as in Definition 2.3, the tent T is given by a fan $\Phi\left(\begin{smallmatrix} r & a \\ b & s \end{smallmatrix}\right)$ if and only if the continued fractions

$$\frac{r}{r - \alpha} = [a_1, \dots, a_{k-1}] \quad \textit{and} \quad \frac{s}{s - \beta} = [b_1, \dots, b_{k-1}]$$

can be concatenated with a_k and b_l such that

$$\textit{either} \quad [a_2, \dots, a_k, b_l, \dots, b_2, b_1] = 0 \quad \textit{or} \quad [a_1, a_2 \dots, a_k, b_l, \dots, b_2] = 0.$$

Proof x_1 and y_0 are opposite vectors in Figure 2.2, so $\langle x_1, x_2, \dots, y_1, y_0 \rangle$ is a half-space with a basic subdivision. Q.E.D.

2.2.4 Initial cases ss!init

We list here all the cases with r or $s \leq 1$, treating all cases with attitude not covered by Corollary 2.8.

$\begin{pmatrix}1 & 0\\ 0 & 1\end{pmatrix}$	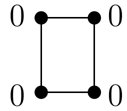	$x_0y_1 = A,$ $x_1y_0 = B.$
$\begin{pmatrix}1 & 0\\ b & 1\end{pmatrix}$	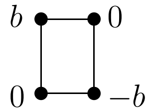	$x_0y_1 = x_1^bA,$ $x_1y_0 = B.$
$\begin{pmatrix}1 & a\\ 0 & 1\end{pmatrix}$	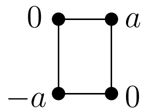	$x_0y_1 = A,$ $x_1y_0 = y_1^aB.$
$\begin{pmatrix}1 & 1\\ s-1 & s\end{pmatrix}$	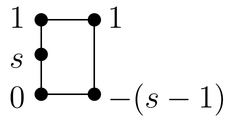	$x_1y_1 = x_2A, x_2y_0 = y_1B,$ $x_0x_2 = x_1^s,$ $x_1y_0 = AB, x_0y_1 = x_1^{s-1}A.$
$\begin{pmatrix}r & 1\\ r-1 & 1\end{pmatrix}$	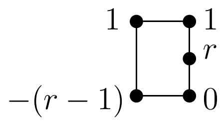	$x_0y_1 = x_2A, x_1y_1 = y_1B,$ $y_0y_2 = y_1^r,$ $x_1y_0 = y_1^{r-1}B, x_0y_1 = AB.$

The cases with a or $b = 1$ and $r, s \geq 2$ are not exceptional; rather, they serve as the first regular example of our construction:

$\begin{pmatrix}r & rs-1\\ 1 & s\end{pmatrix}$ 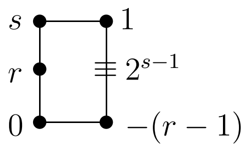

$\begin{pmatrix}r & 1\\ rs-1 & s\end{pmatrix}$ 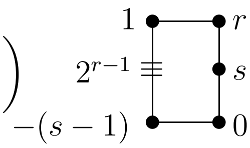

(2.21)

2.3 Construction of $T \subset V_{AB}$ from $\left(\begin{smallmatrix}r & a\\ b & s\end{smallmatrix}\right) \in \mathrm{SL}(2,\mathbb{Z})$ s!bet

For the deformation $T \subset V_{AB}$, we pump up the fan $\Phi\left(\begin{smallmatrix}r & a\\ b & s\end{smallmatrix}\right)$ of 2.2.2 out of the plane $\overline{\mathbb{M}}$ to the cone σ_{AB} of Figure 2.3 in the 4-space of $M = \mathbb{Z}^4$, using the new variables A, B respectively to bend along the ξ and η axes. In more detail, consider the monomial lattice $M \cong \mathbb{Z}^4$ based by ξ, η, A, B, and the cone σ_{AB} in $M_{\mathbb{R}}$ spanned by eq!x0y0

$$\xi, \eta, A, B \quad \text{together with} \quad x_0 = (A\eta^{-1})^r \xi^a, \quad y_0 = \eta^b (B\xi^{-1})^s \qquad (2.22)$$

(compare (2.13)). We draw σ_{AB} projectively, so that it has two quadrilateral f!siAB

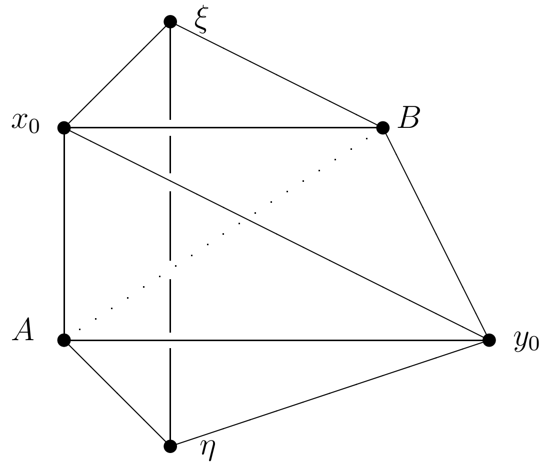

Figure 2.3: The monomial cone σ_{AB}

faces $\xi\eta A x_0$ and $\xi\eta y_0 B$ (the "back"), and four triangles $\xi B x_0$, $B x_0 y_0$, $x_0 y_0 A$ and $y_0 A \eta$ (the "front"). The primitive vectors orthogonal to these faces are, in order, eq!orthv

$$(0,0,0,1)\ (0,0,1,0)\ (0,1,1,0)\ (rb,rs,1,0)\ (rs,as,0,1)\ (1,0,0,1). \quad (2.23)$$

We get σ_{AB} from the simplex $\langle \xi, \eta, x_0, y_0 \rangle$ by pulling out each of the two back faces to quadrilaterals, adding a vertex A in the plane of x_0, ξ, η such that ξ, η, A is basic and the quadrilateral x_0, ξ, η, A is convex as shown, and likewise for B in the plane of y_0, η, ξ. The picture can be viewed from different perspectives (we use some below, see Figure 4.1), and trying to read metric properties from these can be misleading.

The dual cone $\sigma_{AB}^\vee$ is the convex hull of the orthogonal vectors (2.23). Since these are all in the hyperplane of weights w with $w(AB) = 1$, the dotted line from A to B is interior to σ_{AB}, and AB generates the ideal of interior monomials. This is Danilov's criterion for the toric variety $V_{AB} = \operatorname{Spec}(\mathbb{C}[\sigma_{AB} \cap M])$ to be Gorenstein. The unextended simplex $\langle \xi, \eta, x_0, y_0 \rangle$ itself does not in general determine A, B or the matrixes (2.14).

The 2-faces $\langle x_0, \xi \rangle$ and $\langle y_0, \eta \rangle$ of the simplicial cone $\langle \xi, \eta, x_0, y_0 \rangle$ are also faces of σ_{AB}, basic in $\mathbb{M}$ if and only if $r = 1$, respectively $s = 1$; they are the monomial cones of toric surfaces S_1 and S_3, and to determine these, we want the monomials of $\mathbb{M}$ along these sides, and the tag relations between them, including those at the four corners[6] (we explain this below). All this comes from the relations (2.22) and their inverses eq!xi,eta

$$\eta = (A^r B^a x_0^{-1})^s y_0^{-a}, \quad \xi = x_0^{-b}(A^b B^s y_0^{-1})^r. \tag{2.24}$$

Indeed (2.22) and (2.24) give eq!4mon

$$\left.\begin{array}{ll} (x_0\xi^{-a})^{1/r} = A\eta^{-1} & \text{and} \quad (y_0\eta^{-b})^{1/s} = B\xi^{-1} \\ (x_0^b\xi)^{1/r} = A^b B^s y_0^{-1} & \text{and} \quad (y_0^a\eta)^{1/s} = A^r B^a x_0^{-1} \end{array}\right\} \in M. \tag{2.25}$$

This implies that S_1 and S_3 are the quotient singularities eq!2way

$$S_1 \cong \frac{1}{r}(a,1) \cong \frac{1}{r}(1,-b) \quad \text{and} \quad S_3 \cong \frac{1}{s}(b,1) \cong \frac{1}{s}(1,-a). \tag{2.26}$$

The more precise statement is the following:

l!mon

Lemma 2.10 *The face $\langle x_0, \xi\rangle$ spans a 2-dimensional vector space in $M_{\mathbb{R}}$, that intersects $\mathbb{M}$ in the sublattice generated as a $\mathbb{Z}$-module by x_0, ξ together with* either *of*

$$(x_0^b\xi)^{1/r} = A^b B^s y_0^{-1} \quad \textit{or} \quad (x_0\xi^{-a})^{1/r} = A\eta^{-1}.$$

Write $x_0, x_1, \dots, x_{k-1}, x_k = \xi$ for the successive monomials along the Newton boundary of $\langle x_0, \xi\rangle$. The number k and the monomials themselves come from either of the continued fraction expansions eq!b/s2

$$[a_0, a_1, \dots, a_{k-1}] = \frac{-b}{r} \quad \textit{and} \quad [a_k, \dots, a_1] = \frac{a}{r} \tag{2.27}$$

by the following constructions:

1. *From the bottom, x_0 is given, and $x_1 = (x_0^\gamma\xi)^{1/r}$, where γ is the least residue of b modulo r. Thus $a_0 = \lceil\frac{-b}{r}\rceil = \frac{-b+\gamma}{r} \le 0$ and*

$$x_1 = (x_0^\gamma\xi)^{1/r} = A^b B^s x_0^{a_0} y_0^{-1}, \quad \textit{that is,} \quad x_1 y_0 = A^b B^s x_0^{a_0}. \tag{2.28}$$

[6]Repetition, needs a little pruning.

If $\gamma = 0$ then r divides b, whereas $rs - ab = 1$ implies that r, b are coprime; thus $r = 1$, so that $k = 1$ and $x_1 = \xi$. Otherwise $x_2, \dots, x_k$ are determined as usual by tag equations

$$x_{i-1}x_{i+1} = x_i^{a_i} \quad \text{for } i = 1, \dots, k-1,$$

where $[a_1, \dots, a_{k-1}] = \frac{r}{\gamma}$ (see Remark 2.2).

2. *From the top, $x_k = \xi$ is given; if $r \mid a$ then, as before, $r = 1$ and the only monomials are $x_0, x_1 = \xi$. Otherwise, set $x_{k-1} = (x_0\xi^{r-\alpha})^{1/r}$, where α is the least residue of a mod r. Then $r - \alpha = a_k r - a$ where $a_k = \lceil \frac{a}{r} \rceil \geq 1$, and*

$$x_{k-1} = \xi^{a_k}(x_0\xi^{-a})^{1/r} = x_k^{a_k} A\eta^{-1} \quad \text{that is,} \quad x_{k-1}\eta = Ax_k^{a_k}.$$

The remaining monomials are determined by

$$x_{i-1}x_{i+1} = x_i^{a_i}, \quad \text{where } [a_{k-1}, \dots, a_1] = \tfrac{r}{r-\alpha}.$$

The ring $\mathbb{C}[M \cap \langle x_0, \xi\rangle]$ (the coordinate ring $\mathbb{C}[S_1]$ of S_1) is isomorphic to the invariant ring of the cyclic quotient singularity $\frac{1}{r}(a, 1) \cong \frac{1}{r}(1, -b)$; here $ab = rs - 1$, so that $ab \equiv -1 \bmod s$.

In the same way, $\langle y_0, \eta\rangle \cong \frac{1}{s}(b, 1) \cong \frac{1}{s}(1, -a)$ with initial monomials y_1 and y_{l-1} determined by the corner tag equations

$$x_0y_1 = A^rB^ay_0^{b_0} \quad \text{and} \quad \xi y_{l-1} = B\eta^{b_l},$$

with $b_0 = \lceil \frac{-a}{s} \rceil \leq 0$ and $b_l = \lceil \frac{b}{s} \rceil \geq 1$, and the remaining monomials for S_3 are $y_0, y_1, \dots, y_{l-1}, y_l$ tagged by eq!a/r

$$[b_0, b_1, \dots, b_{l-1}] = \frac{-a}{s} \quad \text{and} \quad [b_l, \dots, b_1] = \frac{b}{s}. \tag{2.29}$$

l!be

Lemma 2.11 *Let*

$$T = S_0 \cup S_1 \cup S_2 \cup S_3$$

be a tent with two given cyclic quotient singularities in reduced form $S_1 = \frac{1}{r}(\alpha, 1)$ and $S_3 = \frac{1}{s}(\beta, 1)$. Then toric deformations $T \subset V_{AB}$ that smooth the ξ and η axes correspond one-to-one with matrixes

$$\begin{pmatrix} r & a \\ b & s \end{pmatrix} \in \mathrm{SL}(2, \mathbb{Z}) \quad \text{with} \quad \begin{matrix} a \equiv \alpha \bmod r, \\ b \equiv \beta \bmod s. \end{matrix}$$

Since $ab = rs - 1$ *obviously implies that* $a < r$ *or* $b < s$, *this means that*

$$\begin{aligned} \textit{either} \quad & a = \alpha \mid rs - 1 \quad \textit{and} \quad b = \tfrac{rs-1}{\alpha}\,, \\ \textit{or} \quad & b = \beta \mid rs - 1 \quad \textit{and} \quad a = \tfrac{rs-1}{\beta}\,. \end{aligned}$$

There may be 0, 1 *or* 2 *solutions.*

3 Classification of diptychs

ch!Cl

3.1 A second panel V_{LM}

s!2ndp

Our[7] construction in 2.3 of the toric deformation $T \subset V_{AB}$ was given by the fan $\Phi\left(\begin{smallmatrix} r & a \\ b & s \end{smallmatrix}\right)$ dividing the plane $\overline{\mathbb{M}}$ into the four cones of Figure 2.2. Its key properties are that its 4 cones give the 4 sides of T, and the union of its three top cones is *one step beyond convex*; by this we mean that shaving either x_0 or y_0 off the two side cones makes the union of the three top cones convex. (More specifically, in Figure 2.2, the tag 0 at x_0 means that $x_1, 0, y_0$ are collinear, so that every monomial except x_0 is in the upper half-space; and the negative tag $b_0 < 0$ at y_0 means that all the monomials from $x_0, \dots, x_k, y_l, \dots, y_1$ are strictly within a half-plane.)

3.1.1 A second fan $\Phi'\left(\begin{smallmatrix} r & g \\ h & s \end{smallmatrix}\right)$

ss!2Ph

For the right panel V_{LM} of our diptych, we need a second fan Φ' in a plane $\overline{\mathbb{M}}'$ (not identified with $\overline{\mathbb{M}}$), defining the same tent T, but this time the big end of Φ' is the top $\langle \xi, \eta \rangle$ corresponding to S_2, and its little end the bottom $\langle x_0, y_0 \rangle$ corresponding to S_0. For this, replace (2.13) with the base change

$$x_0 = \eta^{-r}\xi^{-g}, \quad y_0 = \eta^{-h}\xi^{-s} \quad \text{and} \quad \eta = x_0^{-s}y_0^{g}, \quad \xi = x_0^{h}y_0^{-r} \tag{3.1}$$

based on the inverse pair $\left(\begin{smallmatrix} -r & -g \\ -h & -s \end{smallmatrix}\right)$ and $\left(\begin{smallmatrix} -s & g \\ h & -r \end{smallmatrix}\right)$, with $g, h \geq 0$. As before, x_0, ξ, η, y_0 define a fan Φ' of 4 cones, but with signs giving the inclusion $-\langle x_0, y_0 \rangle \subseteq \langle \xi, \eta \rangle$ opposite to (2.20), so that $\langle \xi, \eta \rangle$ is the big end.

Lemma 3.1 *In Φ' the cone $\langle x_0, \xi \rangle$ corresponding is $\frac{1}{r}(1, h) \cong \frac{1}{r}(-g, 1)$; the cone $\langle y_0, \eta \rangle$ is $\frac{1}{s}(1, g) \cong \frac{1}{s}(-h, 1)$.*

Hence Φ' defines the same tent T as Φ of 2.2.2 if and only if $-g \equiv \alpha \bmod r$ and $-h \equiv \beta \bmod s$.

We say that Φ and Φ' related in this way are *partners*. Section 3.2 classifies all partner pairs.

l!2nd

Lemma 3.2 *From V_{AB}, the cone $\langle x_0, \xi \rangle$ is $\frac{1}{r}(a, 1) \cong \frac{1}{r}(1, -b)$ and from V_{LM} it is $\frac{1}{r}(1, g) \cong \frac{1}{r}(-h, 1)$. The cone $\langle y_0, \eta \rangle$ is $\frac{1}{s}(b, 1) \cong \frac{1}{s}(1, -a)$ and also $\frac{1}{s}(1, h) \cong \frac{1}{s}(-g, 1)$. Therefore $ag \equiv 1 \bmod r$ and $bh \equiv 1 \bmod s$; together with $rs - ab = rs - gh = 1$, these imply that* eq!9

[7]This material needs organising as a coherent narrative.

$$a + h \equiv b + g \equiv 0 \bmod r \textit{ and } \bmod s. \tag{3.2}$$

3.1.2 A second panel V_{LM}

ss!VLM

I fix notation: the left panel V_{AB} was specified by the matrix

$$\begin{pmatrix} r & a \\ b & s \end{pmatrix} \quad \text{via the monomials} \quad \begin{array}{rcl} x_0 & = & (A\eta^{-1})^r \xi^a, \\ y_0 & = & \eta^b (B\xi^{-1})^s. \end{array}$$

Likewise, the right panel V_{LM} is Spec of the cone σ_{LM} in the same $M_{\mathbb{R}}$ generated by x_0, y_0, L, M together with monomials

$$\begin{array}{rcl} \xi & = & (Ly_0^{-1})^r x_0^g, \\ \eta & = & y_0^h (Mx_0^{-1})^s \end{array} \quad \text{specified by} \quad \begin{pmatrix} r & g \\ h & s \end{pmatrix} \in \mathrm{SL}(2, \mathbb{Z}).$$

We draw the two monomial cones σ_{AB} and σ_{LM} together in Figure 4.1

l!2nd2

Lemma 3.3 *From V_{AB}, the cone $\langle x_0, \xi \rangle$ is $\frac{1}{r}(a,1) \cong \frac{1}{r}(1,-b)$ and from V_{LM} it is $\frac{1}{r}(1,g) \cong \frac{1}{r}(-h,1)$. The cone $\langle y_0, \eta \rangle$ is $\frac{1}{s}(b,1) \cong \frac{1}{s}(1,-a)$ and also $\frac{1}{s}(1,h) \cong \frac{1}{s}(-g,1)$. Therefore $ag \equiv 1 \bmod r$ and $bh \equiv 1 \bmod s$; together with $rs - ab = rs - gh = 1$, these imply that* eq!9

$$a + h \equiv b + g \equiv 0 \bmod r \textit{ and } \bmod s. \tag{3.3}$$

r!convx

Remark 3.4 The union $\sigma_{AB} \cup \sigma_{LM}$ has convex hull a cone with a vertex. Indeed, in the $\mathbb{R}$-basis x_0, y_0, x_k, y_l of $\mathbb{M}$, the condition for a linear form $(\alpha, \beta, \gamma, \delta)$ to be positive on A, B is

$$\alpha - a\gamma + r\delta > 0 \quad \text{and} \quad \beta + s\gamma - b\delta > 0.$$

This is achieved by taking

$$\frac{s}{b} > \frac{\delta}{\gamma} > \frac{a}{r}, \quad \text{that is,} \quad \frac{\delta}{\gamma} \in \left(\frac{a}{r}, \frac{s}{b} \right),$$

independently of α, β. Similarly, $\frac{\alpha}{\beta} \in \left(\frac{h}{s}, \frac{r}{g} \right)$ gives positivity on L, M.

3.2 Classification of partner pairs

s!Cl

Classifying all partner pairs Φ, Φ' of fans is an elementary "infinite descent" exercise similar to playing with Fibonacci numbers.

Rules of the game: Given integers eq!10

$$\begin{aligned} r,s\ge 1,\quad a,b,g,h\ge 0,\quad \text{with}\quad ab=gh=rs-1\\ \text{and}\quad a+h\equiv b+g\equiv 0 \bmod r \text{ and} \bmod s. \end{aligned} \tag{3.4}$$

Use the congruences to define δ and ε: eq!10a

$$a+h=\varepsilon s \quad\text{and}\quad b+g=\delta r. \tag{3.5}$$

The following two operations preserve all the equalities and congruences while interchanging δ and ε: eq!22

$$\begin{aligned} \begin{pmatrix} r & a\\ b & s\end{pmatrix} &\mapsto \begin{pmatrix} 0 & 1\\ -1 & \varepsilon\end{pmatrix}\begin{pmatrix} r & a\\ b & s\end{pmatrix} = \begin{pmatrix} b & s\\ \varepsilon b-r & g\end{pmatrix}\\ \begin{pmatrix} r & g\\ h & s\end{pmatrix} &\mapsto \begin{pmatrix} r & g\\ h & s\end{pmatrix}\begin{pmatrix} \delta & 1\\ -1 & 0\end{pmatrix} = \begin{pmatrix} b & r\\ \delta h-s & h\end{pmatrix} \end{aligned} \tag{3.6}$$

and ("its inverse with ε, δ interchanged") eq!23

$$\begin{aligned} \begin{pmatrix} r & a\\ b & s\end{pmatrix} &\mapsto \begin{pmatrix} \delta & -1\\ 1 & 0\end{pmatrix}\begin{pmatrix} r & a\\ b & s\end{pmatrix} = \begin{pmatrix} g & \delta a-s\\ r & a\end{pmatrix}\\ \begin{pmatrix} r & g\\ h & s\end{pmatrix} &\mapsto \begin{pmatrix} r & g\\ h & s\end{pmatrix}\begin{pmatrix} 0 & -1\\ 1 & \varepsilon\end{pmatrix} = \begin{pmatrix} g & \varepsilon g-r\\ s & a\end{pmatrix} \end{aligned} \tag{3.7}$$

It turns out that a series of these operations with alternating δ, ε reduces to the *initial case* $\left(\begin{smallmatrix} 1 & \delta\\ 0 & 1\end{smallmatrix}\right)$, $\left(\begin{smallmatrix} 1 & 0\\ \varepsilon & 1\end{smallmatrix}\right)$ and then down to $\left(\begin{smallmatrix} 0 & 1\\ -1 & 0\end{smallmatrix}\right)$, $\left(\begin{smallmatrix} 0 & -1\\ 1 & 0\end{smallmatrix}\right)$. Inverting the procedure gives the following result.

th!d-e

Theorem 3.5 (Classification Theorem I) *Each solution of (3.4–3.5) is one of the exceptional solutions* (3.10) *below, or is given by* eq!d-e

$$\begin{aligned} \begin{pmatrix} r & a\\ b & s\end{pmatrix} &= \begin{pmatrix} \delta & -1\\ 1 & 0\end{pmatrix}\begin{pmatrix} \varepsilon & -1\\ 1 & 0\end{pmatrix}\cdots\begin{pmatrix} \varepsilon \text{ or } \delta & -1\\ 1 & 0\end{pmatrix}\begin{pmatrix} 0 & 1\\ -1 & 0\end{pmatrix},\\ \begin{pmatrix} r & g\\ h & s\end{pmatrix} &= \begin{pmatrix} 0 & 1\\ -1 & 0\end{pmatrix}\begin{pmatrix} 0 & -1\\ 1 & \delta \text{ or } \varepsilon\end{pmatrix}\cdots\begin{pmatrix} 0 & -1\\ 1 & \delta\end{pmatrix}\begin{pmatrix} 0 & -1\\ 1 & \varepsilon\end{pmatrix} \end{aligned} \tag{3.8}$$

or the same with the two righthand sides interchanged. The δ, ε alternate, the two lines have the same number $k+1$ of factors (for some $k \ge 1$), and the values of δ, ε and k that are allowed are exactly the following: eq!lt6

$\delta\varepsilon$	0	1	2	3	≥ 4
k	1	≤ 2	≤ 3	≤ 5	any

(3.9)

Exceptional solutions *The cases $b = g = 0$ or $a = h = 0$, the matrixes* eq!ex

$$\begin{pmatrix} r & a \\ b & s \end{pmatrix} = \begin{pmatrix} 1 & a \\ 0 & 1 \end{pmatrix} \quad \text{and} \quad \begin{pmatrix} r & g \\ h & s \end{pmatrix} = \begin{pmatrix} 1 & 0 \\ h & 1 \end{pmatrix}, \tag{3.10}$$

for any $a, g \geq 0$, or the same with both matrixes transposed.

Remark 3.6 (1) The exceptional cases correspond to the not-very-long rectangles and not-very-surprising diptych varieties:

$$\begin{array}{cc} a & 0 \\ \hline \\ \hline 0 & -a \end{array} \qquad \begin{array}{cc} -h & 0 \\ \hline \\ \hline 0 & h \end{array} \qquad \begin{array}{l} x_0y_1 = Ax_1^a + My_0^h \\ x_1y_0 = B + L \end{array}$$

and we do not need to mention them again. They do not give rise to Mori flips because they do not admit weights with $\operatorname{wt} B = 0$ and $\operatorname{wt} L > 0$.

(2) The cases $b = h = 0$ or $a = g = 0$ are regular solutions in Theorem 3.5 with $k = 1$ and (say) $\delta = a$, $\varepsilon = g$: eq!in

$$\begin{pmatrix} 1 & a \\ 0 & 1 \end{pmatrix} = \begin{pmatrix} \delta & -1 \\ 1 & 0 \end{pmatrix} \begin{pmatrix} 0 & 1 \\ -1 & 0 \end{pmatrix}, \quad \begin{pmatrix} 1 & g \\ 0 & 1 \end{pmatrix} = \begin{pmatrix} 0 & 1 \\ -1 & 0 \end{pmatrix} \begin{pmatrix} 0 & -1 \\ 1 & \varepsilon \end{pmatrix}. \tag{3.11}$$

They provide the endpoint of our infinite descent, and correspond to case $\mathrm{I}(a, g, 1)$ in Theorem 3.9:

$$\begin{array}{cc} a & 0 \\ \hline \\ \hline 0 & -a \end{array} \qquad \begin{array}{cc} 0 & -g \\ \hline \\ \hline g & 0 \end{array} \qquad \begin{array}{l} x_0y_1 = Ax_1^a + M \\ x_1y_0 = B + Lx_0^g \end{array}$$

(3) The restriction on k when $\delta\varepsilon \leq 3$ in (3.9) arises because the product in (3.8) no longer satisfies $r, s, a, b \geq 0$ for bigger values of k. Thus

$$\begin{pmatrix} \delta & -1 \\ 1 & 0 \end{pmatrix} \begin{pmatrix} \varepsilon & -1 \\ 1 & 0 \end{pmatrix} \begin{pmatrix} 0 & 1 \\ -1 & 0 \end{pmatrix} = \begin{pmatrix} \delta & \delta\varepsilon - 1 \\ 1 & \varepsilon \end{pmatrix}$$

has top righthand entry < 0 for $\delta\varepsilon = 0$ and $k = 2$. For $\delta\varepsilon = 1, 2, 3$ and $k = 3, 4, 6$ respectively, the product of k factors is -1:

$$\begin{pmatrix} \delta & -1 \\ 1 & 0 \end{pmatrix} \begin{pmatrix} \varepsilon & -1 \\ 1 & 0 \end{pmatrix} \cdots \begin{pmatrix} \delta \text{ or } \varepsilon & -1 \\ 1 & 0 \end{pmatrix} = \begin{pmatrix} -1 & 0 \\ 0 & -1 \end{pmatrix},$$

so we are basically into elements of finite order in $\mathrm{SL}(2, \mathbb{Z})$.

Sketch proof The proof is based on a case division according to the relative sizes of $r, \dots, h$; in each case, an appropriate combination of (3.6–3.7) decreases the entries of both matrixes, down to one of the initial cases. When $\delta, \varepsilon \geq 2$ and $b > h$, (3.6) decreases all the entries of both matrixes and then the resulting factorisation is the stated one ((3.7) increases all the entries). The interchanged version occurs for $b < h$. The cases when δ or $\varepsilon = 1$ is indeterminate: either operation decreases some entries and increases others, but composing the two decreases them all.

3.3 Mori billiards and quadratic irrationalities

s!Mbill

Our analysis boils down to the 2-step recurrent continued fraction

$$x = [\,\underline{\delta, \varepsilon}\,] = [\delta, \varepsilon, \delta, \dots], \quad \text{a root of} \quad \varepsilon x^2 - \delta\varepsilon x + \delta = 0. \tag{3.12}$$

Following Mori [M3], p. 167, introduce the quadratic form

$$Q_{\delta,\varepsilon}(x, y) = \delta x^2 - \delta\varepsilon xy + \varepsilon y^2,$$

The columns of our matrix solutions to (3.4–3.5) are equipotentials for $Q_{\varepsilon,\delta} = \delta$ or ε with alternating δ, ε:

Lemma 3.7 *In the notation of Theorem 3.5*

$$\Big(Q_{\delta,\varepsilon}(r, b), Q_{\delta,\varepsilon}(s, a)\Big) = \begin{cases} (\varepsilon, \delta) & \textit{for } k \textit{ odd,} \\ (\delta, \varepsilon) & \textit{for } k \textit{ even.} \end{cases}$$

(see Figure 3.1 and Mori [M3], p. 167).

Example 3.8 For $\delta = 7$, $\varepsilon = 3$, the matrixes $\left(\begin{smallmatrix} r & a \\ b & s \end{smallmatrix}\right)$ are

$$\begin{pmatrix} 1 & 3 \\ 0 & 1 \end{pmatrix}, \quad \begin{pmatrix} 3 & 20 \\ 1 & 7 \end{pmatrix}, \quad \begin{pmatrix} 20 & 57 \\ 7 & 20 \end{pmatrix}, \quad \begin{pmatrix} 57 & 379 \\ 20 & 133 \end{pmatrix}, \quad \text{etc.,}$$

and they have

$$Q_{\delta,\varepsilon}(1, 0) = 7, \quad Q_{\delta,\varepsilon}(3, 1) = 3, \quad Q_{\delta,\varepsilon}(20, 7) = 7,$$
$$Q_{\delta,\varepsilon}(57, 20) = 3, \quad Q_{\delta,\varepsilon}(379, 133) = 7, \quad \text{etc.}$$

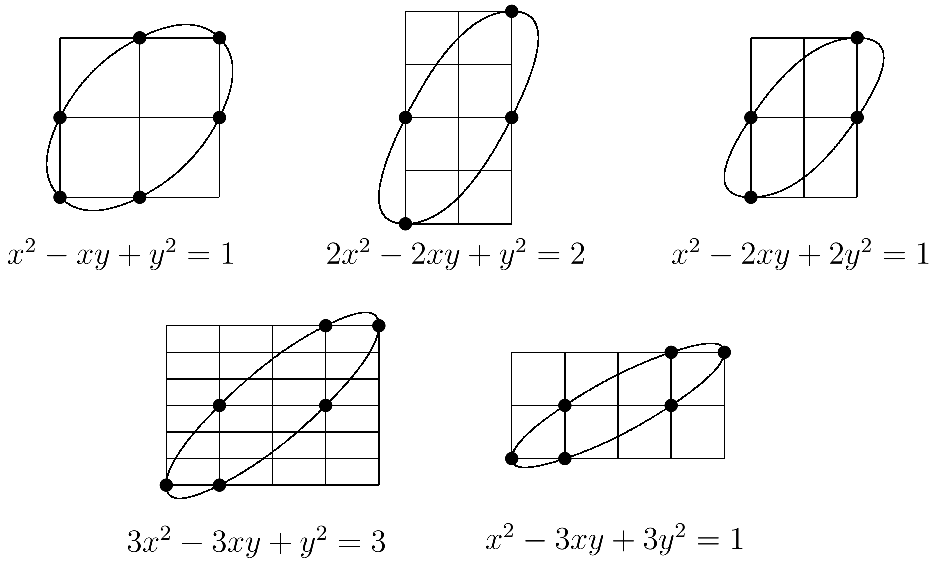

Figure 3.1: Mori billiards when $\delta\varepsilon < 4$

3.4 The four families of minimal models of pairs

s!min

Theorem 3.5 with $\delta, \varepsilon \geq 2$ gives the main family $\mathrm{I}(d, e, k)$ of long rectangles: just use the output $[\delta, \varepsilon, \delta, \dots]$ of the theorem as the lefthand tags. When δ or $\varepsilon = 1$, this is incompatible (as it stands) with the tags of Lemmas 2.5 and 2.10; in fact we worked there with minimal generators of monomial cones, and so all the tags are $a_i \geq 2$. Eliminating redundant generators corresponds to the blowdown of Proposition 2.1.b. Successively striking out 1s and decrementing adjacent tags by 1 gives the following result.

th!cl

Theorem 3.9 (Classification Theorem II) *Up to reflection symmetries, any pair of long rectangles is one of the following:*

Name	*parameters*	*case of Theorem 3.5*
$\mathrm{I}(d, e, k)$	$d, e \geq 2,\ k \geq 1$	$d = \delta,\ e = \varepsilon$
$\mathrm{II}(e, h)$	$e \geq 3,\ h \geq 0$	$\delta = 1,\ e = \varepsilon,\ k = 2h + 2$ *even*
$\mathrm{III}(d, h)$	$d \geq 3,\ h \geq 0$	$d = \delta,\ \varepsilon = 1,\ k = 2h + 2$ *even*
$\mathrm{IV}(d, h)$	$d \geq 3,\ h \geq 0$	$d = \delta,\ \varepsilon = 1,\ k = 2h + 1$ *odd*

where the families I–IV *are described below.*

Here "up to reflection symmetries" means interchanging x_i and y_j if necessary, and swapping the two rectangles with a top-to-bottom inversion.

Swapping the two rectangles with a top-to-bottom inversion take one solution to another. It takes families I, II and III to themselves. Its purpose in the statement is to put $\delta = 1$, $\varepsilon \geq 3$ and k odd into Family IV.

For example, if we start from a chain $1, e, 1, e, \dots, 1, e$ in Theorem 3.5 of even length $k = 2h + 2$ with $e \geq 4$, then contracting out all the intermediate 1s gives the tags $1, e-1, e-2, \dots, e-2, e-1$ of family $\mathrm{II}(e, h)$.

In the detailed list below we omit the corner annotations A, B at the top of the lefthand rectangle, and L, M at the bottom of the righthand one. The shorthand 2^x denotes a column of 2s repeated x times. We usually write the torso on the lefthand rectangle only, taken it as read on the righthand one.

Family $\mathrm{I}(d, e, k)$ **for** $d, e \geq 2$**,** $k \geq 1$

We treat separately the case $\mathrm{I}(d, e, 1)$, which has empty torso:

$$\begin{array}{cc} d & 0 \\ \hline \emptyset & \\ \hline 0 & -d \end{array} \qquad \begin{array}{cc} 0 & -e \\ \hline & \\ \hline e & 0 \end{array} \tag{3.13}$$

Case $d, e \geq 3,\ k \geq 2$ There are $k-2$ alternating brackets; at the bottom left, the tags are $a = e$, $b = d$ if k is odd, or $a = d$, $b = e$ if k is even.

$$\begin{array}{cc}
d & 1 \\ \hline
 & 2 \\
 & 2^{d-3} \\
\left\{\begin{array}{c} e \\ \end{array}\right. & \left.\begin{array}{c} 3 \\ 2^{e-3} \end{array}\right\} \\
\left\{\begin{array}{c} d \\ \end{array}\right. & \left.\begin{array}{c} 3 \\ 2^{d-3} \end{array}\right\} \\
\vdots & \vdots \\
\left\{\begin{array}{c} a \\ \end{array}\right. & \left.\begin{array}{c} 3 \\ 2^{a-3} \end{array}\right\} \\
b & 2 \\ \hline
0 & -(b-1)
\end{array}
\qquad
\begin{array}{cc}
0 & -(e-1) \\ \hline
 & \\ \hline
a & 1
\end{array}$$

When $k = 2$ the torso has 2^{d-1} on the right (as in (2.21)).

CASE $d \geq 3, e = 2$ The expression $3, 2^{e-3}, 3$ for the righthand tags does not make sense. Instead each occurrence is replaced with 4. At the bottom there is a slightly different outcome for k even or odd:

$$\begin{array}{cc} d & 1 \\ \hline & 2^{d-2} \\ \{\,2 & 4\,\} \\ \{\,d & 2^{d-3}\,\} \\ \vdots & \vdots \\ 2 & 2 \\ \hline 0 & -1 \end{array} \qquad \begin{array}{cc} 0 & -1 \\ \hline \\ \\ \\ \\ \\ \hline d & 1 \end{array} \qquad \text{or} \qquad \begin{array}{cc} d & 1 \\ \hline & 2^{d-2} \\ \{\,2 & 4\,\} \\ \{\,d & 4\,\} \\ \vdots & \vdots \\ 2 & 3 \\ d & \\ \hline 0 & -(d-1) \end{array} \qquad \begin{array}{cc} 0 & -1 \\ \hline \\ \\ \\ \\ \\ \\ \hline 2 & 1 \end{array}$$

CASE $d = 2, e \geq 3$ In the same way, replace each fragment $3, 2^{d-3}, 3$ with 4.

CASE $d = e = 2,\ k \geq 2$

$$\begin{array}{cc} 2 & 1 \\ \hline 2^{k-1} & k+1 \\ \hline 0 & -1 \end{array} \qquad \begin{array}{cc} 0 & -1 \\ \hline \\ \hline 2 & 1 \end{array}$$

Family $\mathrm{II}(e,h)$ **for** $e \geq 3,\ h \geq 0$

The case $\mathrm{II}(e,0)$ is the same as $\mathrm{I}(1,e,2)$ with $d = 1$:

$$\begin{array}{cc} 1 & 1 \\ \hline e & \\ \hline 0 & -(e-1) \end{array} \qquad \begin{array}{cc} 0 & -(e-1) \\ \hline \\ \hline 1 & 1 \end{array}$$

Case $e \geq 5,\ h \geq 1$ There are $h-1$ repeating brackets.

$$
\begin{array}{cc}
1 & 2 \\
\hline
e-1 & 2 \\
 & 2^{e-5} \\
\left\{ \begin{array}{c} e-2 \\ \\ \end{array} \right. & \left. \begin{array}{c} 3 \\ 2^{e-5} \end{array} \right\} \\
\vdots & \vdots \\
\left\{ \begin{array}{c} e-2 \\ \\ \end{array} \right. & \left. \begin{array}{c} 3 \\ 2^{e-5} \end{array} \right\} \\
e-1 & 2 \\
\hline
0 & -(e-2)
\end{array}
\qquad\qquad
\begin{array}{cc}
0 & -(e-2) \\
\hline
 & \\
 & \\
 & \\
\hline
1 & 2
\end{array}
$$

Case $e = 4$

$$
\begin{array}{cc}
1 & 2 \\
\hline
3 & \\
2^{h-1} & h+1 \\
3 & \\
\hline
0 & -2
\end{array}
\qquad\qquad
\begin{array}{cc}
0 & -2 \\
\hline
 & \\
 & \\
\hline
1 & 2
\end{array}
$$

Family III(d, h) **for** $d \geq 3$**,** $h \geq 0$

Case $d \geq 5$ There are h repeating brackets. When $h = 0$ the left torso is empty, the right is 2^{d-1}.

$$
\begin{array}{cc}
d-1 & 1 \\
\hline
 & 2^2 \\
 & 2^{d-5} \\
\left\{ \begin{array}{c} d-2 \\ \\ \end{array} \right. & \left. \begin{array}{c} 3 \\ 2^{d-5} \end{array} \right\} \\
\vdots & \vdots \\
\left\{ \begin{array}{c} d-2 \\ \\ \end{array} \right. & \left. \begin{array}{c} 3 \\ 2^{d-5} \end{array} \right\} \\
 & 2^2 \\
\hline
-1 & 0
\end{array}
\qquad\qquad
\begin{array}{cc}
-1 & 0 \\
\hline
 & \\
 & \\
 & \\
\hline
d-1 & 1
\end{array}
$$

Case $d = 4$

$$
\begin{array}{cc}
3 & 1 \\ \hline
 & 2 \\
2^h & h+2 \\
 & 2 \\ \hline
-1 & 0
\end{array}
\qquad
\begin{array}{cc}
-1 & 0 \\ \hline
 & \\
 & \\
 & \\ \hline
3 & 1
\end{array}
$$

Case $d = 3$ Now h only takes the values $h = 0$ and 1, giving

$$
\begin{array}{cc}
2 & 1 \\ \hline
 & 3 \\ \hline
-1 & 0
\end{array}
\qquad
\begin{array}{cc}
-1 & 0 \\ \hline
 & \\ \hline
2 & 1
\end{array}
\qquad \text{and} \qquad
\begin{array}{cc}
2 & 1 \\ \hline
 & 2 \\
 & 2 \\ \hline
-1 & 0
\end{array}
\qquad
\begin{array}{cc}
-1 & 0 \\ \hline
 & \\
 & \\ \hline
2 & 1
\end{array}
$$

Family $\mathrm{IV}(d,h)$ **for** $d \geq 3$, $h \geq 0$

Case $d \geq 5$ The case $h = 0$ is the same as $\mathrm{I}(d,e,1)$ (the case (3.13) with empty torso) specialised to $e = 1$.

There are $h - 1$ repeating brackets. When $h = 1$ the torso consists of a single $d - 1$ against 2^{d-2}.

$$
\begin{array}{cc}
d-1 & 1 \\ \hline
 & 2^2 \\
 & 2^{d-5} \\
\left\{ \begin{array}{c} d-2 \\ \\ \end{array} \right. & \left. \begin{array}{c} 3 \\ 2^{d-5} \end{array} \right\} \\
\vdots & \vdots \\
\left\{ \begin{array}{c} d-2 \\ \\ \end{array} \right. & \left. \begin{array}{c} 3 \\ 2^{d-5} \end{array} \right\} \\
d-1 & 2 \\ \hline
0 & -(d-2)
\end{array}
\qquad
\begin{array}{cc}
-1 & 0 \\ \hline
 & \\ \hline
1 & 2
\end{array}
$$

Case $d = 4$

$$
\begin{array}{cc}
3 & 1 \\ \hline
2^{h-1} & 2 \\
3 & h+1 \\ \hline
0 & -2
\end{array}
\qquad
\begin{array}{cc}
-1 & 0 \\ \hline
 & \\
 & \\ \hline
1 & 2
\end{array}
$$

Case $d = 3$ In this case h is no longer a parameter.

2	1	−1	0
2	2		
0	−1	1	2

4 Combining monomial cones σ_{AB} and σ_{LM}

ch!pp

4.1 The pretty polytope $\Pi(d, e, k)$

s!pp

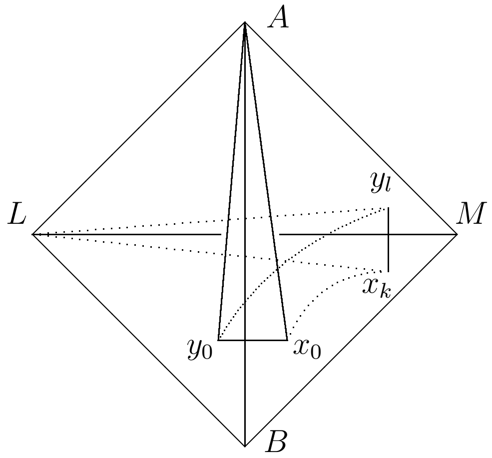

Figure 4.1: Pretty polytope Π: Starting from simplex $ABLM$, pull out x_0 on plane ABL, etc., with crosspiece x_0y_0 on the edge AB in ratio $1 : d$, and x_ky_l on the edge LM in ratio $1 : e$. Π has 8 vertices and 12 triangular faces; A, B, L, M have valency 5, and x_0, y_0, x_k, y_l valency 4.

f!pp

All our varieties $T, V_{AB}, V_{LM}, V_{ABLM}$ are equivariant under the same torus $\mathbb{T} = \mathbb{G}_m^4$; write $\mathbb{M} = \mathrm{Hom}(\mathbb{T}, \mathbb{G}_m)$ for its character lattice, identified with the monomial lattice of both V_{AB} and V_{LM}. The coordinate ring of V_{ABLM} constructed in Chapter 5 is $\mathbb{M}$-graded (that is, $\mathbb{T}$-equivariant). Write $f \overset{\mathbb{T}}{\sim} g$ to mean that f and g are eigenfunctions with the same $\mathbb{T}$-weight or eigenvalue in $\mathbb{M}$. This chapter mostly treats the $\mathbb{T}$-weights of monomials; we mix additive and multiplicative notation, and sometimes write $=$ for $f \overset{\mathbb{T}}{\sim} g$, so that, for example, the first equation of (4.1) means $x_0 \overset{\mathbb{T}}{\sim} L^{-1/d}A^\gamma B^\delta$.

The *pretty polytope* Π of Figure 4.1 combines the two polytopes σ_{AB} of Section 2.3 and σ_{LM} of Section 3.1. While V_{AB} and V_{LM} each provided many possible $\mathbb{Z}$-bases of $\mathbb{M}$, we use instead the *impartial* $\mathbb{Q}$-basis L, M, A, B, writing out the $\mathbb{T}$-weights of $x_{0\dots k}, y_{0\dots l}$ as follows: eq!-1/d

$$x_0 = (-\tfrac{1}{d}, 0, \gamma, \delta) \quad \text{and} \quad x_1 = (0, \tfrac{1}{e}, \alpha, \beta), \tag{4.1}$$

where eq!maca

$$\begin{pmatrix}\alpha & \beta\\ \gamma & \delta\end{pmatrix} = \begin{cases} \begin{pmatrix}0 & 1\\ -1 & e\end{pmatrix}\cdots\begin{pmatrix}0 & 1\\ -1 & e\end{pmatrix}\begin{pmatrix}-\frac{1}{d} & 0\\ 0 & \frac{1}{e}\end{pmatrix} & \text{if } k \text{ is even}\\ \begin{pmatrix}0 & 1\\ -1 & e\end{pmatrix}\cdots\begin{pmatrix}0 & 1\\ -1 & d\end{pmatrix}\begin{pmatrix}-\frac{1}{e} & 0\\ 0 & \frac{1}{d}\end{pmatrix} & \text{if } k \text{ is odd}\end{cases} \tag{4.2}$$

(k factors in each product). Compared to (3.8), we simply remove the first and last tags (d at x_k and 0 at x_0), and put in denominators d, e corresponding to the index of the sublattice $\mathbb{M}' = \mathbb{Z}\cdot(L, M, A, B) \subset \mathbb{M}$ (see Corollary 4.7).

The impartial basis gives $\mathbb{M}$ two projections eq!pi

$$\pi_{AB}\colon \mathbb{M} \to \mathbb{Q}^2 \quad \text{and} \quad \pi_{LM}\colon \mathbb{M} \to \mathbb{Q}^2 \tag{4.3}$$

that track the exponents of A, B and of L, M. The image group $\mathbb{Q}^2$ is ordered, and we write $\pi_{LM}(m) \le 0$ to mean that $m \in \mathbb{M}$ has nonpositive L, M exponents, etc.

p!xys

Proposition 4.1 *In the impartial basis L, M, A, B, the monomials $x_0, \dots, y_l$ have $\mathbb{T}$-weights of the form (for even k):*

$$\begin{array}{llll} x_0 = (\ -\frac{1}{d} & 0 & \gamma & \delta\ ) \\ x_1 = (\ 0 & \frac{1}{e} & \alpha & \beta\ ) \\ x_2 = (\ \frac{1}{d} & 1 & \cdot & \cdot\ ) \\ x_3 = (\ 1 & d-\frac{1}{e} & \cdot & \cdot\ ) \end{array} \qquad \begin{array}{l} \cdots \\ x_{k-2} = (\ \cdot \quad \cdot \quad \frac{1}{d} \quad 1\ ) \\ x_{k-1} = (\ \alpha \quad \beta \quad 0 \quad \frac{1}{e}\ ) \\ x_k = (\ \gamma \quad \delta \quad -\frac{1}{d} \quad 0\ ) \end{array} \tag{4.4}$$

and

$$\begin{array}{lcl} y_0 & = & (\ 0 \quad -\frac{1}{e} \quad d\gamma-\alpha \quad d\delta-\beta\ ) \\ y_1 & = & (\ \frac{1}{d} \quad 1-\frac{1}{e} \quad \cdot \quad \cdot\ ) \\ & \cdots & \\ y_{j+1} & = & b_j y_j - y_{j-1} \\ & \cdots & \\ y_{l-1} & = & (\ \cdot \quad \cdot \quad \frac{1}{d} \quad 1-\frac{1}{e}\ ) \\ y_l & = & (\ d\gamma-\alpha \quad d\delta-\beta \quad 0 \quad -\frac{1}{e}\ ) \end{array} \tag{4.5}$$

where the b_j in (4.5) are the tags at y_j (usually 2 or 3).

When k is odd, the top-to-bottom symmetry swaps d and e. At the top, we don't change anything (recall that we define $\alpha, \beta, \gamma, \delta$ in x_1, x_0 by the other choice in (4.2)); at the bottom we do $d \leftrightarrow e$ and modify $\alpha, \beta, \gamma, \delta$ accordingly, giving $x_k = (\gamma', \delta', -\frac{1}{e}, 0)$ and $y_l = (e\gamma' - \alpha', e\delta' - \beta', 0, -\frac{1}{d})$.

Proof The matrix product in (4.2) ensures that the $k-1$ changes of basis of the form $x_2 = x_1^e x_0^{-1}$, etc., take the last two entries $\left(\begin{smallmatrix}\alpha & \beta \\ \gamma & \delta\end{smallmatrix}\right)$ of x_1, x_0 into the last two entries $\left(\begin{smallmatrix}-1/d & 0 \\ 0 & 1/e\end{smallmatrix}\right)$ of x_k, x_{k-1}. The first two columns then just record known data from V_{LM}, and the last two from V_{AB}. Q.E.D.

c!ming

Corollary 4.2 *(i) Except for the explicit* $-\frac{1}{d}$ *and* $-\frac{1}{e}$ *in* x_0, x_k, y_0, y_l *at the four corners, all the entries are* ≥ 0.

(ii) (From here on, we assume $d, e \geq 2$*; the other cases are treated elsewhere.) The* L *and* M *exponents* $\pi_{LM}(x_i)$ *and* $\pi_{LM}(y_j)$ *increase monotonically with* i *and* j *(in fact, increase* exponentially *if* $de > 4$*, as illustrated in Figure 4.2), while* $\pi_{AB}(x_i)$ *and* $\pi_{AB}(y_j)$ *decrease.*

(iii) None of $x_{0\dots k}$ *or* $y_{0\dots l}$ *is* $\mathbb{T}$*-equivalent to a monomial in the other variables (all the* x_i*,* y_j*,* A, B, L, M*).*

For (iii), notice that the x_i, y_j, A and B are minimal generators of the coordinate ring of V_{AB} by the results of Section 2.3. So it is impossible to write even the first two entries of x_i or y_j as a positive integral combination of the other variables.

x!k=2

Example 4.3 (Case $k = 2$) Then

$$\begin{pmatrix}\alpha & \beta \\ \gamma & \delta\end{pmatrix} = \begin{pmatrix}0 & 1 \\ -1 & e\end{pmatrix}\begin{pmatrix}-\frac{1}{d} & 0 \\ 0 & \frac{1}{e}\end{pmatrix} = \begin{pmatrix}0 & \frac{1}{e} \\ \frac{1}{d} & 1\end{pmatrix}$$

The variables $x_{0\dots 2}, y_{0\dots d}$ are

$$\begin{aligned} x_0 &= (-\tfrac{1}{d}, 0, \tfrac{1}{d}, 1) \\ x_1 &= (0, \tfrac{1}{e}, 0, \tfrac{1}{e}) \\ x_2 &= (\tfrac{1}{d}, 1, -\tfrac{1}{d}, 0) \end{aligned} \qquad \begin{aligned} y_0 &= (0, -\tfrac{1}{e}, 1, d-\tfrac{1}{e}) \\ y_i &= (\tfrac{i}{d}, i-\tfrac{1}{e}, 1-\tfrac{i}{d}, d-i-\tfrac{1}{e}) \\ &\quad \text{for } i = 0, \dots, d \\ y_d &= (1, d-\tfrac{1}{e}, 0, -\tfrac{1}{e}) \end{aligned}$$

Check top-to-bottom symmetry. Check the two tag equations at x_0:

$$dx_0 + (1,0,0,0) = x_1 + y_0; \text{ and } 0x_0 + (0,0,1,d) = (0,0,1,d)$$

corresponding to the corner tag equations $x_1 y_0 = x_0^d L$ in V_{LM} and $x_1 y_0 = AB^d$ in V_{AB}. Check the tag equations at y_0: $1y_0 + (0,1,0,0) = x_0 + y_1$, and

$$(e-1)x_1 + (0,0,1,d-1) = (0, 1-\tfrac{1}{e}, 1, d-\tfrac{1}{e})$$

corresponding to $x_0 y_1 = y_0 M$ in V_{LM} and $x_0 y_1 = x_1^{e-1} AB^{d-1}$ in V_{AB}.

Example 4.4 (Case $k = 3$) Then x!k=3

$$\begin{pmatrix} \alpha & \beta \\ \gamma & \delta \end{pmatrix} = \begin{pmatrix} 0 & 1 \\ -1 & e \end{pmatrix} \begin{pmatrix} 0 & 1 \\ -1 & d \end{pmatrix} \begin{pmatrix} -\frac{1}{e} & 0 \\ 0 & \frac{1}{d} \end{pmatrix} = \begin{pmatrix} \frac{1}{e} & 1 \\ 1 & e - \frac{1}{d} \end{pmatrix}$$

So $x_{0\ldots3}, y_{0\ldots d+e-2}$ are

$$\begin{aligned} x_0 &= (-\tfrac{1}{d}, 0, 1, e - \tfrac{1}{d}) \\ x_1 &= (0, \tfrac{1}{e}, \tfrac{1}{e}, 1) \\ x_2 &= (\tfrac{1}{d}, 1, 0, \tfrac{1}{d}) \\ x_3 &= (1, d - \tfrac{1}{e}, -\tfrac{1}{e}, 0) \end{aligned}$$

$$\begin{aligned} y_0 &= (0, -\tfrac{1}{e}, d - \tfrac{1}{e}, de - 2) \\ y_1 &= (\tfrac{1}{d}, 1 - \tfrac{1}{e}, d - 1 - \tfrac{1}{e}, (d-1)e - 2 + \tfrac{1}{d}) \\ &\ldots \\ y_i &= (\tfrac{i}{d}, i - \tfrac{1}{e}, d - i - \tfrac{1}{e}, (d-i)e - 2 + \tfrac{i}{d}) \\ &\text{for } i = 0, \ldots, d-1 \\ y_{d-2} &= (1 - \tfrac{2}{d}, d - 2 - \tfrac{1}{e}, 2 - \tfrac{1}{e}, 2e - 1 - \tfrac{2}{d}) \end{aligned}$$

$$\begin{aligned} y_{d-1} &= (1 - \tfrac{1}{d}, d - 1 - \tfrac{1}{e}, 1 - \tfrac{1}{e}, e - 1 - \tfrac{1}{d}) \\ y_d &= (2 - \tfrac{1}{d}, 2d - 1 - \tfrac{2}{e}, 1 - \tfrac{2}{e}, e - 2 - \tfrac{1}{d}) \\ &\ldots \\ y_{d-2+i} &= (i - \tfrac{1}{d}, id - 1 - \tfrac{i}{e}, 1 - \tfrac{i}{e}, e - i - \tfrac{1}{d}) \\ &\text{for } i = 1, \ldots, e \\ y_{d+e-3} &= (e - 1 - \tfrac{1}{d}, d(e-1) - 2 + \tfrac{1}{e}, \tfrac{1}{e}, 1 - \tfrac{1}{d}) \\ y_{d+e-2} &= (e - \tfrac{1}{d}, de - 2, 0, -\tfrac{1}{d}) \end{aligned}$$

Same checks; note especially the effect of the tag 3 at y_{d-1}.

x!46

Example 4.5 (Case $d = 4$, $e = 6$, $k = 6$)

$$\begin{array}{llcclllll} & & & & L & M & A & B & \\ & x_0 & = & (& -1/4 & 0 & 505/4 & 483 &) \\ 6 & x_1 & = & (& 0 & 1/6 & 22 & 505/6 &) \\ 4 & x_2 & = & (& 1/4 & 1 & 23/4 & 22 &) \\ 6 & x_3 & = & (& 1 & 23/6 & 1 & 23/6 &) \\ 4 & x_4 & = & (& 23/4 & 22 & 1/4 & 1 &) \\ 6 & x_5 & = & (& 22 & 505/6 & 0 & 1/6 &) \\ & x_6 & = & (& 505/4 & 483 & -1/4 & 0 &) \end{array} \qquad (4.6)$$

and eq!bigm

$$
\begin{array}{ccccccccc}
 & & & & L & M & A & B & \\
 & y_0 & = & (& 0 & -1/6 & 483 & 11087/6 &) \\
2 & y_1 & = & (& 1/4 & 5/6 & 1427/4 & 8189/6 &) \\
2 & y_2 & = & (& 1/2 & 11/6 & 461/2 & 5291/6 &) \\
3 & y_3 & = & (& 3/4 & 17/6 & 417/4 & 2393/6 &) \\
2 & y_4 & = & (& 7/4 & 20/3 & 329/4 & 944/3 &) \\
2 & y_5 & = & (& 11/4 & 21/2 & 241/4 & 461/2 &) \\
2 & y_6 & = & (& 15/4 & 43/3 & 153/4 & 439/3 &) \\
3 & y_7 & = & (& 19/4 & 109/6 & 65/4 & 373/6 &) \\
2 & y_8 & = & (& 21/2 & 241/6 & 21/2 & 241/6 &) \\
3 & y_9 & = & (& 65/4 & 373/6 & 19/4 & 109/6 &) \\
2 & y_{10} & = & (& 153/4 & 439/3 & 15/4 & 43/3 &) \\
2 & y_{11} & = & (& 241/4 & 461/2 & 11/4 & 21/2 &) \\
2 & y_{12} & = & (& 329/4 & 944/3 & 7/4 & 20/3 &) \\
3 & y_{13} & = & (& 417/4 & 2393/6 & 3/4 & 17/6 &) \\
2 & y_{14} & = & (& 461/2 & 5291/6 & 1/2 & 11/6 &) \\
2 & y_{15} & = & (& 1427/4 & 8189/6 & 1/4 & 5/6 &) \\
 & y_{16} & = & (& 483 & 11087/6 & 0 & -1/6 &)
\end{array}
\qquad (4.7)
$$

We read this table in several ways. Omitting the A and B columns describes σ_{LM} in the impartial basis. Notice the tag equations

bottom: $x_1y_0 = x_0^4L$ and $x_0y_1 = y_0M$;
sides: $x_0x_2 = x_1^6$, $x_1x_3 = x_2^4$ and so on;
top: $x_5y_{16} = L^{505}M^{1932}$ and $x_6y_{15} = x_5^5L^{373}M^{1427}$.

f!sciss

Figure 4.2 plots the first two columns of (4.7) as "scissors" controlled by the points $x_0 = (-\frac{1}{d}, 0)$ and $y_0 = (0, -\frac{1}{e})$ and the origin $(0,0)$ (implicit but crucial). To describe it in words, the sequence of y_i starts from y_0 and tries to grow along the line Λ of slope $1/[4,6,4,6,\dots] \doteq 0.261387212$, without crossing it. It first tries x_0 (slope $-\infty$), then x_1 (slope 0) and x_2 (slope 1/4, so under Λ), then takes one step back to $y_1 = x_2y_0$ (slope 3/10, so above Λ). Now y_0, y_1, y_2, y_3, x_3 is an arithmetic progression of length $5 = d+1$ with increment x_2 (and $y_{i+1} = y_ix_2$, so $0y_0y_1x_2$, $0y_1y_2x_2$, etc., are parallelograms); but x_3 (slope 6/23) is below L; so take one step back to y_3 and construct the next arithmetic progression $y_3, y_4, y_5, y_6, y_7, x_4$ of length $6 = e$ with increment x_3, and so on. Compare Figure 2.2, where the scissors were more open.

r!sciss

Remark 4.6 The abstract continued fraction $[e, d, \dots,]$ and its complement $[2, 2, \dots, 3, \dots,]$ has two different "scissors" embeddings into the L, M-plane

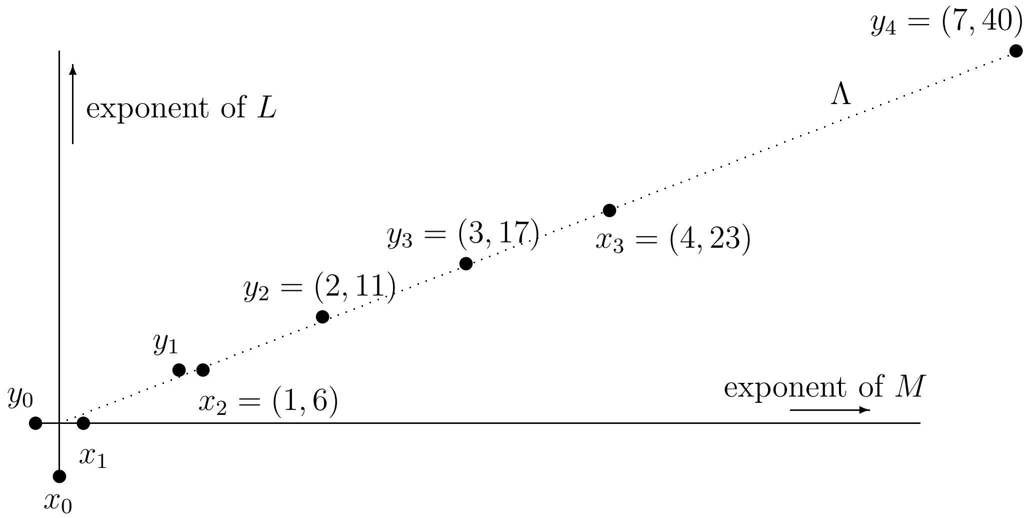

Figure 4.2: Scissors (compare the dots of Figure 2.2.b). The exponents of L are in units of 1/4 and those of M in units of 1/6. The initial points are $x_0 = (-1, 0)$, $y_0 = (0, -1)$, $x_1 = (0, 1)$, $y_1 = (1, 5)$.

(as the dots of Figures 2.2 and 4.2) and into the A, B-planes, and the pretty polytope $\Pi(d, e, k)$ is just the diagonal embedding into the product.

We don't see this clearly at present, but there must be a sense in which Figure 4.2 puts together Mori billiards 3.3 with the Riemenschneider staircase of [R], §3, pp. 220–3. It's still an exercise to turn this from a philosophical slogan into technically true propositions.

4.2 The quotient Q and the padded cell

s!pad

The exponents of $x_{0\dots k}, y_{0\dots l}$ in Proposition 4.1 also behave in a characteristic way modulo the integers (see Figure 4.3). To understand this, we write $\mathbb{M}' = \mathbb{Z} \cdot (L, M, A, B) \subset \mathbb{M}$ for the sublattice generated by A, B, L, M, and $Q = \mathbb{M}/\mathbb{M}'$ for the quotient. We think of Q pictorially as a fundamental domain in $\mathbb{M}$ for the translation lattice $\mathbb{M}'$, as in Figure 4.3.

c!Q

Corollary 4.7 *(iv)* $\mathbb{Q} \cong \mathbb{Z}/d \oplus \mathbb{Z}/e$*, based by:*

if $k = 2\kappa$ *is even:*

$$x_0 \equiv (-\tfrac{1}{d}, 0, \mp\tfrac{1}{d}, 0); \quad \textit{and} \quad y_0 \equiv (0, -\tfrac{1}{e}, 0, \pm\tfrac{1}{e}); \qquad (4.8)$$

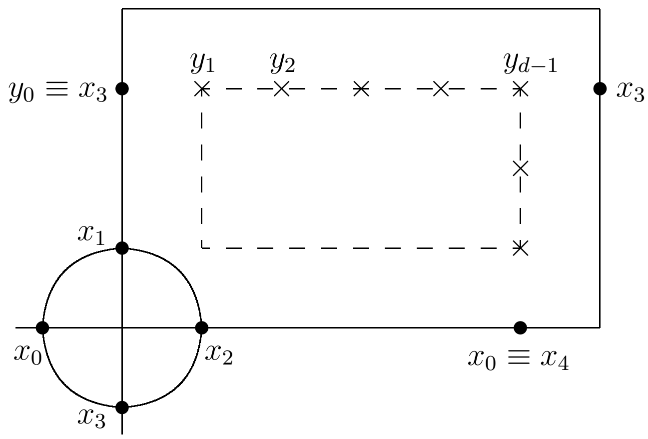

Figure 4.3: The padded cell (with sides identified): the values of x_i and y_j in the torus $Q = \mathbb{M}/\mathbb{M}'$. The x_i cycle around the 4 points $(\pm\frac{1}{d}, 0)$ and $(0, \pm\frac{1}{e})$ closest to the origin, while the y_i walk around the path of Figure 4.3, performing $k-1$ quarter-circuits around the padding of the cell, starting from $x_3 \equiv y_0$. Each quarter-circuit takes place in steps of x_i and has endpoint x_{i+1}.

if $k = 2\kappa + 1$ is odd:

$$x_0 \equiv (-\tfrac{1}{d}, 0, 0, \pm\tfrac{1}{d}) \quad \textit{and} \quad y_0 \equiv (0, -\tfrac{1}{e}, \pm\tfrac{1}{e}, 0), \tag{4.9}$$

where in either case $\pm = (-1)^\kappa$.

(v) *The classes in Q of monomials $x_0, \dots, y_l$ are given as follows (for even k):*

$$\begin{aligned} x_1 \equiv -y_0 \equiv (0, \tfrac{1}{e}, 0, \mp\tfrac{1}{e}), \quad x_i \equiv -x_{i-2} \quad \textit{for } i \geq 2 \\ \textit{and} \quad y_{j+1} = y_j + x_{i(j)} \end{aligned} \tag{4.10}$$

for j in the appropriate interval. In particular, in Q, the x_i are periodic with period 4, with $x_3 \equiv y_0$.

Note that in Q, the different corner tags on the two long rectangles say the same thing; thus

$$\begin{aligned} x_1 y_0 = x_1^0 A^\alpha B^\beta = x_0^d L \quad \text{both give} \quad x_1 \equiv y_0^{-1} \in Q \\ x_0 y_1 = y_0^{-(e-1)} A^\gamma B^\delta = y_0 M \quad \text{both give} \quad y_0 \equiv x_0 y_1 \in Q \end{aligned}$$

because $x_0^d, y_0^e \in \mathbb{M}$.

5 Proof of Main Theorem 1.2.3

ch!pf

Structure of the proof

The proof of Main Theorem 1.2.3 builds a staircase: first, we drop a chain of projections down from the top of V_{AB}, using Corollary 2.9 and the blowdowns of Proposition 2.1.d to eliminate the generator $x_{2\dots k}$ and $y_{2\dots l}$ one at a time. This chain will serve as a guiding rail in the main construction; it records the order of variables and the current state of the tags and annotations as we eliminate them (Proposition 5.2): as each $s_\nu = x_{i+1}$ or y_{j+1} is eliminated from $V_{AB,\nu+1}$, it has tag 1, and appears in an equation $s_\nu h_\nu = x_i y_j$ with its neighbours, where $h_\nu = h_\nu(A,B)$ is the monomial in A, B defined in 5.1.3.

We then build the 6-fold V_{ABLM} up from the bottom, holding tight to our guiding rail, the chain of projections of V_{AB}. Each step $V_{\nu+1} \to V_\nu$ of the induction is a Kustin–Miller unprojection (see [PR]), and adjoins an unprojection variable $s_\nu = x_{i+1}$ or y_{j+1}. The current V_ν is contained in the ambient space $\mathbb{A}_\nu = \mathbb{A}^{i+j+6}_{\langle x_{0\dots i}, y_{0\dots j}, A, B, L, M\rangle}$. The main point is to set up the unprojection divisor $D_\nu \subset V_\nu$; we *define* it by the ideal

$$I_{D_\nu} = (x_{0\dots i-1}, y_{0\dots j-1}, h_\nu), \qquad (5.1)$$

with $h_\nu(A,B)$ as in 5.1.3, so that D_ν is the hypersurface eq!Dnu

$$D_\nu : (h_\nu(A,B) = 0) \subset \mathbb{A}^6_{\langle x_i, y_j, A, B, L, M\rangle}. \qquad (5.2)$$

Thus D_ν is by definition the product of affine 4-space $\mathbb{A}^4_{\langle x_i, y_j, L, M\rangle}$ with the monomial curve $h_\nu(A,B) = 0$; the elements L, M form a regular sequence for D_ν, and the section $L = M = 0$ in D_ν is the unprojection divisor for $V_{AB,\nu+1} \to V_{AB,\nu}$. The remaining issue is to prove that $D_\nu \subset V_\nu$, or equivalently, that eq!DV

$$I_{V_\nu} \subset I_{D_\nu} = \big(x_{0\dots i-1}, y_{0\dots j-1}, h_\nu\big). \qquad (5.3)$$

For this, rather than working with the actual equations of V_ν (that we cannot always calculate in closed form, and include complicated terms), we prove the stronger result: *any monomial in $x_{0\dots i}, y_{0\dots j}, A, B, L, M$ with the same $\mathbb{T}$-weight as a generator of I_{V_ν} is in $I_{D_\nu} = (x_{0\dots i-1}, y_{0\dots j-1}, h_\nu)$.*[8] Thus, every $\mathbb{T}$-homogeneous generator of I_{V_ν} is a sum of monomials in I_{D_ν}.

[8] Is this correct? In addition, we prove that in appropriate cases (with luck all the Pfaffian equations in pentagrams) the 3 monomials known to occur in the Pfaffian are the only possible monomials in that degree. Say here that the italicised claim is only true in the main case $d, e \geq 2$, $de > 4$, other cases treated elsewhere.

It turns out in the end, much to our regret, that our proof does not involve any explicit pentagrams or Pfaffians; however, they are close at hand if we ever felt the compulsion to use them.

5.1 The projection sequence of V_{AB}

s!pseq

This section and the next lay the groundwork for the proof of the Main Theorem 1.2.3 by setting out facts and notation for the chains of birational projections down from V_{AB} and up from V_{LM}. Either chain is provided by the blowdown of Proposition 2.1.d applied to the conclusion $[a_2,\dots,b_1]=0$ of Corollary 2.9.

ex!decon

Example 5.1 Consider the long rectangle of Figure 1.2. The concatenated continued fraction $[4,2,1,3,2,2]=0$ is deconstructed as

$$[4,\underline{2,1,3},2,2]\mapsto[\underline{4,1,2},2,2]\mapsto[\underline{3,1,2},2]\mapsto[\underline{2,1,2}]\mapsto[1,1]=0$$

This is a recipe for a chain of birational projections, each eliminating a monomial from σ_{AB} with tag 1:

$$\begin{array}{lll} & & {}_1\,B \\ A & 2 & 3 \\ & 4 & 2 \\ & 2 & 2 \\ & 0 & -1 \end{array} \mapsto \begin{array}{lll} AB & 1 & {}_2\,B \\ & 4 & 2 \\ & 2 & 2 \\ & 0 & -1 \end{array} \mapsto \begin{array}{lll} & & {}_1\,AB^2 \\ AB & 3 & 2 \\ & 2 & 2 \\ & 0 & -1 \end{array} \mapsto$$

$$\begin{array}{lll} A^2B^3 & 2 & {}_1\,AB^2 \\ & 2 & 2 \\ & 0 & -1 \end{array} \mapsto \begin{array}{lll} A^3B^5 & 1 & \\ & 2 & {}_1\,AB^2 \\ & 0 & -1 \end{array} \mapsto \begin{array}{lll} A^3B^5 & 1 & {}_0\,A^4B^7 \\ & 0 & -1 \end{array}$$

For example, on the second line, we read $x_1y_2=x_2^2A^2B^3$ and $x_2y_1=y_2AB^2$ from the tags and annotation of the first rectangle, that we can check against (1.6). Each rectangle is the monomial cone $\sigma_{AB,\nu}$ of a Gorenstein affine toric variety $V_{AB,\nu}$ with the given monomials in A,B as annotations, and each step $V_{AB,\nu+1}\to V_{AB,\nu}$ is a birational projection.

5.1.1 Order of monomials

ss!order

Our construction inverts this type of chain, up from a codimension 2 complete intersection in x_0, x_1, y_0, y_1, A, B, adding x_2, y_2 and so on one at a time, to recover V_{AB}. For this, we order the $k+l-2$ steps *inverse to the elimination* of the monomials $x_{2\dots k}, y_{2\dots l}$; that is, we rename the nth eliminated monomial s_ν with $\nu = k+l-2-n$, so that $s_0 = x_2$ and $s_1 = y_2$. We work by induction on this ν. At the same time, we name the annotation h_ν on the monomial s_ν as it is eliminated; the chain starts from the top with

$$s_{k+l-3} = y_l \quad \text{and} \quad h_{k+l-3} = B \quad \text{and} \quad b_l = 1. \tag{5.4}$$

(This assumes the main case $d, e \geq 2$ so that $b_l = 1$. Otherwise, if $a_k = 1$ then this line should be $s_{k+l-3} = x_k$ and $h_{k+l-3} = A$.)

Thus in Example 5.1, $[s_0, s_1, s_2, s_3, s_4] = [x_2, y_2, y_3, x_3, y_4]$ and

$$[h_0, h_1, h_2, h_3, h_4] = [A^3B^5, AB^2, AB^2, AB, B].$$

The scissors of Figure 4.2 strongly suggest this ordering of the monomials, although there is a choice to make at the end between y_1 and x_2, which both have tag 1; we always eliminate $s_1 = x_2$.

5.1.2 The projection $V_{AB,\nu+1} \to V_{AB,\nu}$

ss!snu

The projection sequence gives cones $\sigma_{AB,\nu}$ that depend on the induction parameter ν. The top corners of each $\sigma_{AB,\nu}$ are monomials x_i and y_j with $i = i(\nu)$ and $j = j(\nu)$ (Table 5.1 keeps track of these functions), and we know the equations of $V_{AB,\nu}$ including

$$x_{i-1}y_j = x_i^{\alpha_\nu} A_\nu \quad \text{and} \quad x_i y_{j-1} = y_j^{\beta_\nu} B_\nu, \tag{5.5}$$

given by the tags and annotations at x_i and y_j in $V_{AB,\nu}$ as in Figure 5.1. f!mod

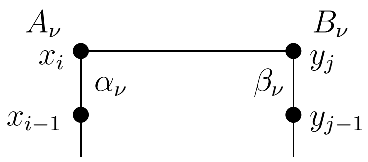

Figure 5.1: The *bar* x_i——y_j at the top of $\sigma_{AB,\nu}$, with tag equations (5.5).

Proposition 5.2 *The chain of projections $V_{AB,\nu+1} \to V_{AB,\nu}$ reduces V_{AB} down to a codimension 2 complete intersection $V_{AB,0} \subset \mathbb{A}^6_{\langle x_0,x_1,y_0,y_1,A,B\rangle}$. The step $V_{AB,\nu+1} \to V_{AB,\nu}$ eliminates $s_\nu = x_{i+1}$ or y_{j+1}, with two possible cases for the top of $\sigma_{AB,\nu+1}$:* p!snu

$$\begin{array}{cccccc} & s_\nu & & & & s_\nu \\ \textit{either} & x_i & y_j & \textit{or} & x_i & y_j \\ & x_{i-1} & y_{j-1} & & x_{i-1} & y_{j-1} \end{array}$$

In the left case $s_\nu = x_{i+1}$, the top of $\sigma_{AB,\nu}$ is determined in terms of $\nu+1$ and the original tag a_i at x_i by

$$A_\nu = A_{\nu+1}, \quad B_\nu = A_{\nu+1}B_{\nu+1}, \quad \alpha_\nu = a_i - 1, \quad \beta_\nu = \beta_{\nu+1} - 1, \qquad (5.6)$$

and similarly in the right case by

$$A_\nu = A_{\nu+1}B_{\nu+1}, \quad B_\nu = B_{\nu+1}, \quad \alpha_\nu = \alpha_{\nu+1} - 1, \quad \beta_\nu = b_j - 1. \qquad (5.7)$$

5.1.3 Choice of $h_\nu(A,B)$

ss!hnu

We set $h_\nu = \mathrm{hcf}(A_\nu, B_\nu)$, equal to A_ν or B_ν by (5.6–5.7). The unprojection divisor of $V_{AB,\nu+1} \to V_{AB,\nu}$ is the hypersurface $(h_\nu = 0) \subset \mathbb{A}^4_{x_i,y_j,A,B}$; in the main construction of V_{ABLM} in 5.3, the unprojection divisor of $V_{\nu+1} \to V_\nu$ is $(h_\nu = 0) \subset \mathbb{A}^6_{\langle x_i,y_j,A,B,L,M\rangle}$.

The initial case $n = 0$ or $\nu = k+l-2$ is $V_{AB,\nu} = V_{AB}$; in our construction of V_{ABLM}, it is the final goal: if we reach it, there is nothing more to check. Then $A = A_\nu$, $B = B_\nu$, $h_\nu = 1$, and divisibility by h_ν is trivial.

5.1.4 Unprojecting $D_{AB,\nu} \subset V_{AB,\nu}$

ss!upAB

Proposition 5.2 described the projection $V_{AB,\nu+1} \to V_{AB,\nu}$ that eliminates the variable s_ν; inverting this, we construct $V_{AB,\nu+1}$ as an unprojection from $V_{AB,\nu}$ adjoining s_ν. For this, define $D_{AB,\nu} \subset \mathbb{A}^{i+j+4}_{\langle x_{0\dots i},y_{0\dots j},A,B\rangle}$ by the ideal $(x_{0\dots i-1}, y_{0\dots j-1}, h_\nu)$; thus $D_{AB,\nu}$ is the hypersurface $(h_\nu = 0) \subset \mathbb{A}^4_{\langle x_i,y_j,A,B\rangle}$.

Claim $D_{AB,\nu} \subset V_{AB,\nu}$. *In other words, every generator of the ideal of $V_{AB,\nu}$ is in the ideal $(x_{0\dots i-1}, y_{0\dots j-1}, h_\nu)$ of $D_{AB,\nu}$.*

This is an exercise in toric geometry. [Hint: The main case goes as follows. Consider an equation $x_i y_{j'} = x_i^\xi y_j^\eta A^\alpha B^\beta$ for some $j' < j$. First $\xi = 0$, for otherwise we could divide through by x_i to get a monomial expression for $y_{j'}$. Now comparing our equation with the tag equation $x_i y_{j-1} = y_j^{\beta_j} B_\nu$ gives

$$y_{j'} y_j^{\beta_j - \eta} y_{j-1}^{-1} = A^\alpha B^\beta B_\nu^{-1}. \tag{5.8}$$

However, both sides of (5.8) must be 1, since the span of $y_{0\dots l}$ is complementary to the span of A, B in the vector space $\mathbb{M}_\mathbb{Q}$ (compare Figure 2.3). Therefore $A^\alpha B^\beta = B_\nu$, and both sides of our equation are in the ideal.]

The analogous claim in the more complicated context of Proposition 5.8 is the key point in the proof of the existence of V_{ABLM}.

5.2 Crosses, pitchforks and pentagrams

5.2.1 The spreadsheet for V_{AB}

As just explained, our construction of $V_{\nu+1}$ from V_ν reverses the projection sequence down from the top of V_{AB}. Our proof also needs information derived from the projection sequence up from the bottom of V_{LM}. Thus in Extended Example 1.1, we deconstructed V_{LM} by eliminating y_0, y_1, y_2, x_0, x_1 from the bottom of Figure 1.3. Here we establish how the two projection sequences interleave, as an exercise in patient bookkeeping.

Table 5.1 gives the function $i = i(\nu)$, $j = j(\nu)$ of 5.1.2 describing the top of $V_{AB,\nu}$ as in Figure 5.1. The table repeats periodically with period $d+e-2$, or alternate half periods of $d-1$, $e-1$. We set $v = \nu \bmod d+e-2$ and write $\nu = C(d+e-2) + v$. t!spsh

The starting point $\nu = 0$ is $V_{AB,\nu}$ with x_1, y_1 at its top bar. We describe the odd case $k = 2\kappa + 1$. Set $C = 0$ and enter the first round: the line $v = a = 1$ adds an x_i, then $a = 2, \dots, e-1$ is a half round that adds $e-2$ terms y_j; similarly, the line $v = e$ (so $b = 1$) adds an x_i and then $b = 2, \dots, d-1$ is a half round that adds $d-2$ terms y_j. We then increment $C \mapsto C+1$ and loop. Each half round adds one x_i and $d-2$ or $e-2$ terms y_j. There are $k-1$ half rounds, ending with $\nu = (d+e-2)\kappa$ if $k = 2\kappa+1$ or $\nu = (d-1)\kappa + (e-1)(\kappa-1)$ if $k = 2\kappa$.

The above treatment assumes that we are in the main case $d, e \geq 2$; everything remains true when d or e or both are 2. Then the intervals $2 \leq a \leq d-1$ or $2 \leq b \leq e-1$ are empty, so the corresponding half periods add one x_i and no y_j.

v	i	j	
0	$2C+1$	$(d+e-4)C+1$	
a	$2C+2$	$(d+e-4)C+a$	for $1 \leq a \leq e-1$
$e+b-1$	$2C+3$	$(d+e-4)C+e-2+b$	for $1 \leq b \leq d-1$
Final	$k=2\kappa+1$	$l=(d+e-4)\kappa+2$	

v	i	j	
0	$2C+1$	$(d+e-4)C+1$	
a	$2C+2$	$(d+e-4)C+a$	for $1 \leq a \leq d-1$
$d+b-1$	$2C+3$	$(d+e-4)C+d-2+b$	for $1 \leq b \leq e-1$
a	$2C+2$	$(d+e-4)C+a$	for $1 \leq a \leq d-1$
Final	$k=2\kappa$	l	

Table 5.1: Numbering the unprojection sequence for V_{AB}. The even case $k=2\kappa$ has one fewer half round. The final line is irregular: it adds a final y_l instead of x_{k+1} with $l=(d+e-4)\kappa+2$ or $l=(d-2)\kappa+(e-2)(\kappa-1)+2$.

5.2.2 Comparing the projection sequences for V_{AB} and V_{LM}

We want to compare the bars x_i, y_j at the top of $V_{AB,\nu}$ with the corresponding thing at the bottom of V_{LM} after a number of projections. To see this, we divide the monomials y_j up into intervals according to the lines of Table 5.1, writing Y_{i-1} for the ith half period. In more detail, for k even, the line for even $i=2C+2$ gives the interval f!pfpi

$$Y_{i-1} = \{y_j \mid \text{for } j \in [n_i+1, \dots, n_i+d-1]\} \tag{5.9}$$

where $n_i = (d+e-4)\frac{i-2}{2}$; similarly, the line $i'=2C+3$ gives

$$Y_{i'-1} = \{y_j \mid \text{for } j \in [n_{i'}+1, \dots, n_{i'}+e-1]\} \tag{5.10}$$

where $n_{i'} = (d+e-4)\frac{i'-3}{2}+d-2$.

Notice the adjacency between the intervals: the last entry n_i+d-1 of Y_{i-1} equals the first entry $n_{i'}+1$ of the following interval $Y_{i'}$ with $i'=i+1$, and vice versa. For d or $e=2$, the interval Y_i reduces to one element.

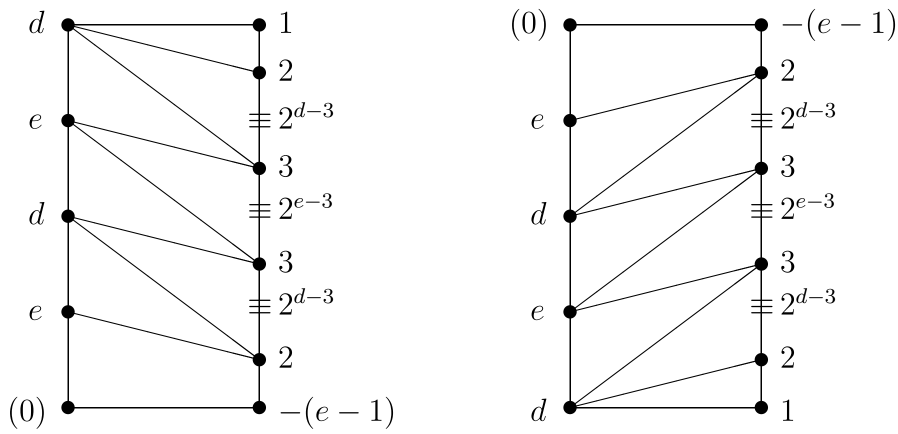

Figure 5.2: Projecting V_{AB} from the top and V_{LM} from the bottom

Lemma 5.3 *The bars at the top of $V_{AB,\nu}$ are precisely x_{i+1}, y_j with $j \in Y_i$.* l!bar

The bars at the bottom of $V_{LM,\nu'}$ (after projecting out ν' monomials from V_{LM}, starting with y_0) are precisely x_{i-1}, y_j with $j \in Y_i$. See Figure 5.2.

The first clause merely repeats the information contained in Table 5.1 about the order of projection. The projection sequence of V_{LM} from the bottom is enumerated by a symmetric and more or less identical spreadsheet, which proves the second clause.

The following simple consequence is a key point of our proof in Section 5.3.

c!kil

Corollary 5.4 *Suppose that we project out n_1 monomials from the top of V_{AB} down to the top bar x_i, y_j and n_2 monomials from the bottom of V_{LM} up to the bottom bar $x_{i'}, y_{j'}$, where $n_1 + n_2 = k + l - 2$, so that just 4 monomials remain. Then $i' < i$ and $j' \leq j$.*

Equivalently, either $i' = i - 1$ and $j' = j - 1$ or $i' = i - 2$ and $j' = j$, so that any such projection leads to a "cross" or "pitchfork" of the shape

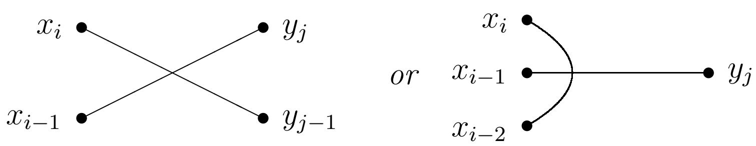

(5.11)

The same phenomenon was already implicit in the cascade of pentagrams of Example 1.1; we include this, although it is not essential for our proof.

Corollary 5.5 *Projecting out n_1 monomials from the top of V_{AB} and n_2 from the bottom of V_{LM} with $n_1 + n_2 = k + l - 3$ gives a pentagram of one of the two shapes*

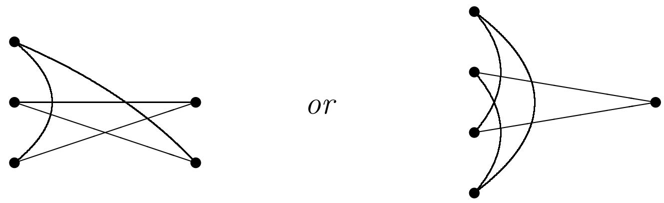

or (5.12)

5.3 Proof by induction

s!pf

We construct $V = V_{ABLM}$ by serial unprojection. The induction starts from the codimension 2 complete intersection

$$V_0 \subset \mathbb{A}^8_{\langle x_0, x_1, y_0, y_1, A, B, L, M \rangle}$$

defined by

$$x_1 y_0 = T_{x_0}(V_{AB}) + T_{x_0}(V_{LM}) \quad \text{and} \quad x_0 y_1 = T_{y_0}(V_{AB}) + T_{y_0}(V_{LM})$$

where $T_{x_0}(V_{AB})$ is the righthand side of the tag equation at x_0 in V_{AB}, and similarly for the other three terms. Clearly V_0 is Gorenstein and A, B, L, M is a regular sequence, with the regular section $L = M = 0$ in V_0 the variety $V_{AB,0}$. We use the following elementary fact about unprojection.

l!com

Lemma 5.6 *Unprojection commutes with regular sequences: let X, D be as in [PR], Theorem 1.1 and $Y \to X$ the unprojection of D in X. Suppose that $z_1, \dots, z_r \in \mathcal{O}_X$ is a regular sequence for X and for D. Then $z_1, \dots, z_r$ is also a regular sequence for $\mathcal{O}_Y$, and Y_z is the unprojection of D_z in X_z, where $Y_z : (z_i = 0) \subset Y$ and similarly for D_z and X_z.* $\square$

indas

Inductive assumption 5.7 *We own a variety $V_\nu = V_{ABLM,\nu}$ having a $\mathbb{T}$-action, together with a regular sequence L, M made up of $\mathbb{T}$-eigenfunctions such that $V_\nu \cap (L = M = 0) = V_{AB,\nu}$.*

We start with $\nu = 0$, and $V_{ABLM,\nu} = V_0$ as above. The induction has $k + l - 2$ steps, adjoining $x_{2\dots k}$ and $y_{2\dots l}$ in the order determined in 5.1.1. When ν reaches $k + l - 2$ then $V_{ABLM} = V_\nu$ and we are finished. Otherwise, if $\nu < k + l - 2$, the induction step consists of proving that V_ν has a divisor

D_ν on which L, M is a regular sequence, and the section $D_\nu \cap (L = M = 0)$ is the divisor $D_{AB,\nu} \subset V_{AB,\nu}$.

If $\nu < k + l - 2$, by 5.1.4, the step $V_{AB,\nu+1} \to V_{AB,\nu}$ of the chain down from V_{AB} is the unprojection adjoining the element s_ν with unprojection ideal $\bigl(x_{0\dots i-1}, y_{0\dots j-1}, h_\nu\bigr)$, where h_ν is the monomial in A, B defined in 5.1.3. We seek to imitate this for the 6-fold V_ν; for this, define D_ν by

$$D_\nu \subset \mathbb{A}^8_{\langle x_{0\dots i}, y_{0\dots j}, A, B, L, M\rangle} \quad \text{with ideal} \quad I_{D_\nu} = \bigl(x_{0\dots i-1}, y_{0\dots j-1}, h_\nu\bigr).$$

Clearly, it is the hypersurface $D_\nu : (h_\nu = 0) \subset \mathbb{A}^6_{\langle x_i, y_j, A, B, L, M\rangle}$, and is the product of $\mathbb{A}^4_{\langle x_i, y_j, L, M\rangle}$ with the plane curve $h_\nu(A, B) = 0$. The issue is to prove that $D_\nu \subset V_\nu$.

p!k

Proposition 5.8 (Key point) $I_{V_\nu} \subset I_{D_\nu} = (x_{0\dots i-1}, y_{0\dots j-1}, h_\nu)$ *for every* $\nu < k + l - 2$.

We prove this by a general argument on $\mathbb{T}$-weights of monomials that may appear in a relation, without any need to analyse the actual equations of V_ν. We introduce the notation $R(\nu)$ for the $\mathbb{T}$-weights of homogeneous generators of $I_{V_{AB,\nu}}$ or equivalently, of I_{V_ν} (by $\mathbb{T}$-equivariance); we write $f \in R(\nu)$ to indicate that f is a homogeneous polynomial with $\mathbb{T}$-weight in $R(\nu)$. The precise statement we prove is the following:

cl!div

Claim 5.9 *Any monomial* $x_i^\xi y_j^\eta A^\alpha B^\beta L^\lambda M^\mu \in R(\nu)$ *is divisible by* h_ν.

Recall that $h_\nu = \operatorname{hcf}(A_\nu, B_\nu)$; we usually prove divisibility by A_ν or B_ν. By definition, any alleged monomial in $R(\nu)$ is $\mathbb{T}$-equivalent to a relation in $I_{V_{AB,\nu}}$ for $x_{i'} y_{j'}$ or $x_{i'} x_{i''}$ or $y_{j'} y_{j''}$. The main mechanism of the proof is to compare it with one of the two equations (5.5), or more precisely, with one of the model monomials eq!mod2

$$x_{i-1} y_j \overset{\mathbb{T}}{\sim} x_i^{\alpha_\nu} A_\nu \quad \text{and} \quad x_i y_{j-1} \overset{\mathbb{T}}{\sim} y_j^{\beta_\nu} B_\nu, \tag{5.13}$$

coming from the top corners of $V_{AB,\nu}$ as in Figure 5.1.

Step 1 *Claim 5.9 holds for every monomial in* $R(\nu - 1)$. Indeed, it is divisible by $h_{\nu-1}$ by induction, and by (5.6–5.7) the h_ν increase as ν decreases.

Step 2 The first actual calculation in the proof: *Claim 5.9 holds for all the monomials* $x_{i'} y_j$ *with* $i' = 0, \dots, i - 1$ *and* $x_i y_{j'}$ *with* $j' = 0, \dots, j - 1$ *appearing in* cross-over *relations.*

Proof We write out the proof for $x_{i'}y_j$ in detail as a model case. The method is to compare an alleged monomial

$$x_i^\xi y_j^\eta m \overset{\mathbb{T}}{\sim} x_{i'}y_j \in R(\nu), \quad \text{where } m \text{ is a monomial in } A, B, L, M$$

with the known monomial $x_i^{\alpha_\nu}A_\nu \overset{\mathbb{T}}{\sim} x_{i-1}y_j$ from (5.13). We have $\eta = 0$: otherwise dividing both sides by y_j contradicts Corollary 4.2.iii. Consider

$$\frac{x_{i'}}{x_{i-1}} \overset{\mathbb{T}}{\sim} x_i^{\xi-\alpha_\nu}\frac{m}{A_\nu} \tag{5.14}$$

By Corollary 4.2.ii and the fact that $i' \le i-1$, the lefthand side has L, M exponents $\pi_{LM}(\frac{x_{i'}}{x_{i-1}}) \le 0$ (see (4.3) for the notation π_{LM} and π_{AB}); thus $\alpha_\nu \ge \xi$, and the equivalence takes the form eq!gt-1

$$x_i^{\alpha_\nu-\xi}\frac{x_{i'}}{x_{i-1}} \overset{\mathbb{T}}{\sim} \frac{m}{A_\nu} \quad \text{with} \quad \alpha_\nu \ge \xi. \tag{5.15}$$

Now for the same reason, $\pi_{AB}(\frac{x_{i'}}{x_{i-1}}) \ge 0$. The same goes for $x_i^{\alpha_\nu-\xi}$, except for the case $x_i = x_k$, at the top left of the rectangle for V_{AB}.

This initial case is important: $\pi_{AB}(x_k) = (-\frac{1}{d}, 0)$ (see Proposition 4.1); because of the negative exponent, we cannot get our conclusion by convexity alone. Instead we use a congruence argument based on intuition derived from the padded cell 4.3: in fact, the negative exponent is the smallest possible value $-\frac{1}{d}$, and we claim that α_ν is one of $d-1, d-2, \dots, 1$. Indeed, if $\nu = k+l-2$ we are at the end of the induction, and there is nothing to prove. Otherwise, the tag at x_k has decreased by at least one from its pristine value d. It follows that the lefthand side of (5.15) has A exponent > -1 and B exponent ≥ 0. On the other hand, the righthand side of (5.15) is a Laurent monomial. Therefore m is divisible by A_ν, as required.

The argument for $x_iy_{j'}$ is similar but slightly easier. Suppose that eq!topc

$$x_iy_{j'} \overset{\mathbb{T}}{\sim} x_i^\xi y_j^\eta m \quad \text{with} \quad m = A^\alpha B^\beta L^\lambda M^\mu. \tag{5.16}$$

First $\xi = 0$, because otherwise dividing through by x_i would contradict Corollary 4.2.iii. Next, dividing through by the monomials in the second expression of (5.13) gives

$$\frac{y_{j'}}{y_{j-1}} = y_j^{\eta-\beta_\nu} \times \frac{m}{B_\nu}. \tag{5.17}$$

As before, since $j' \le j-1$, Corollary 4.2.ii gives that $\pi_{LM}(\frac{y_{j'}}{y_{j-1}}) \le 0$. Therefore $\eta - \beta_\nu \le 0$. Taking that term to the lefthand side gives

$$y_j^{\beta_\nu - \eta} \frac{y_{j'}}{y_{j-1}} = \frac{m}{B_\nu} \quad \text{with} \quad \beta_\nu \ge \eta. \tag{5.18}$$

Now $j' \le j-1$, so $\pi_{AB}(\frac{y_{j'}}{y_{j-1}}) \ge 0$; the same goes for y_j except if $j = l$ and y_j is at the top of the long rectangle, and we are finished, with $V_\nu = V_{ABLM}$. Therefore the exponents of A, B on the lefthand side are ≥ 0, and hence m is divisible by B_ν.

This proves Step 2. Q.E.D.

The proof of Step 2 used Corollary 4.2.ii to compare the exponents of $x_i/x_{i'}$ and $y_j/y_{j'}$, with typical implication $i > i' \Rightarrow \pi_{LM}(x_i) > \pi_{LM}(x_{i'})$. For Step 3 we need a similar comparison for monomials $x_i/y_{j'}$ and $y_j/x_{i'}$. Care is needed here to distinguish the order of monomials in the projection sequences from the top of V_{AB} and from the bottom of V_{LM}: the L, M exponents behave monotonically in the projection sequences of V_{AB}, and vice versa.

l!cmp

Lemma 5.10 *Given two monomials $m_1, m_2 \in \{x_{0\dots k}, y_{0\dots l}\}$, suppose that the projection sequence for V_{AB} eliminates m_1 before m_2; then*

$$\pi_{LM}(m_1) \ge \pi_{LM}(m_2). \tag{5.19}$$

Similarly, if the projection sequence for V_{LM} eliminates m_1 before m_2 then

$$\pi_{AB}(m_1) \ge \pi_{AB}(m_2). \tag{5.20}$$

See Scissors, Figure 4.2 for a picture. Example 4.5 provides a numerical sanity check, with the respective orders of elimination

$$V_{AB} : y_{16}, y_{15}, y_{14}, x_6, y_{13}, y_{12}, y_{11}, y_{10}, x_5, y_9, y_8, x_4, y_7, y_6, y_5, y_4, x_3, y_3, y_2, x_2;$$
$$V_{LM} : y_0, y_1, y_2, x_0, y_3, y_4, y_5, y_6, x_1, y_7, y_8, x_2, y_9, y_{10}, y_{11}, y_{12}, x_3, y_{13}, y_{14}, x_4.$$

Step 3 *Claim 5.9 holds for all monomials $y_j y_a$ with $a = 0, \dots, j-2$.*

First, Corollary 5.4 implies that the V_{LM} projection sequence eliminates y_a before x_{i-1}. Indeed, x_{i-1} is joined to y_j in a cross or pitchfork involving at most y_j and y_{j-1}, so this is a party to which no y_a with $a \le j-2$ is invited. Therefore Lemma 5.10 gives eq!piAB

$$\pi_{AB}\Big(\frac{y_a}{x_{i-1}}\Big) \geq 0. \tag{5.21}$$

As before, comparing the alleged monomial with the first of (5.13) gives eq!ya

$$\frac{y_a}{x_{i-1}} \overset{\mathbb{T}}{\sim} x_i^{\xi-\alpha_\nu}\frac{m}{A_\nu}. \tag{5.22}$$

The proof divides into two cases.

Case 1 The projection sequence for V_{AB} eliminates x_i before y_a.

Lemma 5.10 says that $\xi - \alpha_\nu \geq 1$ is impossible in (5.22) (the lefthand side would have π_{LM} strictly smaller than the right). Thus eq!yaw

$$x_i^{\alpha_\nu-\xi}\frac{y_a}{x_{i-1}} \overset{\mathbb{T}}{\sim} \frac{m}{A_\nu} \quad \text{with} \quad \alpha_\nu \geq \xi, \tag{5.23}$$

and (5.21) implies that A_ν divides m.

Case 2 The projection sequence for V_{AB} eliminates y_a before x_i. This means that y_a, y_j are both contained in the interval Y_{i-1} of Lemma 5.3, and that y_a is not at the bottom:

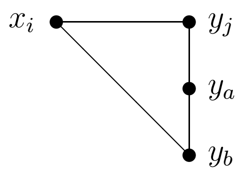

Suppose that x_i is tagged with d (or simply replace $d \leftrightarrow e$ in what follows), and write $Y_{i-1} = [b, b+d-2]$ for the interval of Lemma 5.3. Our conclusion in this case is that $\xi - \alpha_\nu < a - b + 1$ and $\equiv a - b + 1 \mod d$. Therefore $\xi \leq \alpha_\nu$, and the argument of Case 1 works as before.

The proof goes as follows:

(a) For $y_a \in Y_{i-1}$

$$\pi_{LM}(y_a) = (a-b)\pi_{LM}(x_i) + \pi_{LM}(y_b) < (a-b+1)\pi_{LM}(x_i). \tag{5.24}$$

(b) On the other hand, taking π_{LM} in (5.22) gives

$$(\xi - \alpha_\nu)\pi_{LM}(x_i) = \pi_{LM}(y_a) - \pi_{LM}(x_{i-1}) < \pi_{LM}(y_a) \tag{5.25}$$

Therefore $\xi - \alpha_\nu < a - b + 1 \leq d - 2$.

(c) Moreover modulo $\mathbb{M}'$, we have

$$y_a \equiv \frac{x_i^{a-b+1}}{x_{i-1}} \in Q. \tag{5.26}$$

(d) Therefore in (5.22), $\xi - \alpha_\nu \equiv a - b + 1 \bmod d$.

Proof (a) follows from the tag equations for the toric variety V_{AB} at the successive y_α: as $y_{\alpha+1}$ is eliminated it has tag 1 and tag equation eq!yal

$$x_i y_\alpha = y_{\alpha+1} A^{u_\alpha} B^{v_\alpha}. \tag{5.27}$$

Applying π_{LM} gives the equality in (5.24), and the inequality comes from Lemma 5.10.

(b) When we reach the bottom of this interval, we eliminate x_i, with tag 1 and tag equation

$$x_{i-1} y_b = x_i A^{u_b} B^{v_b}. \tag{5.28}$$

Viewing this equation modulo $\mathbb{M}'$ gives $y_b \equiv x_i/x_{i-1}$, and together with (5.27) this gives the value of y_a in Q as eq!ysuba

$$y_a \equiv y_b x_i^{(a-b)} \equiv \frac{x_i^{a-b+1}}{x_{i-1}}, \tag{5.29}$$

which proves (c).

In the coordinates of the padded cell Q, we know that x_{i-1} is $(0, \pm\frac{1}{e})$ and x_i is $(\pm\frac{1}{d}, 0)$. The alleged monomial tells us that $y_\alpha \equiv x_i^{\xi-\alpha}/x_{i-1}$ modulo $\mathbb{M}'$, and (d) follows. Q.E.D.

Step 4 *Claim 5.9 holds for all monomials $x_i x_a$ with $a = 0, \dots, i-2$.*

We only consider the case eq!star

$$d, e \geq 2 \quad \text{and} \quad de > 4. \tag{$*$}$$

In fact,[9] we must use this assumption, since the claim fails when $d = e = 2$. Given this, the argument turns out to be rather coarse compared to Step 3, and we win with something to spare.

[9] Say this, if true?: This is the (only?) place in the proof that uses $de > 4$? Also, deal with case assumption $d, e \geq 2$, $de > 4$ in the statement of Main Claim 5.9.

Proof We compare an alleged monomial $x_i x_a \overset{\mathbb{T}}{\sim} y_j^\eta m$ with the first of (5.13) as usual; move the y_j term across, this time regardless of sign, obtaining

$$y_j^{\beta_\nu - \eta} \frac{x_a}{y_{j-1}} \overset{\mathbb{T}}{\sim} \frac{m}{B_\nu}. \tag{5.30}$$

Our conclusion in this case is that $\beta_\nu - \eta - 1 > -2$ and d divides $\beta_\nu - \eta - 1$; this implies that $\pi_{AB}(m/B_\nu) \geq \pi_{AB}(x_a y_j / y_{j-1}) \geq 0$, so that B_ν divides m as required.

The proof goes as follows:

(1) Arguing from the top, we see that y_j goes before x_{i-2} in the projection sequence for V_{AB}; the tag equation in V_{AB} as y_j is eliminated is eq!pfAB

$$x_{i-2} y_{j-1} \overset{\mathbb{T}}{\sim} y_j A^u B^v. \tag{5.31}$$

(2) From the bottom, the existence of the pitchfork $(x_{i\dots i-2}, y_j)$ implies that in the projection sequence for V_{LM}, the tag equation as y_{j-1} is eliminated is eq!pfLM

$$x_{i-2} y_j \overset{\mathbb{T}}{\sim} y_{j-1} L^s M^t. \tag{5.32}$$

(3) Now substitute for y_j / y_{j-1} from (5.31), obtaining

$$y_j^{\beta_\nu - \eta - 1} \frac{x_{i-2} x_a}{A^u B^v} \overset{\mathbb{T}}{\sim} \frac{m}{B_\nu}. \tag{5.33}$$

Taking L, M parts gives

$$(\beta_\nu - \eta - 1)\pi_{LM}(y_j) \geq -\pi_{LM}(x_{i-2}) - \pi_{LM}(x_a). \tag{5.34}$$

Now since y_j goes before x_{i-2} in the V_{AB} sequence, Lemma 5.10 says that $\pi_{LM}(y_j)$ is bigger than either summand on the right. Therefore

$$\beta_\nu - \eta - 1 > -2. \tag{5.35}$$

(4) Now substitute for x_{i-2} / y_{j-1} from (5.32), obtaining eq!mB

$$y_j^{\beta_\nu - \eta - 1} L^s M^t \overset{\mathbb{T}}{\sim} \frac{m}{B_\nu}. \tag{5.36}$$

Now the usual padded cell congruence argument implies that d divides $\beta_\nu - \eta - 1$. In fact m/B_ν and $L^s M^t \in \mathbb{M}'$, whereas y_j is at the endpoint of an interval Y_{i-1} and so has coordinates $(\pm\frac{1}{d}, 0)$ in Q.

Finally, either $a = i - 2$ and the tag equation (5.32) at y_{j-1} gives $\pi_{AB}(x_a y_j / y_{j-1}) = 0$, or x_a goes before y_{j-1} in the projection sequence for V_{LM}, so that $\pi_{AB}(m/B_\nu) \geq \pi_{AB}(x_a y_j / y_{j-1}) \geq 0$, and B_ν divides m as required.

Q.E.D.

6 The other cases

The above treatment assumed $d, e \geq 2$ and $de > 4$. The remaining cases are

(i) $d = 1, e \geq 5$ or $d \geq 5, e = 1$.

(ii) $d = e = 2$.

(iii) $(d, e) = (1, 4)$ or $(4, 1)$.

(iv) $de \leq 3$.

6.0.1 Rough notes

$de - 4$ is a discriminant, compare 3.3.

The cases $d = e = 2$ and $\{d, e\} = \{1, 4\}$ provide mild counterexamples to Claim 5.9 in the preceding proof. The difference with the cases $de \neq 4$ is that the $\mathbb{T}$-weights of $x_0, \dots, x_k \in \mathbb{M}$ include long arithmetic progressions, so that 5.3, Step 4 for $x_i x_a$ often fails: it is not true that every monomial $\mathbb{T}$-equivalent to a relation R is divisible by h_ν. These cases are discussed in the separate chapter [BR].

In the cases $de \leq 3$, at least one of d, e equals 1, and k is small (see (3.9)). This handful of cases can almost certainly be treated as easy initial cases of the main family $I(1, e, k)$ or $I(d, 1, k)$.

In the cases with d or $e = 1$, the main difference is that we have a choice as to which monomials it makes sense to project out. Any x_i tagged with a 1 could be projected out at any time, and different order of projections will lead to different forms of the equations (some with redundant generators and some without). The phenomenon was already present in the previous chapter: every one of our deconstructions ended with the two monomials x_2, y_1 both tagged with a 1, and we chose to project out the x_2.

In the bigger cases with d or $e = 1$, the monomials x_i and y_j still have coordinates in the impartial basis A, B, L, M, and we can use this to determine a preferred order of projections down from the top of V_{AB} and up from the bottom of V_{LM}. These orders are different from the straightforward lexicographic order $x_0, x_1, x_2, \dots$, but if we follow them we still get our crosses, pitchforks and pentagrams, and most of the remaining ingredients of our proof.

6.1 $d = 1, e \geq 5$

(The variables tagged with 1 can be eliminated, and then it should be the same as $d, e \geq 2$ and $de > 4$.)

There is a choice here: one strategy is to start by eliminating the variables tagged with 1 as redundant generators, and put together a whole new proof from scratch similar to the argument for $d, e \geq 2$ and $de > 4$. However, it turns out to be more convenient to leave in the redundant generators: this obliges us to rearrange the order of projection, but it has the advantage that the main equations remain Pfaffians with monomial entries.

We illustrate the issues involved by working out the case $I(1, e, 1)$, that is, $d = 1$, $e \geq 3$ and $k = 3$. The equations from the bottom are f!131

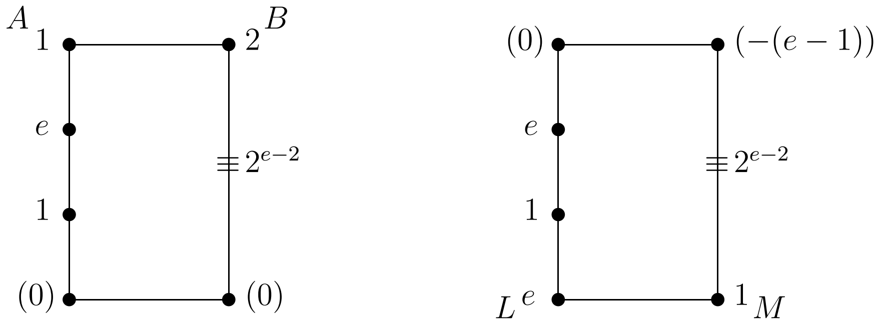

Figure 6.1: The case $I(1, 3, 1)$

$$x_0 y_1 = A^{e-1}B^{e-2} + y_0 M \quad \text{and} \quad x_1 y_0 = A^e B^{e-1} + x_0^e L \tag{6.1}$$

Although the monomial x_1 is redundant as a generator, it does no harm to leave him in throughout the unprojection calculation. The Pfaffian equations come from the chain

$$\begin{pmatrix} y_j & x_2^j A^{e-j-1} B^{e-j-2} & -x_0^{e-j-1} L & -y_{j+1} \\ & x_0 & AB & -1 \\ & & x_1 & M \\ & & & x_2 \end{pmatrix} \tag{6.2}$$

for $j = 0, \dots, e-2$ and the final coda introducing x_3 as unprojection variable

$$\begin{pmatrix} y_{e-1} & x_2^j A^{e-j-1} B^{e-j-2} & -x_0^{e-j-1} L & -x_3 \\ & x_0 & A & -1 \\ & & x_1 & BM \\ & & & x_2 \end{pmatrix} \tag{6.3}$$

The two top tag equations are

$$x_2y_3 = x_3A + LM^3 \quad \text{and} \quad x_3y_2 = y_3^2B + x_2^2LM^2 \tag{6.4}$$

The effect of leaving in the redundant generator $x_1 = x_0x_2 + ABM$ is that these matrixes have a unit entry. But eliminating him messes up the shape of the remaining equations.

e.g. $d = 1$, $e = 6$, $k = 10$.

Lefthand tags: $1, 6, 1, 6, 1, 6, 1, 6, 1, 6, 0$.

Righthand tags: $2, 2, 2, 3, 2, 3, 2, 3, 2, 2, -4$.

```
> Matrix([x10,x9,x8,x7,x6,x5,x4,x3,x2,x1,x0]);

[  265   209     -1      0]
[   56 265/6      0    1/6]
[   71    56      1      1]
[   15  71/6      1    5/6]
[   19    15      5      4]
[    4  19/6      4   19/6]
[    5     4     19     15]
[    1   5/6     15   71/6]
[    1     1     71     56]
[    0   1/6     56  265/6]
[   -1     0    265    209]

> Matrix([y10,y9,y8,y7,y6,y5,y4,y3,y2,y1,y0]);

[  209 989/6      0   -1/6]
[  153 362/3      1    2/3]
[   97 153/2      2    3/2]
[   41  97/3      3    7/3]
[   26  41/2      7   11/2]
[   11  26/3     11   26/3]
[    7  11/2     26   41/2]
[    3   7/3     41   97/3]
[    2   3/2     97  153/2]
[    1   2/3    153  362/3]
[    0  -1/6    209  989/6]
```

The matrices when $d = 1$, $e = 6$, $k = 6$

1. x_6 (out), x_5, x_3 (in), y_6, y_5

$$\begin{pmatrix} y_5 & x_5^4 & By_6 & x_3 \\ & y_6 & L^{14}M^{11} & A \\ & & x_6 & L^5M^4 \\ & & & x_5 \end{pmatrix}$$

2. x_5, x_4 (in), x_3, y_6 (out), y_5

$$\begin{pmatrix} x_3 & Ax_5^4 & L^5M^4 & x_4 \\ & y_5 & 1 & AB \\ & & y_6 & L^{14}M^{11}X_3 \\ & & & x_5 \end{pmatrix}$$

3. x_5, x_4, x_3, y_5 (out), y_4 (in)

$$\begin{pmatrix} y_5 & L^9M^7x_3^2 & A^2Bx_5^3 & y_4 \\ & x_5 & L^5M^4 & 1 \\ & & x_4 & AB \\ & & & x_3 \end{pmatrix}$$

4. x_5, x_4, x_3, y_4 (out), y_3 (in)

$$\begin{pmatrix} y_4 & L^4M^3x_3^2 & A^3B^2x_5^2 & y_3 \\ & x_5 & L^5M^4 & 1 \\ & & x_4 & AB \\ & & & x_3 \end{pmatrix}$$

5. x_5, x_4 (out), x_3, x_1 (in), y_3

$$\begin{pmatrix} y_3 & x_3^3 & A^4B^3x_5 & x_1 \\ & x_5 & L^4M^3 & 1 \\ & & x_4 & ABLM \\ & & & x_3 \end{pmatrix}$$

6. x_5 (out), x_3, x_2 (in), x_1, y_3

$$\begin{pmatrix} x_1 & x_3^2 & ABLM & x_2 \\ & y_3 & 1 & A^4B^3 \\ & & x_5 & L^4M^3x_1 \\ & & & x_3 \end{pmatrix}$$

6.2 $d = e = 2$

s!22

Weights (assume k even).

y_2	$k/2$	$(k+1)/2$	0	$-1/2$
y_1	$1/2$	$1/2$	$1/2$	$1/2$
y_0	0	$-1/2$	$k/2$	$(k+1)/2$
x_k	$(k-1)/2$	$k/2$	$-1/2$	0
x_{k-1}	$(k-2)/2$	$(k-1)/2$	0	$1/2$
$\vdots$				$\vdots$
x_1	0	$1/2$	$(k-2)/2$	$(k-1)/2$
x_0	$-1/2$	0	$(k-1)/2$	$k/2$

Notice that all the x_i are collinear in $\mathbb{Z}^4$, and in any projection, so that arguing on $\mathbb{T}$-weights will not effectively deter monomials in the equations for $x_i x_j$.

The actual equations include

$$x_{i-1}x_{i+1} = x_i^2 + (AB)^{k-i-1}(LM)^{i-1}BM$$
$$y_1 x_i = ABx_{i+1} + LMx_{i-1}$$

All the equations not involving y_0, y_2 come from

$$\begin{matrix} y_1 & AB & x_0 & x_1 & \dots & x_{k-2} \\ & LM & x_2 & x_3 & \dots & x_k \\ & & x_1 & x_2 & \dots & x_{k-1} \\ & & & m_{01} & \dots & m_{0,k-1} \\ & & & & m_{ij} & \end{matrix}$$

where

$$m_{i,i+1} = (AB)^{k-3-i}(LM)^i BM$$

and (exponents need correcting)

$$m_{i,j} = \frac{(AB)^{i-j} - (LM)^{i-j}}{AB - LM}(AB)^i (LM)^{k-j} BM$$

On the other hand the $\mathbb{T}$-weight of $y_0 y_2$ does force all monomials in the long equations to be divisible by h.

Try again

$k = 7$

y_1	AB	x_0	x_1	x_2	x_3	x_4	x_5
	LM	x_2	x_3	x_4	x_5	x_6	x_7
		x_1	x_2	x_3	x_4	x_5	x_6
			A^4B^5M	$y_1A^3B^4M$	$y_1^2A^2B^3M - A^3B^4LM^2$	$y_1^3AB^2M - 2y_1A^2B^3LM^2$	dunno
				$A^3B^4LM^2$	$y_1A^2B^3LM^2$	$y_1^2AB^2LM^2 - A^2B^3L^2M^3$	$y_1^3BLM^2 - 2y_1AB^2L^2M^3$
					$A^2B^3L^2M^3$	$y_1AB^2L^2M^3$	$y_1^2BL^2M^3 - AB^2L^3M^4$
						$AB^2L^3M^4$	$y_1BL^3M^4$
							BL^4M^5

Same but subst $BM = z$, $AB = C$, $LM = D$

$k = 7$

y_1	C	x_0	x_1	x_2	x_3	x_4	x_5
	D	x_2	x_3	x_4	x_5	x_6	x_7
		x_1	x_2	x_3	x_4	x_5	x_6
			C^4z	y_1C^3z	$y_1^2C^2z - C^3Dz$	$y_1^3Cz - 2y_1C^2Dz$	dunno
				C^3Dz	y_1C^2Dz	$y_1^2CDz - C^2D^2z$	$y_1^3Dz - 2y_1CD^2z$
					C^2D^2z	y_1CD^2z	$y_1^2D^2z - CD^3z$
						CD^3z	y_1D^3z
							D^4z

with dunno $= (y_1^4 - 3y_1^2CD + C^2D^2)z$.

Same but float z

$$
\begin{array}{cccccccc}
y_1 z & Cz & x_0 & x_1 & x_2 & x_3 & x_4 & x_5 \\
 & Dz & x_2 & x_3 & x_4 & x_5 & x_6 & x_7 \\
 & & x_1 & x_2 & x_3 & x_4 & x_5 & x_6 \\
 & & & C^4 & y_1 C^3 & y_1^2 C^2 - C^3 D & y_1^3 C - 2y_1 C^2 D & y_1^4 - 3y_1^2 CD + C^2 D^2 \\
 & & & & C^3 D & y_1 C^2 D & y_1^2 CD - C^2 D^2 & y_1^3 D - 2y_1 CD^2 \\
 & & & & & C^2 D^2 & y_1 CD^2 & y_1^2 D^2 - CD^3 \\
 & & & & & & CD^3 & y_1 D^3 \\
 & & & & & & & D^4
\end{array}
$$

The bottom 6×6 matrix is the second wedge of

$$
\begin{array}{cccccc}
y_1^2 C/D - C^2 & y_1 C & CD & 0 & -D^2 & -y_1 D^2/C \\
-y_1 C^2/D & -C^2 & 0 & CD & y_1 D & y_1^2 D/C + D^2
\end{array}
$$

The general case

$$
\begin{array}{cccccccc}
y_1 z & Cz & x_0 & \dots & x_{i-1} & x_i & \dots & x_{k-2} \\
 & Dz & x_2 & \dots & x_{i+1} & x_{i+2} & \dots & x_k \\
 & & x_1 & \dots & x_i & x_{i+1} & \dots & x_{k-1} \\
 & & & C^{k-3} & \dots & & \dots & \dots \\
 & & & & C^{k-1-i} D^{i-2} & y_1 C^{k-2-i} D^{i-2} & \dots & \dots \\
 & & & & & C^{k-2-i} D^{i-1} & \dots & \dots \\
 & & & & & & \dots & \dots \\
 & & & & & & & D^{k-3}
\end{array}
$$

The bottom $(k-1) \times (k-1)$ block is the second wedge of a $2 \times (k-1)$ matrix any two consecutive columns of which (say $i-1, i$) reduce to

$$\begin{matrix} \dots & C^aD^b & 0 & \dots \\ \dots & 0 & C^cD^d & \dots \end{matrix}$$

with $a+c = k-2-i$ and $b+d = i-1$, and the rest of which is then fixed by requiring the $j-1, j$ minor to be $C^{k-2-j}D^{j-1}$ and the $j-2, j$ minor to be $y_1C^{k-2-i}D^{i-2}$.

$$\begin{matrix} \dots & y_1C^aD^{b-1} & C^aD^b & 0 & \dots \\ \dots & -C^{c+1}D^{d-1} & 0 & C^cD^d & \dots \end{matrix}$$

Part II
Mori flips of Type A

7 Introduction to Part II

To go from a diptych 6-fold V_{ABLM} to a Mori flip involves

(1) a suitable choice of 1-parameter subgroup $\mathbb{G}_m \subset \mathbb{T}$, or equivalently a grading of the coordinate ring $k[V_{ABLM}]$;

(2) a suitable regular codimension 2 section (or regular pullback) homogeneous under the $\mathbb{G}_m$-action;

(3) passing to the GIT quotient by this $\mathbb{G}_m$ action as described in Reid [Wf?] and in 1.3.2.

We explain how to make these choices for any diptych 6-fold in Theorem 8.5, to construct Mori flips of Type A. We sketch the converse: finding a diptych variety to realise a given flip in this way (Theorem 8.6). The key is Mori's division algorithm [M3].

7.1 First example

exa!first

Let V_{ABLM} be the short diptych I$(d, e, 1)$ of Figure 7.1.

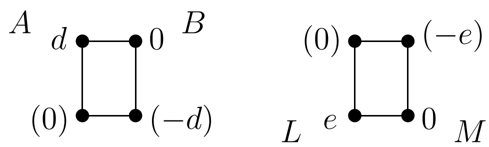

Figure 7.1: The short diptych with tags d, e

Then V_{ABLM} is just $\mathbb{A}^6_{\langle x_{01} y_{01} AL\rangle}$ with B, M given by the two righthand tag equations

$$V_{ABLM}\colon \qquad x_0y_1 = Ax_1^d + M, \quad x_1y_0 = B + Lx_0^e. \tag{7.1}$$

Setting $A = u^\alpha$, $B = u^\beta$, $L = t^\lambda$, $M = t^\mu$ defines a regular pullback of V_{ABLM}, the codimension 2 complete intersection

$$V_{ut}\colon \qquad x_0y_1 = u^\alpha x_1^d + t^\mu, \quad x_1y_0 = u^\beta + t^\lambda x_0^e. \tag{7.2}$$

We make these equations homogeneous, giving the "section" u and "elephant" t the weights $\operatorname{wt} u = 0$, $\operatorname{wt} t = 1$; we choose $\lambda = em_1$ and $\mu = dm_2$, and give the top x_1, y_1 positive weights $\operatorname{wt} x_1 = m_2$, $\operatorname{wt} y_1 = m_1 + dm_2$; homogeneity of the two equations fixes the bottom weights to be negative: $\operatorname{wt} x_0 = -m_1$, $\operatorname{wt} y_0 = -m_2 < 0$.

These weights determine an action of $\mathbb{G}_m$ on V_{ut} as a 1-parameter subgroup $\mathbb{G}_m \subset \mathbb{T}$ of the torus $\mathbb{T} = (\mathbb{G}_m)^4$ that acts on V_{ABLM}. Passing to the GIT quotient by this $\mathbb{G}_m$ action, in other words to the Proj, describes a flip $X \to T \leftarrow X^+$. The two flipping curves $C \subset X$ and $C^+ \subset X^+$ are weighted $\mathbb{P}^1$s represented by the top and bottom of our diptych panel: $C = \mathbb{P}(m_2, m_1 + dm_2)_{x_k, y_l}$ and $C^+ = \mathbb{P}(m_1, m_2)_{x_0, y_0}$, so that $C^+ = \mathbb{P}^1$ with homogeneous coordinates the weighted ratio $x_0^{m_2} : y_0^{m_1}$ between the bottom two monomials in Figure 7.1. Before the flip, the extremal neighbourhood X is a union of two affine pieces $x_k \neq 0$, each a Type A terminal hyperquotient given by

$$x_k = 1 \;\; (x_0 y_1 = u^\alpha x_1^d + t^\mu)/\tfrac{1}{m_2}(-m_1, m_1, 0, 1) \quad \text{with} \quad y_0 = B + L x_0^e, \text{ and}$$

$$y_l = 1 \;\; (x_1 y_0 = u^\beta + t^\lambda x_0^e)/\tfrac{1}{m_1 + dm_2}(-m_2, m_2, 0, 1) \quad \text{with} \quad x_0 = u^\alpha x_1^d + t^\mu.$$

This explains our choice of tents having top and bottom $S_0 = S_2 = \mathbb{A}^2$ rather than more general toric surfaces, and thus our choice of long rectangles.

7.2 The explicit manifesto

The *Mori category* consists of (quasi-)projective 3-folds with $\mathbb{Q}$-factorial terminal singularities. The singularities were classified into explicit lists by Mori [M2]; see also [YPG], Theorem 6.1. The other ingredients of the Mori category are the steps of the minimal model program

(i) divisorial contractions (surface $\to$ point) (Kawakita [Kk1], [Kk2]);

(ii) divisorial contractions (surface $\to$ curve) (Tziolas [Tz1], [Tz2]);

(iii) flips (Mori [M1], [M3], Kollár and Mori [KM]);

the final models

(iv) Mori fibre space conic bundles $X \to S$ (Prokhorov [Pr1], [Pr2], Mori and Prokhorov [MP]);

(v) Mori fibre space del Pezzo fibrations (Corti [Co1], Pukhlikov [Pu1], [Pu2]);

(vi) Fano 3-folds ([Si]);

and

(vii) Sarkisov links between the 3-fold Mfs in (iv–vi) (Sarkisov [Sa], Corti [Co1], [Co02], Corti, Pukhlikov and Reid [CPR], Corti and Mella [CM], Brown, Corti and Zucconi [BCZ]).

As indicated by the selective references, much progress has been made on each of these items since the Minimal Model program was established in the 1980s; one hopes in the fullness of time to see many more explicit results, even concrete lists of varieties.

8 Mori flips and diptych varieties

8.1 Mori's continued division algorithm

8.1.1 A summary of Mori's algorithm

Theorem 2.2 of [M3] proves that any semistable extremal neighbourhood $C \subset X$ has completion along C isomorphic to the completion of the following model for suitable m_i, a_i, g_i.

Input Two patches of an extremal neighbourhood with glueing rules: for $i = 1, 2$,

$$U_i \colon \big(\xi_i \eta_i = g_i(\zeta_i^{m_i}, u)\big) \subset \frac{1}{m_i}(1, -1, a_i, 0)$$

where the variables are in order $\xi_i, \eta_i, \zeta_i, u$ and $g_i \in \mathbb{C}[\![u]\!][\zeta_i^{m_i}]$. The glueing is achieved by

$$\xi_1^{m_1} = \xi_2^{-m_2}, \quad \zeta_1 \xi_1^{-a_1} = \zeta_2 \xi_2^{m_2 - a_2}$$

with the glueing of η_i implicit in the equations.

Initial data from the input Two types of data, for $i = 1, 2$.

Discrete data: read off the integers m_i, a_i and set

$$\rho_i = \deg_T g_i(T, u), \quad \alpha_i = \operatorname{val}_u g_i(T, u).$$

Set two auxilliary integers

$$\delta = a_1 m_2 + a_2 m_1 - m_1 m_2,$$

and

$$\varepsilon = (\delta \rho_1 \rho_2)^2 - 4\rho_1 \rho_2 = \operatorname{discr}(\rho_1 x_1^2 - \delta \rho_1 \rho_2 x_1 x_2 + \rho_2 x_2^2).$$

(The δ, ε appearing here are quite different from those of Theorem 3.5. Note that $\delta > 0$ since it comes from the canonical class. And, except in a handful of small cases having in particular $\rho_1, \rho_2 \leq 4$, also $\varepsilon > 0$.) It is a requirement coming from the $\mathbb{G}_m$ action that $2m_1 > \delta \rho_2 m_2$: if this is not the case, swap the roles of $1, 2$ in the indexing and compute again.

Continuous data: construct the homogeneous polynomials

$$G_i(T, S) = g_i(T/S, u) S^{\rho_i} \in \mathbb{C}[\![u]\!][S, T]$$

and note that $G_i(T, 1)$ is reduced. We arrange for $G_i(0, 1) = u^{\alpha_i}$ using coordinate change in x_i, y_i.

Discrete part of the algorithm Define

n	1	2	3	4	
ρ_i	ρ_1	ρ_2	ρ_1	ρ_2	repeat 4-periodically
α_i	α_1	α_2	$\alpha_1(\rho_1-1)$	$\alpha_2(\rho_2-1)$	repeat 4-periodically
$\alpha_{i,2}$	α_1	α_2			repeat 2-periodically

The powers of z in the tag equations (or, equally, the $\mathbb{G}_m$ weights) come from

n	1	2	$\cdots$	$d(k+1)$
$d(n)$	m_1	m_2	$(*)$	$-d(k-1)$

where the missing entries $(*)$ are computed by $d(n+1)+d(n-1)=\delta\rho_n d(n)$, and k is the first positive integer for which the $d(k)\leq 0$; no further values of $d(n)$ are required. (Here Mori also defines the modified sequence $d^*(n)$; in diptych terms, this computes the grading around the bottom of the long rectangle as well as down the d,e side.)

The powers of u in the tag equations come from

n	0	1	2	3
$e(n)$	0	$-\alpha_1$	$-\alpha_2$	0

and $e(n+1)+e(n-1)=\delta\rho_n e(n)+\delta\alpha_{n-2}-\alpha_{n-1,2}$.

The polarisations of the singularities are generated by

n	1	2	$\cdots$	$k+1$	$k+2$
$c(n)$	a_1	m_2-a_2	$(*)$	$-c(k-1)$	$-c(k)$

where the missing entries $(*)$ are computed by $c(n+1)+c(n-1)=\delta\rho_n c(n)$.

Continuous part of the algorithm Set

n	1	2	3	4	
G_i	G_1	G_2	$G_1(u^{\alpha_1}S,T)/u^{\alpha_1}$	$G_2(u^{\alpha_2}S,T)/u^{\alpha_2}$	repeat 4-periodically.

Then compute sections of bundles $F_i\in H^0(X,L_i)$ – we treat them simply as new variables. We arrange them schematically (together with alternative notation $x_1,\dots,y_2'$ that is used later) as

$$\begin{array}{cc} F_2 & F_1 \\ \hline F_3 & F_0 \\ F_4 & \\ \vdots & \\ F_{k-2} & \\ F_{k-1} & F_{k+2} \\ \hline F_k & F_{k+1} \end{array} \quad = \quad \begin{array}{cc} x_1 & x_2 \\ \hline y_2 & y_1 \\ & \\ \vdots & \\ & \\ y_2' & x_1' \\ \hline y_1' & x_2' \end{array}$$

satisfying equations

$$F_3F_1 = G_2(z^{m_2}, F_2^\delta) \quad \text{and} \quad F_2F_0 = G_1(z^{m_1}, F_1^\delta)$$

at the top and then defined by tag equations

$$F_{n+1}F_{n-1} = G_{n-2}(F_n^\delta, u^{e(n)}z^{d(n)}) \quad \text{for} \quad 3 \le n \le k-1.$$

(Theorem 3.10 of [M3] proves that F_{n-1} divides G_{n-2}.) We extend beyond F_k by

$$\begin{aligned} F_{k+1}F_{k-1} &= G_{k-2}(F_k^\delta, u^{e(k)}z^{d(k)})z^{-\rho_{k-2}d(k)} \\ F_{k+2}F_k &= G_{k-1}(F_{k+1}^\delta, u^{e(k+1)}z^{d(k+1)})z^{-\rho_{k-1}d(k+1)}. \end{aligned}$$

(Theorem 3.12 of [M3] proves this extended division.)

Output when $d(k) < 0$ The neighbourhood $C \subset X$ is a flipping neighbourhood. Set

$$\begin{matrix} m_1' = -d(k+1), & a_1' = c(k-1) \bmod m_1' \\ m_2' = -d(k), & a_2' = c(k) \bmod m_2' \end{matrix} \quad \text{and} \quad g_i'(T,u) = G_i'(T,1)$$

where $c \bmod m$ means the residue of c in $1,\dots,m$. (Note that the m_i' are indexed in the opposite order to Section 8.2 below.)

Two patches of the flipped neighbourhood with glueing rules:

$$U_i' \colon \bigl(\xi_i'\eta_i' = g_i'((\zeta_i')^{m_i'}, u)\bigr) \subset \frac{1}{m_i'}(1,-1,a_i',0)$$

where the variables are in order $\xi_i', \eta_i', \zeta_i', u$ and $g_i' \in \mathbb{C}[\![u]\!][(\zeta_i')^{m_i'}]$. The glueing is achieved by

$$(\xi_1')^{m_1'} = (\xi_2')^{-m_2'}, \quad \zeta_1'(\xi_1')^{-a_1'} = \zeta_2'(\xi_2')^{m_2'-a_2'}$$

with the glueing of η_i' implicit in the equations.

Output when $d(k) = 0$ The neighbourhood $C \subset X$ is a divisorial neighbourhood. Set

$$m = -d(k+1), \quad a = c(k-1) \bmod m \quad \text{and} \quad g(T,u) = G_{k-1}(T,1).$$

A patch on the image of the contraction:

$$U\colon \big(\xi\eta = g(\zeta^m, u)\big) \subset \frac{1}{m}(1,-1,a,0)$$

where the variables are in order ξ, η, ζ, u and $g \in \mathbb{C}[\![u]\!][\zeta^m]$.

Mori calculates much more from these equations. For example, [M3], Theorem 3.13 shows that $C = (F_{k-1} = F_{k+2} = u = 0) \subset X$, and Proposition 3.14 then calculates that

$$L_n \cdot C = \frac{d(n)}{m_1 m_2}.$$

8.1.2 Mori's projective model of the flip

Given discrete parameters as above together with the polynomials G_1, G_2, Mori describes the variety

$$\mathcal{X} = \begin{pmatrix} x_1y_1 & = & G_1(z^{m_1}, x_2^\delta) \\ x_2y_2 & = & G_2(z^{m_2}, x_1^\delta) \end{pmatrix} \subset \mathbb{A}^5_{\langle x_1,x_2,y_1,y_2,z\rangle} \times \Delta(u), \qquad (8.1)$$

where $\Delta(u)$ is a formal neighbourhood of the origin, $\operatorname{Spec}\mathbb{C}[\![u]\!]$. This variety has a $\mathbb{G}_m$ action, described explicitly in [M3] Remark 2.7, and the flip (or divisorial contraction) of the initial extremal neighbourhood is described by the variation of this $\mathbb{G}_m$ action. This is carried out explicitly in Theorem 4.7 of [M3] to compute the output of the algorithm described above.

8.2 Mori flips from diptych varieties

s!lrflip

We explain how a diptych variety determines a family of canonical covers of Mori flips. There are several steps: we choose a $\mathbb{G}_m$ action on V, then specialise the annotation variables A, B, L, M to reduce V to a 4-fold; the standard variation of GIT quotient now describes a 3-fold flip, and we must check whether it is a Mori flip.

8.2.1 Diptych varieties and $\mathbb{G}_m$ actions

Let $V = V_{ABLM}$ be a diptych variety based on the pair of long rectangles X_{AB} and Y_{LM} intersecting in the tent T. We determine a $\mathbb{G}_m$ action on V by assigning integer weights to all the variables so that the equations are homogeneous with respect to these weights.

l!act

Lemma 8.1 *Any choice of weights for x_0, x_1, y_0, y_1, A, B, L, M for which the tag equations at the bottom corners are homogeneous uniquely determines a $\mathbb{G}_m$ action on V.*

Of course, there are only really 4 degrees of freedom in the choice of weights, since the trinomial tag equations impose 4 linear conditions.

Proof The diptych is constructed by unprojection. This construction is equivariant for the action of $\mathbb{T}$; each unprojection ideal is homogeneous, and then the unprojection variable can be chosen to lie in one homogeneous piece of the unprojection Hom space. Q.E.D.

Nearly following Mori [M3], write

$$\operatorname{wt} x_k = m_2, \ \operatorname{wt} y_l = m_1 \quad \text{and} \quad \operatorname{wt} x_0 = m_1', \ \operatorname{wt} y_0 = m_2'. \tag{8.2}$$

for the weights of the corner variables.

l!wts

Lemma 8.2 *Suppose that V has a $\mathbb{G}_m$ action with $\operatorname{wt} A = \operatorname{wt} B = 0$, and assume that $\operatorname{codim} V > 2$. Let $p/q = [a_k, a_{k-1}, \dots, a_1]$ and $r/s = [b_l, b_{l-1}, \dots, b_1]$. Then*

$$\begin{pmatrix} -m_1' \\ -m_2' \end{pmatrix} = \begin{pmatrix} \operatorname{wt} L/(a_0' - a_0) \\ \operatorname{wt} M/(b_0' - b_0) \end{pmatrix} = \begin{pmatrix} q & -p \\ -r & s \end{pmatrix} \begin{pmatrix} m_1 \\ m_2 \end{pmatrix}.$$

If $m_1', m_2' < 0$ then x_0, y_0, A, B are the only variables with weight ≤ 0.

To construct examples, we usually use the equations expressed in the form

$$\begin{pmatrix} m_1 \\ m_2 \end{pmatrix} = \begin{pmatrix} s & p \\ r & q \end{pmatrix} \begin{pmatrix} -m_1' \\ -m_2' \end{pmatrix} \quad \text{and} \quad \begin{matrix} \operatorname{wt} L = (a_0 - a_0')m_1' \\ \operatorname{wt} M = (b_0 - b_0')m_2' \end{matrix}.$$

Proof Lemma 2.10 shows $\operatorname{wt} x_0 = \operatorname{wt} x_k^p y_l^{-q} A^q$ and $\operatorname{wt} y_0 = \operatorname{wt} x_k^{-s} y_l^r B^s$, implying the first claim, that

$$\operatorname{wt} x_0 = -qm_1 + pm_2 \quad \text{and} \quad \operatorname{wt} y_0 = rm_1 - sm_2.$$

The same lemma computes the tag equations at the bottom corners as

$$x_1 y_0 = y_1^{-a_0} h_{1,0}(A,B) + x_0^{a_0'} L, \quad x_0 y_1 = x_1^{-b_0} h_{0,1}(A,B) + y_0^{b_0'} M \tag{8.3}$$

for monomials $h_{0,1}, h_{1,0}$ in A, B. Suppose that $a_0 = 0$; a similar argument works if instead $b_0 = 0$. The first equation has weight zero and so $\operatorname{wt} x_1 > 0$. Since $b_0 \leq 0$, the second equation has nonnegative weight and so $\operatorname{wt} y_1 > 0$. Both L, M have strictly positive weight since $a_0', b_0' > 0$ (under the codimension restriction). All other variables now have positive weight since the weight function is linear (or by considering the tag equations down the edges of the tent).

For the remaining claim, we first show that

$$\begin{pmatrix} \operatorname{wt} L \\ \operatorname{wt} M \end{pmatrix} = \begin{pmatrix} -a_0 r' + a_0' q & a_0 s' - a_0' p \\ b_0 q' - b_0' r & -b_0 p' + b_0' s \end{pmatrix} \begin{pmatrix} m_1 \\ m_2 \end{pmatrix} \tag{8.4}$$

where $p'/q' = [a_k, a_{k-1}, \dots, a_2]$ and $r'/s' = [b_l, b_{l-1}, \dots, b_2]$. Lemma 2.10 computes that $x_1 = x_k^{p'} y_l^{-q'} A^{q'}$ and $y_1 = x_k^{-s'} y_l^{r'} B^{s'}$, and therefore

$$\operatorname{wt} x_1 = -q' m_1 + p' m_2, \quad \operatorname{wt} y_1 = r' m_1 - s' m_2.$$

Using equations (8.3),

$$\begin{aligned} \operatorname{wt} L &= -a_0 \operatorname{wt} y_1 - a_0' m_1' \\ &= (-a_0)(r' m_1 - s' m_2) - a_0'(-q m_1 + p m_2) \\ &= (-a_0 r' + a_0' q) m_1 + (a_0 s' - a_0' p) m_2 \end{aligned}$$

and

$$\begin{aligned} \operatorname{wt} M &= -b_0 \operatorname{wt} x_1 - b_0' m_2' \\ &= (-b_0)(-q' m_1 + p' m_2) - b_0'(r m_1 - s m_2) \\ &= (b_0 q' - b_0' r) m_1 + (-b_0 p' + b_0' s) m_2, \end{aligned}$$

which proves (8.4). Now if $a_0 = 0$ then also $r = q'$ and $s = p'$, and the claim follows from (8.4) with these values. Q.E.D.

Definition 8.3 An action is *of flipping type* if one of the following sign conditions is met:

$$\text{either} \quad m_1, m_2 > 0 \text{ and } m_1', m_2' < 0, \quad \text{or} \quad m_1, m_2 < 0 \text{ and } m_1', m_2' > 0.$$

Corollary 8.4 *Actions of flipping type on V for which X_{AB} is the $\mathbb{G}_m$ cover of an elephant are determined by a pair $(-m_1', -m_2') \in \mathbb{N}^2$.*

8.2.2 Specialising diptych varieties to 4 dimensions

We replace A, B, L, M by two variables u, z. There are several different ways we could manage the specialisation. In the first place we compute *monomial specialisation*, that is, we make assignments of the form

$$A = u^\alpha, \quad B = u^\beta, \quad L = z^\lambda, \quad M = z^\mu$$

for integers $\alpha, \beta, \lambda, \mu > 0$. (The case when one or more exponent is zero will also give flips, but not of type k2A.) Later we allow more general polynomials or power series, but in any case these expressions must be homogeneous.

th!monfl

Theorem 8.5 *Let $V = V(A, B, L, M)$ be a diptych variety. Any pair of integers $m'_1, m'_2 < 0$ determine a $\mathbb{G}_m$ action on V of flipping type with*

$$\operatorname{wt} x_0 = m'_1, \;\; \operatorname{wt} y_0 = m'_2, \;\; \operatorname{wt} x_k = -(sm'_1 + pm'_2), \;\; \operatorname{wt} y_l = -(rm'_1 + qm'_2)$$
$$\operatorname{wt} A = \operatorname{wt} B = 0, \quad \operatorname{wt} L = (a_0 - a'_0)m'_1, \quad \operatorname{wt} M = (b_0 - b'_0)m'_2.$$

Any pair of integers $\alpha, \beta > 0$ determine a monomial specialisation

$$A = u^\alpha, B = u^\beta, L = z^{(a_0 - a'_0)m'_1}, M = z^{(b_0 - b'_0)m'_2}$$

that is compatible with the $\mathbb{G}_m$ action for $\operatorname{wt} u = 0$, $\operatorname{wt} z = 1$. The resulting flip diagram is a semistable Mori flip in which the quotient of $(u = 0) \subset V$ is a Du Val elephant and the quotient of $(z = 0) \subset V$ is a cyclic quotient hyperplane section. To check

Proof The only thing to check is that X^- has terminal singularities. This is clear from the trinomial form of the two equations at the top of the diptych, as in Example 7.1. Q.E.D.

8.2.3 A comparison of diptychs and the division algorithm

We run Mori's algorithm for a diptych variety in several steps: compute two patches before the flip, that is, the two tag equations at the top of the diptych variety localised away from the origin; determine m_i, a_i, α_i, G_i, ρ_i, F_i from these two patches; apply Mori's algorithm; and compare the outcome of Mori's algorithm with the two patches determined by the localised tag equations at the bottom of the diptych variety.

The diptych variety with a choice of $\mathbb{G}_m$ action Consider the diptych variety

$$\begin{array}{cc} 2 & 1 \\ \hline 5 & 3 \\ 2 & 2 \\ 5 & 2 \\ & 3 \\ \hline 0 & -4 \end{array} \qquad \begin{array}{cc} 0 & -4 \\ \hline 5 & 3 \\ 2 & 2 \\ 5 & 2 \\ & 3 \\ \hline 2 & 1 \end{array} \qquad \text{with flipping weights (the minimal choice):} \qquad \begin{array}{cc} 49 & 87 \\ \hline 11 & 38 \\ 6 & 27 \\ 1 & 16 \\ & 5 \\ \hline -1 & -1 \end{array}$$

This has partial continued fractions

$$\begin{array}{ll} [2,5,2]= 16/9 & [1,3,2,2]= 4/7 \\ [2,5,2,5]= 71/40 = p/q & [1,3,2,2,3]= 9/16 = r/s. \end{array}$$

The top two equations are

$$x_3y_5 = x_4^2A + L^9M^{16} \qquad x_4y_4 = y_5B + x_3^4L^4M^7. \tag{8.5}$$

The choice of weights $m_1 = 87$, $m_2 = 49$ come from setting $m_1' = m_2' = -1$ in Lemma 8.2, the smallest possibility.

Patches on the flip according to the diptych variety We make the specialisation $A = u^{\alpha_2}$, $B = u^{\alpha_1}$. The weights force the specialisation $L = z^{2m_1'}$, $M = z^{5m_2'}$ which in this case is $L = z^2$, $M = z^5$.

The top corner tag equations (8.5) give the two patches

$$x_4 = 1\colon \bigl(x_3y_5 = u^{\alpha_2} + z^{98}\bigr) \quad \subset \quad \frac{1}{49}(11, 87, 0, 1) = \frac{1}{49}(1, -1, 0, 9)$$

$$y_5 = 1\colon \bigl(x_4y_4' = u^{\alpha_1} + z^{435}\bigr) \quad \subset \quad \frac{1}{87}(49, 38, 0, 1) = \frac{1}{87}(1, -1, 0, 16)$$

where the usual second tag equation $x_4y_4 = B + (x_4^2A + L^9M^{16})^4L^4M^7$ is brought to normal form with the coordinate change $y_4' = y_4 - x_4^7A^4L^4M^7 - \cdots$.

The patch equations we get after the flip are

$$x_1y_0 = L + A^9B^{16} = z^2 + u^{16\alpha_1+9\alpha_2}$$

and

$$x_0y_1 = M + (x_0^2L + A^9B^{16})^4A^4B^7 = z^5 + \cdots + u^{71\alpha_1+40\alpha_2},$$

which can be put in standard form by $y_1' = y_1 - \cdots$.

The quotients of this give a semistable flip. The elephant is

$$X_{AB}/\!\!/\mathbb{G}_m = \mathbb{C}[x_0x_1, y_0^5y_1, u]/\text{equations} = \mathbb{C}[u,v,w]/(vw - A^{49}B^{87}).$$

We could compute the section too. As far as the diptych variety is concerned, this is the end of the calculation.

Mori's division algorithm The two patches above are the starting point for Mori's calculations.

$$\rho_1 = 5, m_1 = 87, a_1 = 16\colon \quad U_1\colon (\xi_1\eta_1 = u^{\alpha_1} + z^{435}) \quad \subset \quad \frac{1}{87}(1,-1,0,16)$$
$$\rho_2 = 2, m_2 = 49, a_2 = 40\colon \quad U_2\colon (\xi_2\eta_2 = u^{\alpha_2} + z^{98}) \quad \subset \quad \frac{1}{49}(-1,1,0,40)$$

(Following Mori, we arrange for the local coordinate along the extremal curve to have weight 1 in each local patch; this variable is ξ_1 in the first patch and η_2 in the second.) The auxilliary variables are

$$\delta = a_2m_1 + a_1m_2 - m_1m_2 = 1, \quad \varepsilon = (\delta\rho_1\rho_2)^2 - 4\rho_1\rho_2 = 60.$$

[M3], Definition 3.2 computes $G_i, \rho_i, \alpha_i, \alpha_{i,2}, d(i), e(i)$ and Definition 3.11 gives $d(i)$. Note below that $d(1) > d(3)$, and $d(6) < 0$ so $k = 6$.

n	0	1	2	3	4	5	6	7
ρ_n		5	2	5	2	5	2	
α_n		α_1	α_2	$4\alpha_1$	α_2	α_1	α_2	
$\alpha_{n,2}$		α_1	α_2	α_1	α_2	α_1	α_2	
$d(n)$		m_1	m_2	$2m_2 - m_1$	$9m_2 - 5m_1$	$16m_2 - 9m_1$	$71m_2 - 40m_1$	
		87	49	11	6	1	-1	-1
$e(n)$	0	$-\alpha_1$	$-\alpha_2$	0	α_1	$\alpha_1 + \alpha_2$	$8\alpha_1 + 4\alpha_2$	$14\alpha_1 + 8\alpha_2$
$c(n)$		16	9	2	1	0	-1	

Recall that $d(n)$ are the $\mathbb{G}_m$ weights and that $c(n)$ are computed in the same way as $d(n)$, with initial values $a_1 = 16$, $m_2 - a_2 = 9$ in place of m_1, m_2.

We read G_1, G_2 from the initial patches and compute G_3, G_4 according to the rule. From then on, G_i repeat 4-periodically.

$$\boxed{\begin{array}{rcl} G_1(T,S) & = & T^5 + u^{\alpha_1} S^5 \\ G_2(T,S) & = & T^2 + u^{\alpha_2} S^2 \\ G_3(T,S) := G_1(u^{\alpha_1} S, T)/u^{\alpha_1} & = & T^5 + u^{4\alpha_1} S^5 \\ G_4(T,S) := G_1(u^{\alpha_2} S, T)/u^{\alpha_2} & = & T^2 + u^{\alpha_2} S^2 \\ G_5(T,S) & = & T^5 + u^{\alpha_1} S^5 = G_1(T,S) \end{array}}$$

[M3] Definition 3.9 and Theorem 3.10 compute F_i by the formulas

$$F_{n-1}F_{n+1} = G_{n-2}(F_n^\delta, z^{d(n)} u^{e(n)}) \quad \text{for} \quad 3 \le n \le k-1$$

and

$$F_{k-1}F_{k+1} = G_{k-2}(F_k^\delta z^{-d(k)}, u^{e(k)}),$$
$$F_k F_{k+2} = G_{k-1}(F_{k+1}^\delta z^{d(k-1)}, u^{e(k+1)}).$$

In this example, the F_i will correspond to diptych variety variables as

F_0	F_1	F_2	F_3	F_4	F_5	F_6	F_7	F_8
y_4	y_5	x_4	x_3	x_2	x_1	x_0	y_0	y_1

The equations (with F_i replaced by x_i as above) read:

n	Mori	diptych
3	$x_2x_4 = x_3^5 + u^{\alpha_1} z^{55}$	$x_2x_4 = x_3^5 + BL^5M^9$
4	$x_1x_3 = x_2^2 + u^{2\alpha_1+\alpha_2} z^{12}$	$x_1x_3 = x_2^2 + AB^2LM^2$
5	$x_0x_2 = x_1^5 + u^{9\alpha_1+5\alpha_2} z^5$	$x_0x_2 = x_1^5 + A^5B^9M$
6	$x_1y_0 = x_0^2z^2 + u^{16\alpha_1+9\alpha_2}$	$x_1y_0 = x_0^2L + A^9B^{16}$
7	$x_0y_1 = y_0^5z^5 + u^{71\alpha_1+40\alpha_2}$	$x_0y_1 = y_0M + x_1^4A^4B^7.$

So Mori's algorithm computes the same patches as the diptych variety. (The first four are identical after substitution. The final equation is different, but determines the patch after the flip.)

The first step in Mori's division algorithm is to show that

$$y_5^5(x_3^5 + u^{\alpha_1} z^{55}) z^\# u^\# \equiv 0 \bmod x_4$$

where $x^{\#}$ denotes any sufficiently high power of x for the following calculation. Indeed

$$\begin{aligned} y_5^5(x_3^5 + u^{\alpha_1} z^{55}) z^{\#} u^{\#} &= \big((y_5 x_5)^5 + y_5^5 u^{\alpha_2} z^{55}\big) z^{\#} u^{\#} \\ &= \big((z^{98} + u^{\alpha_2} x_4^2)^5 + y_5^5 u^{\alpha_2} z^{55}\big) z^{\#} u^{\#} \\ &\equiv (z^{435} + y_5^5 u^{\alpha_2}) z^{\#} u^{\#} \\ &= \big((x_4 y_4 - y_5^5 u^{\alpha_1}) + y_5^5 u^{\alpha_2}\big) z^{\#} u^{\#} \\ &\equiv 0. \end{aligned}$$

8.3 Diptych varieties from Mori flips

This is our main application and original motivation.

Theorem 8.6 *Let $C \subset X$ be an extremal neighbourhood of type k2A with $\delta = 1$. Then there is*

- *a diptych variety V_{ABLM}*
- *specialisations of A, B, L, M as functions of the variables $x_1, \dots, x_k$, $y_1, \dots, y_l$ and two additional variables u, z; the variety after specialisation is denoted V_{uz}.*
- *a $\mathbb{G}_m$ action on V_{uz} for which $\operatorname{wt} u = 0$ and $\operatorname{wt} z = 1$*

such that a formal neighbourhood of $C \subset X$ is isomorphic to a formal neighbourhood of $\mathbb{P}^1(x_k, y_l)$ in the $\mathbb{G}_m$ quotient of V_{uz} polarised by positive weight. The contraction of $C \subset X$ (and also its flip, when this is a flipping neighbourhood) is realised by the variation of this $\mathbb{G}_m$ quotient.

Moreover, restricting to the locus $z = 0$ in each quotient describes an elephant of the extremal neighbourhood $C \subset X$, while $u = 0$ describes a section of it.

We want to prove this in two steps. The choice of diptych and of group action corresponds to the discrete part of Mori's algorithm; the specialisations correspond to the continuous part.

8.3.1 The numerical part

A diptych is determined (up to the symmetries of a rectangle) by the pair of tags d, e down one side. Given a flip of type k2A, these are computed by

$$d = \delta\rho_2 = \rho_2, \quad e = \delta\rho_1 = \rho_1,$$

since we restrict attention to the case $\delta = 1$. This provides the diptych variety V_{ABLM}.

The weights of the group action are determined on the x_i and y_j as follows. The indices of the singularities on $C \subset X$ are the orders of the stabilisers along the x_k and y_l axes; so these variables are given weights m_2 and m_1 respectively. The specialisation we make is of the form

$$A = u^{\alpha_2} + \text{higher order terms in } u, \quad B = u^{\alpha_1} + \text{higher order terms in } u.$$

In particular, A and B must both have weight 0. The weights of all other x_i, y_j are then determined by the homogeneity of the tag equations on V_{AB}. Finally, the weights of L, M are determined by the homogeneity of, say, the two equations at the top of the diptych.

8.3.2 Choosing the specialisations

We are required only to solve for A, B, L, M so that the initial (top) two equations of the specialised diptych variety V_{uz} equal the two equations of Mori's projective model (modulo increasing formal powers of u) given in section 8.1.2. We omit this.

9 Open problems

Does V_{ABLM} have more symmetry? We noted in the introduction that the 6-fold V_{ABLM} has an effective action of $(\mathbb{G}_m)^4$. It is possible that it has a bigger group of symmetries, or even that it is quasi-homogeneous under a bigger group, not necessarily preserving the toric sections. A boring example is $\mathrm{I}(d, e, 1)$ when the pair of rectangles has $k = l = 0$ (see also 7.1); then the equations include $B = \cdots$, $M = \cdots$, so that $V_{ABLM} = \mathbb{A}^6$ and has a huge automorphism group.

Recurring continued fractions? Family I is built from 2-step recurrent continued fractions $[d, e, d, e, \dots]$. As is well known, these are convergents to quadratic irrationalities: the quadratic

$$ex^2 - dex + d = 0 \tag{9.1}$$

has roots the recurrent continued fraction $\xi = [d, e, d, e, \dots]$ and its complement $[2, \dots, 2, 3, 2, \dots, 2, 3, \dots]$. Where does the quadratic irrationality come from? In Mori's context, we guess it comes from comparing the two quadratic intersection pairings of two nonsingular surfaces, the minimal resolution of the elephant and section. What does it really mean?

More general tents? We discussed in Section 1.3 how our level of generality is driven by Mori flips of Type A. How widely our methods apply to more general tents and toric extensions forms a portfolio of interesting research problems.

It would be interesting to understand deformations such as those of Lemma 2.11 and Main Theorem 1.2.3 in the general case of a number of cyclic quotient singularities meeting as a cycle transversely in their 1-strata. In this paper, we work out a case in which we deform a union of four surfaces.

More general flips? Can we do the same for flips of type D and E? The ideology of Reid [Wf?] is that passing to the $\mathbb{G}_m$ cover relates a wide class of flips to variation of GIT quotients. Next, this should reduce the study of Mori 3-fold flips to deformation of $\mathbb{G}_m$ covers of Du Val singularities. In this paper we have carried out this program for Type A flips, and in the process stumbled on a vast new theory of diptych varieties. It is possible that $\mathbb{G}_m$ covers of flips of type D and E hold similar treasures. The alternative is that the more exotic flips are much more restricted, and correspond mostly to rather simple graded rings. Extending the results of Brown [B] to codimension 2 and 3 might be a way into this problem area.

The geometry of flips? Diptych varieties and Mori's division algorithm contain many clues to the geometry of flips. As one example, we see one family of flips degenerating into another. The passage to a minimal basis of a long rectangle (which is nontrivial only in the case when one of d, e equals 1) raises the possibility of distinct diptych varieties having a common panel, say X_{AB} being the same in each. For example,

$$X_{AB} = \begin{array}{cc} 2 & 1 \\ \hline 4 & 3 \\ 2 & 2 \\ & 2 \\ \hline 0 & -1 \end{array} \quad \text{can be partnered by either of} \quad \begin{array}{cc} -2 & 0 \\ \hline 4 & 3 \\ 2 & 2 \\ & 2 \\ \hline 1 & 3 \end{array} \quad \text{and} \quad \begin{array}{cc} 0 & -3 \\ \hline 4 & 3 \\ 2 & 2 \\ & 2 \\ \hline 4 & 1 \end{array}.$$

At the level of flips, this gives two distinct families of flips having the same elephant (both before and after the flip). Since the deformation problem for the elephant is unobstructed (see Section 1.3.7), these do not represent two different components of flips, but one family degenerating into the other.

References

[BR] G. Brown and M. Reid, Anyone know these guys? 11 pp. Get from `www.warwick.ac.uk/staff/Miles.Reid/Aflip/index1.html`

Short separate section that we intend to work into this paper.

[Si] S. Altınok, G. Brown and M. Reid, Fano 3-folds, K3 surfaces and graded rings, in Topology and geometry (Singapore, 2001), Ed. A. J. Berrick and others, Contemp. Math. 314, AMS, 2002, pp. 25–53, preprint math.AG/0202092, 29 pp.

[A] Klaus Altmann, One parameter families containing three dimensional toric Gorenstein singularities, in *Explicit birational geometry of* 3*-folds*, A. Corti and M. Reid (eds), CUP 2000, pp. 21–50

[B] Gavin Brown, Flips arising as quotients of hypersurfaces, Math. Proc. Cambridge Philos. Soc. **127** (1999) 13–31

[B2] Gavin Brown, Pluricanonical cohomology across flips, Bull. London Math. Soc. **31** (1999) 513–522

[B3] Gavin Brown (joint work with Miles Reid), Diptych varieties and semistable flips, Oberwolfach Report 5/2006, 298-302. Google "Oberwolfach diptych"

[BCZ] Gavin Brown, Alessio Corti and Francesco Zucconi, Birational geometry of 3-fold Mori fibre spaces, in Proc. Fano Conference (Torino, 2002), A. Conte, A. Collino and M. Marchisio Eds., Torino, 2004, pp. 235–275

[BE] D. Buchsbaum and D. Eisenbud, Algebra structures for finite free resolutions, and some structure theorems for ideals of codimension 3, Amer. J. Math. **99** (1977) 447–485

[CFHR] Fabrizio Catanese, Marco Franciosi, Klaus Hulek and Miles Reid, Embeddings of curves and surfaces, Nagoya Math. J. **154** (1999) 185–220

[CKM] H. Clemens, J. Kollár and S. Mori, Higher-dimensional complex geometry, Astérisque **166** (1988)

[Co1] A. Corti, Del Pezzo surfaces over Dedekind schemes, Ann. of Math. **144** (1996) 641–683

[Co02] A. Corti, 3-fold flips after Shokurov, in Flips for 3-folds and 4-folds, Oxford Univ. Press 2007, pp. 18–48

[CM] A. Corti and M. Mella, Birational geometry of terminal quartic 3-folds. I, Amer. J. Math. 126 (2004) 739–761

[CPR] A. Corti, A.V. Pukhlikov and M. Reid, Fano 3-fold hypersurfaces, in Explicit birational geometry of 3-folds, C.U.P., 2000, pp. 175–258

[CR] Alastair Craw and Miles Reid, How to calculate A-Hilb $\mathbb{C}^3$, in Geometry of toric varieties (Grenoble, 2000), collection Séminaires et Congrès **6** SMF 2002, pp. 129–154; preprint 32 pp., math.AG/9909085

[D] V.I. Danilov, The geometry of toric varieties, Russian Math Surveys **33** (1978) 97–154

[DH] I.V. Dolgachev, and Yi Hu, Variation of geometric invariant theory quotients, IHES Publ. Math. **87** (1998) 5–56

[Fl] A. Iano-Fletcher, Working with weighted complete intersections, in *Explicit birational geometry of* 3*-folds*, A. Corti and M. Reid (eds), CUP 2000, pp. 73–173

[F] P. Francia, Some remarks on minimal models. I, Compositio Math. **40** (1980) 301–313

[JS] T. de Jong and D. van Straten, A deformation theory for nonisolated singularities, Abh. Math. Sem. Univ. Hamburg **60** (1990) 177-208

[Kk1] Masayuki Kawakita, Divisorial contractions in dimension three which contract divisors to smooth points, Invent. Math. **145** (2001) 105–119

[Kk2] Masayuki Kawakita, Divisorial contractions in dimension three which contract divisors to compound A_1 points, Compositio Math. **133** (2002) 95–116

[Kk3] Masayuki Kawakita, General elephants of threefold divisorial contractions, J. Amer. Math. Soc. **16** (2003) 331–362

[Kk4] Masayuki Kawakita, Threefold divisorial contractions to singularities of higher indices, math.AG/0306065, 55 pp.

[KM] János Kollár and Shigefumi Mori, Classification of three-dimensional flips, J. Amer. Math. Soc. **5** (1992) 533–703

[KuMi] A.R. Kustin and M. Miller, Constructing big Gorenstein ideals from small ones, J. Alg. **85** (1983) 303–22

[M1] Shigefumi Mori, Flip theorem and the existence of minimal models for 3-folds, J. Amer. Math. Soc. **1** (1988) 117–253

[M2] S. Mori, On 3-dimensional terminal singularities, Nagoya Math. J. **98** (1985) 43–66

[M3] Shigefumi Mori, On semistable extremal neighborhoods, in Higher dimensional birational geometry (Kyoto, 1997), Adv. Stud. Pure Math. **35**, Math. Soc. Japan, Tokyo, 2002, pp. 157–184

[MP] Shigefumi Mori and Yuri Prokhorov, On $\mathbb{Q}$-conic bundles, preprint math.AG/0603736, 54 pp.

[Mu] MUKAI Shigeru, Curves and symmetric spaces. I, Amer. J. Math. **117** (1995) 1627–1644

[PR] Stavros Papadakis and Miles Reid, Kustin–Miller unprojection without complexes, J. Algebraic Geom. 13 (2004) 563-577, preprint math.AG/0011094, 15 pp.

[P] Stavros Papadadakis, Gorenstein rings and Kustin–Miller unprojection, Univ. of Warwick PhD thesis, Aug 2001, pp. vi + 73, available from http://www.maths.warwick.ac.uk/~miles/doctors/Stavros/

[Pr1] Yuri Prokhorov, On the Mori classification of conic bundles, Algebraic geometry 11, J. Math. Sci. **106** (2001) 3340–3352

[Pr2] Yu. Prokhorov, Mori conic bundles with a reduced log terminal boundary, Algebraic geometry 9, J. Math. Sci. **94** (1999) 1051–1059

[Pu1] A.V. Pukhlikov, Birationally rigid varieties with a pencil of Fano double covers, I. Mat. Sb. **195**:7 (2004) 127–160 = Sb. Math. **195** (2004) 1039–1071

[Pu2] Birationally rigid varieties with a pencil of Fano double covers, II. Mat. Sb. **195**:11 (2004) 119–156 = Sb. Math. **195** (2004) 1665–1702

[dP] M. Reid, Nonnormal del Pezzo surfaces, Math Proc. RIMS 30 (1994) 695–727

[Wf?] M. Reid, What is a flip? Notes 1992–95, available on request

[YPG] M. Reid, Young person's guide to canonical singularities, in Algebraic Geometry (Bowdoin 1985), ed. S. Bloch, Proc. of Symposia in Pure Math. **46**, A.M.S. (1987), vol. 1, pp. 345–414

[Ki] M. Reid, Graded rings and birational geometry, in Proc. of algebraic geometry symposium (Kinosaki, Oct 2000), K. Ohno (Ed.), 1–72. (See my website + 3-folds)

[R1] M. Reid, Decomposition of toric morphisms, in Arithmetic and geometry, papers dedicated to I.R. Shafarevich, Vol. II, Progr. Math. **36**, Birkhäuser, Boston, Mass., 1983, pp. 395–418

[C3-f] M. Reid, Canonical 3-folds, in Journées de géometrie algébrique d'Angers (July 1979), Sijthoff and Noordhoff, Alphen aan den Rijn, pp. 273–310

[McKay] M. Reid, McKay correspondence, in Proc. of algebraic geometry symposium (Kinosaki, Nov 1996), T. Katsura (Ed.), 14–41, alg-geom/9702016, 30 pp., rejected by Geometry and Topology

[More] M. Reid, More chapters on algebraic surfaces, book project; get from http://www.maths.warwick.ac.uk/~miles/surf

[R2] Miles Reid (joint work with Gavin Brown), Diptych varieties and $\mathbb{C}^*$ covers of Mori flips, Oberwolfach Report 7/2005, 442–444. Google "Oberwolfach diptych"

[R] Oswald Riemenschneider, Deformationen von Quotientensingularitäten (nach zyklischen Gruppen), Math. Ann. **209** (1974) 211–248

[Sa] V. G. Sarkisov, Birational maps of standard $\mathbb{Q}$-Fano fiberings, I. Kurchatov Inst. preprint, 1989

[S] Jan Stevens, On the versal deformation of cyclic quotient singularities, in Singularity theory and its applications, Part I. LNM **1462** 1991, pp. 302–319

[Th] M. Thaddeus, Geometric invariant theory and flips, J. Amer. Math. Soc. **9** (1996) 691–723

[Tz1] N. Tziolas, 3-fold divisorial contractions of a surface to a curve, I. Compositio Math. **139** (2003) 239–261

[Tz2] N. Tziolas, Three dimensional divisorial extremal neighborhoods, math.AG/0309010, 37 pp.

[Tz3] N. Tziolas, Families of D-minimal models and applications to 3-fold divisorial contractions, Proc. LMS to appear

[W] Wilton, Richard II presented to the Virgin and Child by his Patron Saint John the Baptist and Saints Edward and Edmund, Diptych, Egg tempera on oak, c. 1395–9, NG4451. Google “Wilton diptych, National Gallery”

Part III

Appendixes

The `\end{document}` can go here.

10 Calculation interlude

It seems certain that the entire ideal of relations of V_{ABLM} can be written starting from an $N \times N$ Pfaffian matrix (with $N = k + l + 2$), allowing cancellation of certain "floating monomials". The phenomenon is the same as Riemenschneider's "quasi-determinantal" formats [R].

10.1 One vertebra

Problem: Understand the variety V defined by the 4×4 Pfaffians of the following $(e+5) \times (e+5)$ skew matrix:

$$\begin{pmatrix} 4 & 3 & 2 & 1 & 0 & 1 & \dots & j & \dots & e \\ \hline & x_0 & B & X & y_0 & y_1 & \dots & y_j & \dots & y_e \\ & & x_1 & M & AB^e & x_2AB^{e1} & \dots & x_2^jAB^{ej} & \dots & x_2^eA \\ & & & x_2 & x_0^eL & x_0^{e1}LM & \dots & x_0^{ej}LM^j & \dots & LM^e \\ & & & & y_1 & y_2 & \dots & y_{j+1} & \dots & y_{e+1} \\ & & & & & & & \vdots & & \\ -y_i & & & & & & & m_{i,j} & & \end{pmatrix}$$

with rows and columns numbered as shown (we ignore $\pm$ signs, but get them right before doing the computer algebra): down to the basement, the first four are labelled $-4, -3, -2, -1$, so that x_1 is m_{-3-2} and y_i heads the ith column. The final $(e+1) \times (e+1)$ box has entries m_{ij} for $0 \le i < j \le e+1$ given by the closed formula eq!mij

$$m_{ij} = XAL(x_0B)^{e-j}(x_2M)^i \times \frac{(x_0x_2)^c - (BM)^c}{x_0x_2 - BM}, \quad \text{where } c = j - i. \quad (10.1)$$

in the i row and j column, making the Pfaffian equation $-3-2.ij$

$$x_1 m_{ij} = \det \begin{vmatrix} x_2^i AB^{e-i} & x_2^j AB^{e-j} \\ x_0^{e-i} LM^i & x_0^{e-j} LM^j \end{vmatrix} \tag{10.2}$$

into an identity (after substituting $x_1 X = x_0 x_2 - BM$). The superdiagonal entries

$$m_{i,i+1} = XAL(x_0 B)^{e-i-1}(x_2 M)^i,$$

are monomials, but no other entries m_{ij} with $j > i+1$.

Simple observations

We know a bit about V: It is a Gorenstein 7-fold in $\mathbb{A}^{e+10}$ with coordinates $X, x_0, x_1, x_2, y_0, \dots, y_{e+1}, A, B, L, M$. The serial unprojection construction of V has cascade of pentagrams $x_0, x_1, x_2, y_{i+1}, y_i$ giving the 5×5 submatrix

$$\begin{pmatrix} x_0 & B & -X & -y_i \\ & x_1 & M & -x_2^i AB^{ei} \\ & & x_2 & x_0^{ei} LM^i \\ & & & y_{i+1} \end{pmatrix}$$

with Pfaffians

$$\begin{aligned} x_0 x_2 &= x_1 X + BM \\ x_1 y_i &= x_2^i AB^{e-i+1} + x_0^{e-i+1} LM^i \\ x_1 y_{i+1} &= x_2^{i+1} AB^{e-i} + x_0^{e-i} LM^{i+1} \\ x_0 y_{i+1} &= x_2^i AB^{e-i} X + y_i M \\ x_2 y_i &= y_{i+1} B + x_0^{e-i} LM^i X \end{aligned}$$

$x_0 \leftrightarrow M$, $B \leftrightarrow x_2$ and $y_i \leftrightarrow y_{e-i}$ is a symmetry of V and of its equations.

Setting $A = B = 0$ gives a toric 5-fold. Likewise setting $L = M = 0$ or $A = x_2 = 0$ or $L = x_0 = 0$.

It makes sense to view the 7-fold as a flat deformation of the 4-fold obtained by setting $X = A = L = 1$.

How to understand the equations

The minors of the $2\times(e+1)$ matrix of y_i on the top right are the equations of the rational normal curve $\Gamma_e \subset \mathbb{P}^e$. At the same time, the rows $B^e, \dots, x_2^e$ and $x_0^e, \dots, M^e$ parametrise copies of $\Gamma_e \subset \mathbb{P}^e$. So we hope to view V as a kind of scroll construction. Now among many different constructions of scrolls there are residual constructions (the complete intersection of k linearly independent quadrics through $\mathbb{P}^{n-2} \subset \mathbb{P}^n$ is a scroll residual to the $\mathbb{P}^{n-2}$) and linear generation constructions (the variety obtained by joining up corresponding points of $k-1$ embedding of $\mathbb{P}^1$ as rational normal curves in $\mathbb{P}^{a_i}$).

Proposition 10.1 *The affine piece $x_1 \neq 0$ of V is isomorphic to $\mathbb{G}_m \times \mathbb{A}^6$ parametrised by $x_1 \neq 0$, x_0, x_2, A, B, L, M.*

The first Pfaffian $x_0x_2 = x_1X + BM$ is a quadric of rank 6 (that is, the affine Grassmannian $\mathrm{aGr}(2,4) \subset \mathbb{A}^6$). If $x_1 \neq 0$ then $X = (x_0x_2 - BM)/x_1$. Next, each Pfaffian involving x_1 times any of the y_i in the last two columns can be solved for y_i, and both give the same value:

At the bottom right, the Pfaffian $Xx_1 = BM + x_0x_2$ is a quadric of rank 6 (that is, the affine Grassmannian $\mathrm{aGr}(2,4) \subset \mathbb{A}^6$). If $x_1 \neq 0$ then $X = (BM + x_0x_2)/x_1$. Next, each Pfaffian involving x_1 times any of the y_i in the last two columns can be solved for y_i, and both give the same value:

$$x_1y_i = x_2^iAB^{e-i+1} + x_0^{e-i+1}LM^i,$$

The point is just that going from x_1 times y_i in the penultimate column to x_1 times y_i in the final row, involves rolling the factors

$$B \mapsto x_2 \quad \text{and} \quad x_0 \mapsto M$$

at the bottom, and this neatly cancels the change

$$x_2^iAB^{e-1} \mapsto x_2^{i-1}AB^{e-i+1} \quad \text{and} \quad x_0^{e-i}LM^i \mapsto x_0^{e-i+1}LM^{i-1}$$

from moving up a row, etc.

10.2 More vertebras – the case $[5,3,5]$

This case is a bit bigger than Example 1.1, and we work it out in more detail; all the equations are derived from the Pfaffians of 11×11 skew matrixes, in fact in 2 different ways. We provide Magma code to automate part of the calculations.

```
5         1         0         -2
----------          ----------
3         2         3         2
5         2         5         2
          2                   2
          3                   3
          2                   2
----------          ----------
0         -4        3         1
```

Write the skew 11×11 matrix $\mathbf{M} =$

$$\begin{pmatrix}
x_3 & LM^3 & -x_2^2 & -y_6 & -y_5 & -y_4 & -y_3 & -y_2M & m_{1,10} & m_{1,11} \\
 & x_2 & B & -L^4M^{11} & -x_1L^3M^8 & -x_1^2L^2M^5 & -x_1^3LM^2 & -x_1^4 & -y_2B & -y_1B \\
 & & x_1 & x_3^4A & x_3^3AB & x_3^2AB^2 & x_3AB^3 & -AB^4M & -x_0LM^2 & -x_0^2LM \\
 & & & y_5 & y_4 & y_3 & y_2 & x_0 & x_2AB^5 & A^2B^{10} \\
 & & & & m_{5,6} & m_{5,7} & m_{5,8} & m_{5,9} & m_{5,10} & m_{5,11} \\
 & & & & & m_{6,7} & m_{6,8} & m_{6,9} & m_{6,10} & m_{6,11} \\
 & & & & & & m_{7,8} & m_{7,9} & m_{7,10} & m_{7,11} \\
 & & & & & & & m_{8,9} & m_{8,10} & m_{8,11} \\
 & & & & & & & & y_1M & y_0M \\
 & & & & & & & & & m_{10,11}
\end{pmatrix}$$

The calculation starts from the top, with the two equations

$$x_2y_6 = x_3^5A + L^5M^{14} \quad \text{and} \quad y_5x_3 = y_6B + x_2^2L^4M^{11}. \qquad (10.3)$$

These are the 2 Pfaffians of the initial submatrix $\mathbf{M}(1,2,3,4,5)$ without x_1.

The 5×5 submatrixes $\mathbf{M}(1,2,3,4,i)$ for $i = 5,6,7,8$ involve only entries in the first 4 rows, and correspond to the magic pentagrams that successively adjoin x_1, y_4, y_3, y_2. The submatrix $\mathbf{M}(1,2,3,4,9)$ corresponds to the "flat" pentagram y_2, x_3, x_2, x_1, x_0 that adjoins x_0. At this point we *float* monomials in $\mathbf{M}(1,2,3,4,9)$, modifying the matrix by eq!float

$$\begin{pmatrix} x_3 & LM^3 & -x_2^2 & -y_2M \\ & x_2 & B & -x_1^4 \\ & & x_1 & AB^4M \\ & & & x_0 \end{pmatrix} \longmapsto \begin{pmatrix} x_3 & LM^2 & -x_2^2 & -y_2 \\ & x_2 & BM & -x_1^4 \\ & & x_1 & AB^4 \\ & & & x_0 \end{pmatrix}$$

$$\longmapsto \begin{pmatrix} x_3 & BLM^2 & -x_2^2 & -y_2B \\ & x_2 & M & -x_1^4 \\ & & x_1 & AB^5 \\ & & & x_0 \end{pmatrix} \tag{10.4}$$

The commmon factor M from the 3 terms $(1,3),(1,9),(3,9)$ floats across to multiply $(2,4)$, and the factor B in $(2,4)$ floats back to multiply the 3 terms $(1,3),(1,9),(3,9)$. Each operation leaves the 4×4 Pfaffians unchanged. We write

$$M\colon (1,3,9)\to(2,4) \quad\text{and}\quad B\colon (2,4)\to(1,3,9).$$

After floating M (and optionally B), the two submatrixes $\mathbf{M}(2,3,4,9,i)$ for $i=10,11$ adjoin the y_1 and y_0. This accounts for all the specified entries.

The 21 unknown entries $m_{i,j}$ are not in pentagrams and have to be calculated. The answer is:

$$\begin{aligned} m_{1,10} &= -x_2^2y_2 + x_2x_3AB^4 \\ m_{1,11} &= -x_2^2y_1 + x_3A^2B^9 \end{aligned}$$

$$\begin{aligned} m_{5,6} &= x_2^2x_3^3AL^3M^8 \\ m_{6,7} &= x_1x_2^2x_3^2ABL^2M^5 \\ m_{7,8} &= x_1^2x_2^2x_3AB^2LM^2 \\ m_{8,9} &= x_1^3x_2^2AB^3 \\ m_{10,11} &= x_0x_1^4AB^5LM \end{aligned}$$

$$\begin{aligned} m_{5,10} &= y_2y_5 - x_2AB^4L^4M^{11} \\ m_{5,11} &= y_1y_5 - A^2B^9L^4M^{11} \\ m_{6,10} &= y_2y_4 - x_1x_2AB^4L^3M^8 \\ m_{6,11} &= y_1y_4 - x_1A^2B^9L^3M^8 \\ m_{7,10} &= y_2y_3 - x_1^2x_2AB^4L^2M^5 \end{aligned}$$

$$\begin{aligned} m_{5,7} &= x_2^2x_3^2AL^2M^5(x_1x_3 + BLM^3) \\ m_{6,8} &= x_1x_2^2x_3ABLM^2(x_1x_3 + BLM^3) \\ m_{7,9} &= x_1^2x_2^2AB^2(x_1x_3 + BLM^3) \\ m_{8,10} &= y_2^2 - x_1^3x_2AB^4LM^2 \\ m_{5,8} &= x_2^2x_3ALM^2(x_1^2x_3^2 + x_1x_3BLM^3 \\ &\qquad + B^2L^2M^6) \\ m_{5,9} &= x_2^2A(x_1^3x_3^3 + x_1^2x_3^2BLM^3 \\ &\qquad + x_1x_3B^2L^2M^6 + B^3L^3M^9) \\ m_{6,9} &= x_1x_2^2AB(x_1^2x_3^2 + x_1x_3BLM^3 \\ &\qquad + B^2L^2M^6) \end{aligned}$$

$$\begin{aligned} m_{7,11} &= y_1y_3 - x_1^2A^2B^9L^2M^5 \\ m_{8,11} &= y_1y_2 - x_1^3A^2B^9LM^2 \end{aligned}$$

Each is determined by the specified entries together with the assumption that B or M is a nonzero-divisor modulo the ideal of 4×4 Pfaffians. Example:

for $m_{5,6}$, consider

$$\mathrm{Pf}_{24.56} = x_1y_5L^3M^8 - y_4L^4M^{11} - Bm_{5,6}$$

Adding L^3M^8 times $\mathrm{Pf}_{13.46} = -x_1y_5 + x_2^2x_3^3AB + y_4LM^3$ kills the first two term, and gives

$$x_2^2x_3^3ABL^3M^8 - BU3$$

Therefore B times $x_2^2x_3^3AL^3M^8 - m_{5,6}$ is in the ideal of Pfaffians, so $m_{5,6} = x_2^2x_3^3AL^3M^8$.

The entries that are not monomial are usually fairly simple, involving things like

$$x_1^2x_3^2 + x_1x_3BLM^3 + B^2L^2M^6 = \frac{(x_1x_3)^3 - (BLM^3)^3}{x_1x_3 - BLM^3}$$

(in $m_{5,8}$). This comes typically from using $R_{x_1x_3} : x_1x_3 = x_2^3 + BLM^3$ repeatedly to substitute for $x_1^3x_3^3$. Compare the $m_{i,j}$ in (10.1).

The ideal I we seek is generated by 44 key relations $R_{x_0x_2}, \dots, R_{y_1y_5}$ that extend the 44 binomial equations of the tent and the two toric faces V_{AB} and V_{LM}; we tabulate them in Section 10.4 below. They include the Pfaffians from our magic pentagrams. The 330 Pfaffians of $\mathbf{M}$ are in I, and the generators of I are derived from them. As with the calculation of the $m_{i,j}$, our derivation of some of the key relations involves cancelling factors of $\mathbb{M}$ or B from Pfaffians or from suitable linear combinations of them. It is probably not possible to obtain all the key relations as Pfaffians of a single matrix $\mathbb{M}$.

10.3 The other way up – the case $[3, 5, 3]$

The same calculation can also be done starting from the bottom using the skew matrix $\mathbf{N} =$

$$\begin{pmatrix}
x_2 & M & x_1^4 & y_1 & y_2 & x_3 & x_1^3LM^3 & x_1^2L^2M^6 & x_1L^3M^9 & L^4M^{12} \\
 & x_1 & AB^5 & x_0^2L & x_0LM & BLM^2 & x_3AB^4 & x_3^2AB^3 & x_3^3AB^2 & x_3^4AB \\
 & & x_0 & A^2B^9 & x_2AB^4 & x_2^2 & y_2M & y_3M & y_4M & y_5M \\
 & & & y_0 & y_1 & y_2B & n_{4,8} & n_{4,9} & n_{4,10} & n_{4,11} \\
 & & & & n_{5,6} & n_{5,7} & n_{5,8} & n_{5,9} & n_{5,10} & n_{5,11} \\
 & & & & & n_{6,7} & n_{6,8} & n_{6,9} & n_{6,10} & n_{6,11} \\
 & & & & & & y_3B & y_4B & y_5B & y_6B \\
 & & & & & & & n_{8,9} & n_{8,10} & n_{8,11} \\
 & & & & & & & & n_{9,10} & n_{9,11} \\
 & & & & & & & & & n_{10,11}
\end{pmatrix}$$

where the two vertebras now correspond to the blocks $[1, 2, 3, 4] \times [5, 6]$ and $[1, 2, 3, 7] \times [8, 9, 10, 11]$ in $\mathbf{N}$. The hinge, corresponding to the flat pentagram, is the diagonal submatrix $[1, 2, 3, 4, 7]$, which (up to permutation) is the righthand matrix in (10.4).

$$\begin{aligned}
n_{4,8} &= x_1^3x_2^2AB^4 \\
n_{4,9} &= x_1^4y_3 - x_0x_1^2L^2M^5 \\
n_{4,10} &= x_1^4y_4 - x_0x_1L^3M^8 \\
n_{4,11} &= x_1^4y_5 - x_0L^4M^{11} \\
n_{5,6} &= -x_0x_1^4AB^4L \\
n_{5,7} &= -x_0x_1^4x_2L - x_1^4AB^5LM \\
n_{6,7} &= -x_1^4x_2LM \\
n_{5,8} &= y_1y_2 - x_1^3A^2B^9LM^2 \\
n_{5,9} &= y_1y_3 - x_1^2A^2B^9L^2M^5 \\
n_{5,10} &= y_1y_4 - x_1A^2B^9L^3M^8 \\
n_{5,11} &= y_1y_5 - A^2B^9L^4M^{11}
\end{aligned}$$

$$\begin{aligned}
n_{6,8} &= y_2^2 - x_1^3x_2AB^4LM^2 \\
n_{6,9} &= y_2y_3 - x_1^2x_2AB^4L^2M^5 \\
n_{6,10} &= y_2y_4 - x_1x_2AB^4L^3M^8 \\
n_{6,11} &= y_2y_5 - x_2AB^4L^4M^{11} \\
n_{8,9} &= -x_1^2x_2^2x_3AB^3LM^3 \\
n_{8,10} &= -x_1^3y_4LM^3 + x_1y_2L^3M^9 \\
n_{8,11} &= -x_1^3y_5LM^3 + y_2L^4M^{12} \\
n_{9,10} &= -x_1x_2^2x_3^2AB^2L^2M^6 \\
n_{9,11} &= -x_1^2y_5L^2M^6 + y_3L^4M^{12} \\
n_{10,11} &= -x_2^2x_3^3ABL^3M^9
\end{aligned}$$

One gets the same 44 key equations tabulated below

Remark 10.2 The shape of the two big matrixes suggest the general form for longer chains of many vertebras. Working with $\mathbf{M}$, we have:

(1) Each vertebra of length d occupies a $4 \times (d-1)$ block of $\mathbf{M}$; in our example, the two vertebra occupy the blocks $[1,2,3,4] \times [5,6,7,8]$ and $[2,3,4,9] \times [10,11]$ of $\mathbf{M}$.

(2) The entries in each row are monomials forming simple progressions; for example $y_6, \dots, y_3$ and $L^4M^{11}, \dots, x_1^3LM^2$.

(3) The row intervals of two consecutive vertebras overlap in 3, so their union is just 5 rows; these 5 indexes define a flat pentagram, for example $[1,2,3,4,9]$ above. A monomial flotation hinges between the monomial progressions in the two vertebras.

(4) The hinge between two vertebras, working down from the top or up from the bottom, is the flotation in (10.4). The middle matrix is the magic pentagram that adjoins x_0 (from the top) or adjoins x_3 (from the bottom). Its first 4×4 block floats to give the constant piece in the first vertebra (rows 1–8 of $\mathbf{M}$). Its bottom 4×4 block floats to give the constant piece of the second vertebra (rows 1–6 of $\mathbf{N}$).

10.4 Table of 44 key equations

$$
\begin{aligned}
R_{x_0x_2} &= x_0x_2 - x_1^5 - AB^5M \\
R_{x_0x_3} &= x_0x_3 - x_1^4x_2^2 - y_2BM \\
R_{x_0y_1} &= x_0y_1 - x_1^4A^2B^9 - y_0M \\
R_{x_0y_2} &= x_0y_2 - x_1^4x_2AB^4 - y_1M \\
R_{x_0y_3} &= x_0y_3 - x_1^3x_2^4AB^3 - y_2^2M \\
R_{x_0y_4} &= x_0y_4 - x_1^4x_2x_3^2AB^2 - y_2y_3M + x_1^2x_2AB^4L^2M^6 \\
&= x_0y_4 - x_1^2x_2^4AB(x_2^3 + 2BLM^3) - y_2y_3M \\
R_{x_0y_5} &= x_0y_5 - x_1^4x_2x_3^3AB - y_2y_4M + x_1x_2AB^4L^3M^9 \\
&= x_0y_5 - x_1x_2^4AB(x_2^6 + 3x_2^3BLM^3 + 3B^2L^2M^6) - y_2y_4M \\
R_{x_0y_6} &= x_0y_6 - x_1^4x_2x_3^4A - y_2y_5M + x_2AB^4L^4M^{12} \\
&= x_0y_6 - x_2^4A(x_2^9 + 4x_2^6BLM^3 + 6x_2^3B^2L^2M^6 + 4B^3L^3M^9) \\
&\qquad - y_2y_5M
\end{aligned}
$$

$$
\begin{aligned}
R_{x_1x_3} &= x_1x_3 - x_2^3 - BLM^3 \\
R_{x_1y_0} &= x_1y_0 - A^3B^{14} - x_0^3L \\
R_{x_1y_1} &= x_1y_1 - x_2A^2B^9 - x_0^2LM \\
R_{x_1y_2} &= x_1y_2 - x_2^2AB^4 - x_0LM^2 \\
R_{x_1y_3} &= x_1y_3 - x_2^2x_3AB^3 - y_2LM^3 \\
R_{x_1y_4} &= x_1y_4 - x_2^2x_3^2AB^2 - y_3LM^3 \\
R_{x_1y_5} &= x_1y_5 - x_2^2x_3^3AB - y_4LM^3 \\
R_{x_1y_6} &= x_1y_6 - x_2^2x_3^4A - y_5LM^3
\end{aligned}
$$

$$
\begin{aligned}
R_{x_2y_0} &= x_2y_0 - y_1AB^5 - x_0^2x_1^4L \\
R_{x_2y_1} &= x_2y_1 - y_2AB^5 - x_0x_1^4LM \\
R_{x_2y_2} &= x_2y_2 - x_3AB^4 - x_1^4LM^2 \\
R_{x_2y_3} &= x_2y_3 - x_3^2AB^3 - x_1^3L^2M^5 \\
R_{x_2y_4} &= x_2y_4 - x_3^3AB^2 - x_1^2L^3M^8 \\
R_{x_2y_5} &= x_2y_5 - x_3^4AB - x_1L^4M^{11} \\
R_{x_2y_6} &= x_2y_6 - x_3^5A - L^5M^{14}
\end{aligned}
$$

$$
\begin{aligned}
R_{x_3y_0} &= x_3y_0 - y_1y_2B - x_0x_1^8x_2L - x_1^8AB^5LM \\
&= x_3y_0 - y_1y_2B - x_1^8L(x_1^5 + 2AB^5M) \\
R_{x_3y_1} &= x_3y_1 - y_2^2B - x_1^8x_2LM \\
R_{x_3y_2} &= x_3y_2 - y_3B - x_1^3x_2^2LM^2 \\
R_{x_3y_3} &= x_3y_3 - y_4B - x_1^2x_2^2L^2M^5 \\
R_{x_3y_4} &= x_3y_4 - y_5B - x_1x_2^2L^3M^8 \\
R_{x_3y_5} &= x_3y_5 - y_6B - x_2^2L^4M^{11}
\end{aligned}
$$

$$
\begin{aligned}
R_{y_0y_2} &= y_0y_2 - y_1^2 - x_0x_1^8AB^4L \\
R_{y_1y_3} &= y_1y_3 - y_2^3 - x_1^7x_2^3AB^3LM + x_1^3x_2y_2AB^4LM^2 \\
&= y_1y_3 - y_2^3 - x_1^7AB^3LM(x_2^3 - BLM^3) \\
&\quad + x_1^2A^2B^8LM^2(x_2^3 + BLM^3) \\
R_{y_2y_4} &= y_2y_4 - y_3^2 - x_1^2x_2^4x_3AB^2LM^2 \\
&= y_2y_4 - y_3^2 - x_1x_2^4AB^2LM^2(x_2^3 + BLM^3) \\
R_{y_3y_5} &= y_3y_5 - y_4^2 - x_1x_2^4x_3^2ABL^2M^5 \\
&= y_3y_5 - y_4^2 - x_2^4x_3ABL^2M^5(x_2^3 + BLM^3) \\
R_{y_4y_6} &= y_4y_6 - y_5^2 - x_2^4x_3^3AL^3M^8
\end{aligned}
$$

$$
\begin{aligned}
R_{y_0y_3} &= y_0y_3 - y_1y_2^2 - x_0x_1^7x_2^3AB^3L - x_1^7x_2^2A^2B^8LM + x_1^3y_2A^2B^9LM^2 \\
&= y_0y_3 - y_1y_2^2 - x_1^7x_2^2AB^3L(x_1^5 + 2AB^5M) + x_1^3y_2A^2B^9LM^2 \\
R_{y_1y_4} &= y_1y_4 - y_2^2y_3 - x_1^2x_2AB^2LM(x_1^5x_2^2x_3 + x_1^4x_2^2BLM^3 - y_2B^2LM^4) \\
&= y_1y_4 - y_2^2y_3 - x_1^7AB^3LM(x_2^3 - BLM^3) \\
&\quad + x_1^2A^2B^8LM(x_2^3 + BLM) \\
R_{y_2y_5} &= y_2y_5 - y_3y_4 - x_1^2x_2^4x_3^2ABLM^2 - x_1x_2^4x_3AB^2L^2M^5 \\
&= y_2y_5 - y_3y_4 - x_2^4ABLM^2(x_2^6 + 3x_2^3BLM^3 + 2B^2L^2M^6) \\
R_{y_3y_6} &= y_3y_6 - y_4y_5 - x_1x_2^4x_3^3AL^2M^5 - x_2^4x_3^2ABL^3M^8 \\
&= y_3y_6 - y_4y_5 - x_2^4x_3^2AL^2M^5(x_2^3 + 2BLM^3)
\end{aligned}
$$

$$
\begin{aligned}
R_{y_0y_4} &= y_0y_4 - y_1y_2y_3 - x_1ABL(x_0x_1^5x_2^3x_3 + x_0x_1^4x_2^3BLM^3 \\
&\quad - x_0x_1^4B^2L^2M^6 + x_1^6y_3B^2M - y_2AB^7LM^5) \\
&= y_0y_4 - y_1y_2y_3 + x_1A^2B^9L^2M^5(x_0LM^2 + x_2^2AB^4) \\
&\quad - x_1^6x_2^2AB^2L(x_2^3 + 2BLM^3)(x_1^5 + 2AB^5M) \\
R_{y_1y_5} &= y_1y_5 - y_2^2y_4 - x_1^7x_2^3x_3^2ABLM - x_1^6x_2^3x_3AB^2L^2M^4 \\
&\quad - x_1^5x_2^3AB^3L^3M^7 + x_1x_2y_2AB^4L^3M^8 \\
&= y_1y_5 - y_2^2y_4 - x_1^5ABLM(x_2^9 + 3x_2^6BLM^3 \\
&\quad + 3x_2^3B^2L^2M^6 - B^3L^3M^9) + AB^8L^3M^8(x_2^3 + BLM^3) \\
R_{y_2y_6} &= y_2y_6 - y_3y_5 - x_2^4x_3ALM^2(x_1^2x_3^2 + x_1x_3BLM^3 + B^2L^2M^6) \\
&= y_2y_6 - y_3y_5 - x_2^4x_3ALM^2(x_2^6 + 3x_2^3BLM^3 + 3B^2L^2M^6)
\end{aligned}
$$

$$
\begin{aligned}
R_{y_0y_5} = y_0y_5 &- y_1y_2y_4 - x_0x_1^7x_2^3x_3^2ABL - x_0x_1^6x_2^3x_3AB^2L^2M^3 \\
&- x_0x_1^5x_2^3AB^3L^3M^6 + x_0x_1^5AB^4L^4M^9 - x_1^8y_4AB^4LM \\
&+ x_1y_2A^2B^9L^3M^8
\end{aligned}
$$

$$
\begin{aligned}
R_{y_0y_5} = y_0y_5 &- y_1y_2y_4 - x_0x_1^7x_2^3x_3^2ABL - x_1^7x_2^2x_3^2A^2B^6LM \\
&- x_1^2x_2^4x_3y_1AB^2LM^2 + x_1^2x_2^2x_3^2A^3B^{11}LM^2 - x_1x_2^4y_1AB^3L^2M^5 \\
&+ x_1x_2^2x_3A^3B^{12}L^2M^5 + x_1y_2A^2B^9L^3M^8
\end{aligned}
$$

$$
\begin{aligned}
R_{y_1y_6} = y_1y_6 &- y_2^2y_5 - x_1^7x_2^3x_3^3ALM - x_1^2x_2^4x_3^2y_2ABLM^2 \\
&+ x_1^2x_2^3x_3^3A^2B^5LM^2 - x_1x_2^4x_3y_2AB^2L^2M^5 + x_1x_2^3x_3^2A^2B^6L^2M^5 \\
&- x_2^4y_2AB^3L^3M^8 + x_2^3x_3A^2B^7L^3M^8 + x_2y_2AB^4L^4M^{11}
\end{aligned}
$$

$$
\begin{aligned}
R_{y_1y_6} = y_1y_6 &- y_2^2y_5 - x_1^7x_2^3x_3^3ALM - x_1^6x_2^3x_3^2ABL^2M^4 - x_1^5x_2^3x_3AB^2L^3M^7 \\
&- x_1^4x_2^3AB^3L^4M^{10} + x_2y_2AB^4L^4M^{11}
\end{aligned}
$$

$$
\begin{aligned}
R_{y_0y_6} = y_0y_6 &- y_1y_2y_5 - x_0x_1^7x_2^3x_3^3AL - x_1^7x_2^2x_3^3A^2B^5LM \\
&- x_1^2x_2^4x_3^2y_1ABLM^2 + x_1^2x_2^2x_3^3A^3B^{10}LM^2 - x_1x_2^4x_3y_1AB^2L^2M^5 \\
&+ x_1x_2^2x_3^2A^3B^{11}L^2M^5 - x_2^4y_1AB^3L^3M^8 + x_2^2x_3A^3B^{12}L^3M^8 \\
&+ y_2A^2B^9L^4M^{11}
\end{aligned}
$$

$$
\begin{aligned}
R_{y_0y_6} = y_0y_6 &- y_1y_2y_5 + y_2A^2B^9L^4M^{11} - x_0x_1^7x_2^3x_3^3AL \\
&- x_0x_1^6x_2^3x_3^2ABL^2M^3 - x_0x_1^5x_2^3x_3AB^2L^3M^6 \\
&- x_0x_1^4x_2^3AB^3L^4M^9 + x_0x_1^4AB^4L^5M^{12} - x_1^8y_5AB^4LM
\end{aligned}
$$

10.5 Several vertebras

Work with II(6, 5, 6, 5), which has monomials

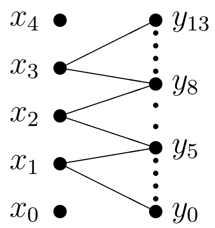

and top equations ("Step 1")

$$\begin{aligned} x_3y_{13} &= x_4^6A + L^{29}M^{168} \\ y_{12}x_4 &= y_{13}B + x_3^4L^{24}M^{139} \end{aligned}$$

"Steps 2–7". The three big wedges of the diagrams give $x_1 \cdot y_{0\dots5}$, $x_2 \cdot y_{5\dots8}$ and $x_3 \cdot y_{8\dots13}$, and are pullbacks from standard vertebras as in Section 10: from the top,

$$\begin{pmatrix} x_4 & M_3 & X_3 & y_{13} & y_{12} & \dots & y_9 \\ & x_3 & -B_3 & L_3M_3^4 & x_2L_3M_3^3 & \dots & x_2^4L_3 \\ & & -x_2 & -x_4^5A & -x_4^4AB & \dots & -x_4AB^4 \\ & & & y_{12} & y_{11} & \dots & y_8 \end{pmatrix}$$

where $A_3 = A$, $B_3 = B$, $L_3 = L^4M^{23}$, $M_3 = L^5M^{29}$, $X_3 = x_3^4$. The lower triangle of entries are given as in (10.1)

$$m_{ij} = AL_3X_3x_4(x_4M_3)^{4-j}(x_2B)^i \times \frac{(x_2x_4)^c - (BM_3)^c}{(x_2x_4 - BM_3)} \quad \text{where } c = j - i;$$

The next column of the matrix is headed by $M_2 = M_3/L_3 = LM^6$ (this is necessary to allow the progression in the second row to continue $x_2^4L_3 \to x_2^5$), giving the pivotal floatation

$$\begin{pmatrix} x_4 & M_3 & X_3 & y_8M_2 \\ & x_3 & B & x_2^5 \\ & & x_2 & A_2M_2 \\ & & & x_1 \end{pmatrix} \longrightarrow \begin{pmatrix} x_4 & L_3 & X_3 & y_8 \\ & x_3 & BM_2 & x_2^5 \\ & & x_2 & A_2 \\ & & & x_1 \end{pmatrix}$$

"Steps 8–10":

$$\begin{pmatrix} X_2 & x_1 & B_2 & y_7 & y_6 & y_5 \\ & M_2 & x_3 & y_8 & y_7 & y_6 \\ & & x_2 & x_3^3A_2 & x_3^2A_2B_2 & x_3A_2B_2^2 \\ & & & x_1L_2M_2^2 & x_1^2L_2M_2 & x_1^3L_2 \end{pmatrix}$$

where $A_2 = AB^5$, $B_2 = AB^6$, $L_2 = LM^5$, $M_2 = LM^6$, $X_2 = x_2^5$.

"Steps 12–16":

$$\begin{pmatrix} X_1 & x_0 & B_1 & y_4 & y_3 & \dots & y_0 \\ & M_1 & x_2 & y_5 & y_4 & \dots & y_1 \\ & & x_1 & x_2^4A_1 & x_2^3A_1B_1 & \dots & A_1B_1^4 \\ & & & x_0L_1M_1^4 & x_0^2L_1M_1^3 & \dots & x_0^5L_1 \end{pmatrix}$$

where $A_1 = A^4B^{23}$, $B_1 = A^5B^{29}$, $L_1 = L$, $M_1 = M$, $X_1 = x_1^4$.

How to join them together into a whole variety?

The key is to understand what happens around a lop-sided pentagram (or "flat" pentagram) such as $y_8x_1x_2x_3x_4$ in Step 7 and its skew matrix

$$\begin{pmatrix} x_1 & B_2 & X_2 & y_8 \\ & x_2 & B_3M_2 & X_3 \\ & & x_3 & L_3 \\ & & & x_4 \end{pmatrix}$$

Adjoining y_7 to this (in Step 8) is an unfaithful Tom unprojection: the unprojection equations should be $y_7 \cdot (x_2, x_3, x_4, M_2)$, but the bottom 4×4 block does not contain M_2, only the products B_3M_2 and L_3 (recall $M_2 = LM^6$ and $L_3 = L^4M^{23}$. We can write out a 6×6 "extrasymmetric" matrix (the top 6×6 of the following display) whose Pfaffians include the unprojection equation for y_7M_2 multiplied by this kind of factor. The same applies in the other direction to adjoining y_9 with unprojection equations $y_9 \cdot (x_1, x_2, x_3, B_3)$.

Its unfaithful Tom is the bottom 6×6 block below.

$$\begin{pmatrix} y_7 & x_3^2B_2 & x_1L_2M_2^2 & y_8B_3 & X_2x_3^2L_2M_2 & * \\ & x_1 & B_2 & X_2 & y_8 & x_2^4X_3AB^4 \\ & & x_2 & B_3M_2 & X_3 & M_2y_8 \\ & & & x_3 & L_3 & x_4AB^4 \\ & & & & x_4 & M_3x_2^4 \\ & & & & & y_9 \end{pmatrix}$$

By calculating 02.46 one gets $* = y_8^2 + x_2^4x_3^2A_2L^?M^?$.

10.6 How to join them together into a whole variety?

How to pass between the first big wedge and the second? Our standard link ("Step 7") is the lop-sided pentagram $y_8x_4x_3x_2x_1$. We can break this up into several intermediate steps to clarify its relation with the preceding Steps 2–6 and the following Steps 8–10. First, given the "rolling factors" pattern, it is natural to try to add a further column after Step 6. "Step 6^+":

$$\begin{pmatrix} X_3 & x_2 & B_3 & \dots & y_8 & \\ & M_3 & x_4 & \dots & y_9 & y_8 \\ & & x_3 & \dots & x_4AB^4 & AB^5 \\ & & & \dots & x_2^4L_3 & x_2^5L_3/M_3 \end{pmatrix}$$

(I write m_{ij} promiscuously as notation for the entries of any 6×6 skew matrix.) Multiply through the last column by $M_3/L_3 = LM^6 = M_2$ to clear denominators: at the same time, adjoin the Tom unprojection variable $m_{16} := x_1$ and fill in the bottom right element m_{56} (say, using the two different occurrences of the equation for x_4y_8):

$$\begin{pmatrix} X_3 & x_2 & B_3 & y_8 & x_1 \\ & M_3 & x_4 & y_9 & y_8M_2 \\ & & x_3 & x_4AB^4 & AB^5M_2 \\ & & & x_2^4L_3 & x_2^5 \\ & & & & x_2^4X_3AB^4 \end{pmatrix}$$

This does not really add anything new – its Pfaffians not involving x_1 are multiples by M_2 or AB^4 of existing Pfaffian equations. The next step is to "float across" the common factors M_2 from the 3 entries m_{23}, m_{26}, m_{36} (the "triangle" 236) to the 3 entries m_{14}, m_{15}, m_{45}, giving

$$\begin{pmatrix} X_3 & x_2 & BM_2 & y_8M_2 & x_1 \\ & L_3 & x_4 & y_9 & y_8 \\ & & x_3 & x_4AB^4 & AB^5 \\ & & & x_2^4M_3 & x_2^5 \\ & & & & AB^4x_2^4X_3 \end{pmatrix}$$

The mechanism behind this: m_{23}, m_{26}, m_{36} are divisible by M_2 (including $M_3 = M_2L_3$). If we divide the rows $2, 3, 6$ by M_2 and multiply the complementary rows $1, 4, 5$ by M_2, the only difference it makes is to multiply or divide some of the Pfaffians by M_2. Deleting column 5 gives the skew matrix of Step 7:

$$\begin{pmatrix} X_3 & x_2 & BM_2 & x_1 \\ & L_3 & x_4 & y_8 \\ & & x_3 & AB^5 \\ & & & x_2^5 \end{pmatrix}$$

How to link up with Steps 8–10?

$$\begin{pmatrix} X_2 & x_1 & B_2 & y_8B_2 & y_7 & y_6 & y_5 \\ & M_2 & x_3 & x_4 & y_8 & y_7 & y_6 \\ & & x_2 & x_3^4A_2 & x_3^3A_2 & x_3^2A_2B_2 & x_3A_2B_2^2 \\ & & & B_2L_2M_2^3 & x_1L_2M_2^2 & x_1^2L_2M_2 & x_1^3L_2 \end{pmatrix}$$

where $A_2 = AB^5$, $B_2 = AB^6$, $L_2 = LM^5$, $M_2 = LM^6$, $X_2 = x_2^5$.

??

In the same way, the 3 entries of the triangle 356 are divisible by AB^4, so I can float these over to 124, obtaining:

$$\begin{pmatrix} AB^4X_3 & x_2 & AB^5M_2 & y_8M_2 & x_1 \\ & L_3 & AB^4x_4 & y_9 & y_8 \\ & & x_3 & x_4 & B \\ & & & x_2^4M_3 & x_2^5 \\ & & & & x_2^4X_3 \end{pmatrix}$$

10.7 Supplement: the tag equations at y_i

This section is preliminary to writing out a systematic list of the "most important" equations. It works out the tag equations down the y side, including the tags at all the y_i and some longer equations; that tag equations at "small" y_i (tagged with 2) are monomial Pfaffians, but the tag equations at the "big" y_i, and the longer equations cannot be reduced to trinomials.

10.7.1 A single vertebra

```
> X := TypeIIPair([7,4]); Print(X);
        7       1       0       -3
        ----------      ----------
        4       2       4       2
                2               2
                2               2
                2               2
                2               2
                2               2
        ----------      ----------
        0       -3      7       1

    -B*M - x1^4 + x0*x2,

    -x1^3*x2^6*A - y6*M + x0*y7,
    -x1^3*x2^5*A*B - y5*M + x0*y6,
    -x1^3*x2^4*A*B^2 - y4*M + x0*y5,
    -x1^3*x2^3*A*B^3 - y3*M + x0*y4,
    -x1^3*x2^2*A*B^4 - y2*M + x0*y3,
```

```
-x1^3*x2*A*B^5 - y1*M + x0*y2,
-x1^3*A*B^6 - y0*M + x0*y1,

-L*M^7 - x2^7*A + x1*y7,
-x0*L*M^6 - x2^6*A*B + x1*y6,
-x0^2*L*M^5 - x2^5*A*B^2 + x1*y5
-x0^3*L*M^4 - x2^4*A*B^3 + x1*y4,
-x2^3*A*B^4 - x0^4*L*M^3 + x1*y3,
-x2^2*A*B^5 - x0^5*L*M^2 + x1*y2,
-x2*A*B^6 - x0^6*L*M + x1*y1,
-A*B^7 - x0^7*L + x1*y0,

-x1^3*L*M^6 - y7*B + x2*y6,
-x0*x1^3*L*M^5 - y6*B + x2*y5,
-x0^2*x1^3*L*M^4 - y5*B + x2*y4,
-x0^3*x1^3*L*M^3 - y4*B + x2*y3,
-x0^4*x1^3*L*M^2 - y3*B + x2*y2,
-x0^5*x1^3*L*M - y2*B + x2*y1,
-x0^6*x1^3*L - y1*B + x2*y0.
```

That is the case $d = 4$ and $e = 7$ of the following general construction:

$$\begin{aligned} x_0x_2 &= x_1^d + BM. \\ x_0y_i &= x_1^{d-1}x_2^{i-1}AB^{e-i} + y_{i-1}M \quad \text{for } i = 1, \dots, e, \\ x_1y_i &= x_2^iAB^{e-i} + x_0^{e-i}LM^i \quad \text{for } i = 0, \dots, e, \\ x_2y_i &= y_{i+1}B + x_0^{e-i-1}x_1^{d-1}LM^i \quad \text{for } i = 0, \dots, e-1, \end{aligned} \tag{10.5}$$

$$\begin{pmatrix} x_0 & -B & -x_1^{d-1} & y_{i-1} \\ & x_1 & -M & -x_2^{i-1}AB^{e-i} \\ & & x_2 & -x_0^{e-i}LM^{i-1} \\ & & & y_i \end{pmatrix} \tag{†}$$

The top 4×4 block remains fixed. The last column has input the second equation $x_1y_{i-1} = \cdots$ and output the equation $x_1y_i = \cdots$, together with a formula for x_0y_i.

10.7.2 The tag equation at small y_i

Adjoining y_{i+1} to the Pfaffian variety (†) is a faithful Tom: we must provide $y_{i+1} \cdot (x_0, x_1, B, y_{i-1})$, which generate the ideal of the bottom 4×4 submatrix.

All but one of these relations fit as the 4×4 Pfaffians of the array

$$\begin{pmatrix} x_0 & -B & -x_1^{d-1} & y_{i-1} & y_i \\ & x_1 & -M & -x_2^{i-1}AB^{e-i} & -x_2^iAB^{e-i-1} \\ & & x_2 & -x_0^{e-i}LM^{i-1} & -x_0^{e-i-1}LM^i \\ & & & y_i & y_{i+1} \\ & & & & * \end{pmatrix} \tag{10.6}$$

Nothing new here – just the equations (†) for i and $i+1$.

Now any of the Pfaffians 12.56 or 23.56 or 34.56 gives the value of *. For example, in 34.56, the 2×2 minor equals $\pm\beta = x_0^{e-i-1}LM^{i-1}$ times

$$x_0y_{i+1} - y_iM = x_1^{d-1}x_2^iAB^{e-i-1} \tag{10.7}$$

(by the second formula of (1)), so

$$* = \alpha\beta x_1^{d-1} \quad \text{with } \alpha = x_2^{i-1}AB^{e-i-1} \text{ and } \beta = x_0^{e-i-1}LM^{i-1}, \tag{10.8}$$

giving the tag equation at y_i:

$$y_{i-1}y_{i+1} = y_i^2 + \alpha\beta x_1^{2d-2}. \tag{10.9}$$

The "extrasymmetric" form of the 6×6 matrix is:

$$\begin{pmatrix} x_0 & -B & -x_1^{d-1} & y_{i-1} & y_i \\ & x_1 & -M & -B\alpha & -x_2\alpha \\ & & x_2 & -x_0\beta & -M\beta \\ & & & y_i & y_{i+1} \\ & & & & \alpha\beta x_1^{d-1} \end{pmatrix} \text{ or } \begin{pmatrix} x_0 & M & x_1 & \alpha B & \alpha x_2 \\ & x_1^{d-1} & B & y_{i-1} & y_i \\ & & x_2 & y_i & y_{i+1} \\ & & & \beta x_0 & \beta M \\ & & & & \alpha\beta x_1^{d-1} \end{pmatrix}. \tag{10.10}$$

10.7.3 Long equation for $y_{i-1}y_{i+2}$?

Rewrite (10.10) in full.

$$\begin{pmatrix} x_0 & -B & -x_1^{d-1} & y_{i-1} & y_i \\ & x_1 & -M & -x_2^{i-1}AB^{e-i} & -x_2^iAB^{e-i-1} \\ & & x_2 & -x_0^{e-i}LM^{i-1} & -x_0^{e-i-1}LM^i \\ & & & y_i & y_{i+1} \\ & & & & x_0^{e-i-1}x_1^{d-1}x_2^{i-1}AB^{e-i-1}LM^{i-1} \end{pmatrix} \tag{10.11}$$

Add another column with a mystery entry $* = m_{57}$:

$$\begin{pmatrix}
x_0 & -B & -x_1^{d-1} & y_{i-1} & y_i & y_{i+1} \\
& x_1 & -M & -x_2^{i-1}AB^{e-i} & -x_2^{i}AB^{e-i-1} & -x_2^{i+1}AB^{e-i-2} \\
& & x_2 & -x_0^{e-i}LM^{i-1} & -x_0^{e-i-1}LM^{i} & -x_0^{e-i-2}LM^{i+1} \\
& & & y_i & y_{i+1} & y_{i+2} \\
& & & & x_0^{e-i-1}x_1^{d-1}x_2^{i-1}AB^{e-i-1}LM^{i-1} & * \\
& & & & & x_0^{e-i-2}x_1^{d-1}x_2^{i}AB^{e-i-2}LM^{i}
\end{pmatrix} \tag{10.12}$$

As before, nothing new here: deleting row-column 5 (projecting out y_{i-1}) is just (10.10) with $i \mapsto i+1$. There are various ways of solving for $*$. For example, $\mathrm{Pf}_{12.57}$ is

$$\begin{aligned}
x_0 * &= x_2^{i-1}y_{i+1}AB^{e-i} - x_2^{i+1}y_{i-1}AB^{e-i-2} && (10.13)\\
&= x_2^{i-1}y_{i+1}AB^{e-i} - (y_iB + x_0^{e-i}x_1^{d-1}LM^{i-1})x_2^{i}AB^{e-i-2} && (10.14)\\
&= -(x_0x_2 + BM)x_0^{e-i-1}x_1^{d-1}x_2^{i-1}AB^{e-i-2}LM^{i-1}, && (10.15)
\end{aligned}$$

giving $* = -(x_0x_2 + BM)x_0^{e-i-2}x_1^{d-1}x_2^{i-1}AB^{e-i-2}LM^{i-1}$. Thus $\mathrm{Pf}_{23.57}$ is the long equation

$$y_{i-1}y_{i+2} = y_iy_{i+1} - (x_0x_2 + BM)x_0^{e-i-1}x_1^{d-1}x_2^{i}AB^{e-i-2}LM^{i-1}. \tag{10.16}$$

Warning One is tempted to make a little optimistic error of sign here (say $x_0x_2 - BM$), and get $*$ as a monomial, but this is definitely *false*: you can use the first relation of (10.10) to swap $x_0x_2 + BM$ into $x_1^d + 2BM$ or into $2x_0x_2 - x_1^d$, but no substitution makes it a monomial. The long equation can be written as a Pfaffian, but not as a trinomial.

10.7.4 Two vertebras and tag equation at big y_i

```
> X := TypeIIPair([6,4,6]); Print(X);
        6         1         0        -3
        ----------          ----------
        4         2         4         2
        6         2         6         2
                  2                   2
```

```
             2                 2
             3                 3
             2                 2
             2                 2
    ----------        ----------
    0        -5       4        1
```

We do not see the tag equation $y_2y_4 = y_2^3 + \mathbf{?}$ as a Pfaffian equation because the series

$$y_2x_0x_1x_2y_3, \quad x_0x_1x_2x_3y_3, \quad y_3x_1x_2x_3y_4,$$

of pentagrams kills y_2 before y_4 appears. The central pentagram is

$$\begin{pmatrix} x_0 & -AB^5 & -x_1^5 & y_3 \\ & x_1 & -BM & -x_2^3 \\ & & x_2 & -LM^3 \\ & & & x_3 \end{pmatrix}$$

To adjoin y_2 and its unprojection equations $y_2 \cdot (x_1, x_2, x_3, M)$ is an unfaithful Tom, because $\mathbb{M}$ is not itself an entry of the bottom 4×4 block; ditto for y_4 with $y_4 \cdot (x_0, x_1, x_2, B)$ and B not in the top 4×4 block. Either of these unprojections is an "unfaithful" 6×6 extrasymmetric formats (the equation for y_2M only appearing multiplied by some factors). These two 6×6 matrixes fit together as the top and bottom blocks of the 7×7 array:

$$\begin{pmatrix} y_2 & -x_2^2AB^6 & -x_0LM^2 & y_3B & x_1^5x_2^2LM^2 & * \\ & x_0 & -AB^5 & -x_1^5 & y_3 & x_1^4x_2^3AB^4 \\ & & x_1 & -BM & -x_2^3 & y_3M \\ & & & x_2 & -LM^3 & -x_3AB^4 \\ & & & & x_3 & -x_1^4LM^4 \\ & & & & & y_4 \end{pmatrix}$$

(Although these are unfaithful, we get Pfaffian relations y_2M and y_4B by going through other pentagrams.)

Number the rows and columns of the big matrix $0 \dots 6$, so that $m_{01} = y_2$, $m_{56} = y_4$ and the mystery entry $*$ is m_{06}. Calculate the Pfaffian $\mathrm{Pf}_{02.46}$:

$$x_1^4x_2^2AB^6LM^4 - y_3^2BM - BM * .$$

This is divisible by BM, which implies that

$$* = -y_3^2 + x_1^4 x_2^2 AB^5 LM^3.$$

The tag equation at y_3 is thus

$$\begin{aligned}\mathrm{Pf}_{01.56} : y_2 y_4 &= y_3(y_3^2 - x_1^4 x_2^2 AB^5 LM^3) + x_1^9 x_2^5 AB^4 LM^2 \\ &= y_3^3 + x_1^4 x_2^2 AB^4 LM^2 (x_1^5 x_2^3 - y_3 BM).\end{aligned}$$

As before, in the last line, one can use the "long equation" $x_0 x_3 = x_1^5 x_2^3 + y_3 BM$ to swap $x_1^5 x_2^3 - y_3 BM$ into $x_0 x_3 - 2y_3 M$ or into $2x_1^5 x_2^3 - x_0 x_3$, but there is no way of reducing it to a monomial.

```
> PfaffianEquations(X);
{   -x2^3*A*B^5 - x0*L*M^3 + x1*y3,
    -y4*L*M^4 - x2^3*x3^2*A*B^3 + x1*y5,
    -y1*A*B^6 - x0^3*x1^5*L + x2*y0,
    -x2^3*L^5*M^19 - y8*B + x3*y7,
    -x1^4*L^2*M^7 - x3^2*A*B^4 + x2*y4,
    -L^6*M^23 - x3^6*A + x2*y8,
    -x1*L^5*M^19 - x3^5*A*B + x2*y7,
    -x1^2*x2^3*L^3*M^11 - y6*B + x3*y5,
    -A^4*B^23 - x0^4*L + x1*y0,
    -y3*A*B^6 - x0*x1^5*L*M^2 + x2*y2,
    -B*L*M^4 - x2^4 + x1*x3,
    -y3*B*M - x1^5*x2^3 + x0*x3,
    -x1^5*x2*A^2*B^11 - y1*M + x0*y2,
    -y6*L*M^4 - x2^3*x3^4*A*B + x1*y7,
    -x1^3*x2^3*L^2*M^7 - y5*B + x3*y4,
    -x1^5*A^3*B^17 - y0*M + x0*y1,
    -x3*A*B^5 - x1^5*L*M^3 + x2*y3,
    -x2^3*x3*A*B^4 - y3*L*M^4 + x1*y4,
    -y7*L*M^4 - x2^3*x3^5*A + x1*y8,
    -y5*L*M^4 - x2^3*x3^3*A*B^2 + x1*y6,
    -x1^5*x2^2*A*B^5 - y2*M + x0*y3,
    -x1*x2^3*L^4*M^15 - y7*B + x3*y6,
    -x1^4*x2^3*L*M^3 - y4*B + x3*y3,
    -A*B^6*M - x1^6 + x0*x2,
    -x1^2*L^4*M^15 - x3^4*A*B^2 + x2*y6,
```

```
    -x2^2*A^2*B^11 - x0^2*L*M^2 + x1*y2,
    -x1^3*L^3*M^11 - x3^3*A*B^3 + x2*y5,
    -y2*A*B^6 - x0^2*x1^5*L*M + x2*y1,
    -x2*A^3*B^17 - x0^3*L*M + x1*y1
}
```

10.8 More calculations

10.9 The $6,1,6,1,6$ case

The monomials are $x_0,\dots,x_5$ with tags $0,6,1,6,1,6$ respectively $y_0,\dots,y_7$ with $-4,2,2,3,2,2,2,1$.

We can treat this as $\mathrm{III}(6,2)$ after passing to a minimal model; but leaving in the redudant generators x_2,x_4 seems to lead to interesting big matrix calculations, where all the unprojections are Toms.

Start from the top with

$$x_4y_7 = Ax_5^6 + L^{24}M^{19} \qquad x_5y_6 = By_7 + L^{19}M^{15}.$$

Add x_3,y_5,y_4,y_3 by the Pfaffians of

$$\begin{pmatrix} x_3 & B & 1 & y_6 & y_5 & y_4 & y_3 \\ & x_4 & L^5M^4 & Ax_5^5 & ABx_5^4 & AB^2x_5^3 & AB^3x_5^2 \\ & & x_5 & L^{19}M^{15} & L^{14}M^{11}x_3 & L^9M^7x_3^2 & L^4M^3x_3^3 \\ & & & y_7 & y_6 & y_5 & y_4 \\ & & & & . & . & . \\ & & & & & \text{etc.} & \end{pmatrix}$$

The terms in the bottom 4×4 are

$$x_3^?x_5^?AB^?L^4M^3(L^5M^4)^? \times \frac{(x_3x_5)^c - (BL^5M^4)^c}{x_3x_5 - BL^5M^4}$$

where the superscript ?? can be determined easily and c is the height above the diagonal: The immediate superdiagonal terms $i,i+1$ have $c=1$ so are monomials.

Writing out pentagrams implies that the next unprojection variable is necessarily x_1 (N.B. not x_2).

(Step 6.) The unprojection is

$$\begin{pmatrix} x_3 & BLM & 1 & x_1 \\ & x_4 & L^4M^3 & AB^4x_5 \\ & & x_5 & x_3^4 \\ & & & y_3 \end{pmatrix}$$

(Step 7.) The only guy to eliminate is x_4. Having done that, we have the choice of adjoining x_2 next, or y_2. The two matrixes are

$$\begin{pmatrix} x_1 & x_3^4 & BLM & x_2 \\ & y_3 & 1 & AB^4 \\ & & x_5 & x_1L^4M^3 \\ & & & x_3 \end{pmatrix} \quad \text{and} \quad \begin{pmatrix} y_3 & x_1L^3M^2 & AB^4 & y_2 \\ & x_5 & LM & x_3^3 \\ & & x_3 & By_3 \\ & & & x_1 \end{pmatrix}$$

We know how to put those two together into a 6×6.

$$\begin{pmatrix} x_1^2L^3M^2 & x_3^4 & x_1BL^4M^3 & x_2 & AB^5x_3^3 \\ & y_3 & x_1L^3M^2 & AB^4 & y_2 \\ & & x_5 & LM & x_3^3 \\ & & & x_3 & By_3 \\ & & & & x_1 \end{pmatrix} \tag{10.17}$$

(To get that, we started by putting x_2 above the col containing x_1 and x_3, then filled in the entries in the top row, then solved for the top right entry.)

Mystery matrix To calculate the tag equation y_2y_4, we wrote down the matrix

$$\begin{pmatrix} x_5^2AB^3 & x_3^2x_5AB^3L^3M^2 & y_3L^4M^3 & y_4 & x_3^2L^8M^6 & y_3^2+x_3^2AB^4L^4M^3 \\ & x_5AB^4 & x_3^2 & x_3LM & x_4 & x_2(=x_1x_3+AB^5LM) \\ & & x_1L^3M^2 & y_3 & x_3^3L^3M^2 & y_2 \\ & & & x_3 & BL^4M^3 & AB^5 \\ & & & & x_5 & x_1 \\ & & & & & y_3B \end{pmatrix}$$

(Steps 8–9.)

In the matrix (10.17), one can float x_3^3 from $(1,3,6)$ to $(2,4,5)$ and float B from (1,4,6) to $(2,3,5)$, to discover most of the remaining equations. We can adjoin the variable y_2, y_1, y_0 in a chain using the big matrix

$$\begin{pmatrix} x_3 & LM & 1 & y_3 & y_2 & y_1 \\ & x_2 & AB^5 & x_1^2L^3M^2 & x_1^3L^2M & x_1^4L \\ & & x_1 & x_3^3AB^4 & x_3^2A^2B^9 & x_3A^3B^{14} \\ & & & y_2 & y_1 & y_0 \\ & & & & \cdot & \cdot \\ & & & & & \cdot \end{pmatrix} \tag{10.18}$$

Then we eliminate x_2 tagged with 1 and put in the final x_0 using the matrix

$$\begin{pmatrix} y_0 & x_1^4 & AB^5 & x_0 \\ & y_1 & L & x_3A^3B^{14} \\ & & x_3 & y_0M \\ & & & x_1 \end{pmatrix} \tag{10.19}$$

10.10 Magma routines for Pfaffian equations

```
> Attach("lr.m");
> SetVerbose("User1",true);
> Attach("lr.m");
> X := TypeIIPair([3,4,3,4]); Print(X);
```

```
3         1         0         -3
----------          ----------
4         2         4         2
3         3         3         3
4         2         4         2
          3                   3
          2                   2
----------          ----------
0         -3        3         1
```

We can ask for `> PfaffianEquations(X);` There are 26 of them: this is a little general calculation: there are $k+1$ monomials down one side, and $l+1$ monomials down the other, so a series of $k+l-2$ pentagrams giving the new variable. Each pentagram gives 2 old Pfaffians and 3 new ones. In our case $k=4$, $l=6$ so there are 8 pentagrams and $2+3\times 8$ Pfaffians. Of these 7 give the tag eqns around big side

```
-x1^3*A^7*B^19 - y0*M + x0*y1,
-A^11*B^30 - x0^3*L + x1*y0,
-A^4*B^11*M - x1^4 + x0*x2,
-A*B^3*L*M^3 - x2^3 + x1*x3,
-B*L^4*M^11 - x3^4 + x2*x4,
-L^11*M^30 - x4^3*A + x3*y6,
-x3^3*L^7*M^19 - y6*B + x4*y5,
```

In each of these, there are 2 known terms, and a third monomial. We should be able to interpret them as a "continued fraction style arithmetic progression".

The remaining 19 Pfaffians are

```
-y5*L^4*M^11 - x3^3*x4^2*A + x2*y6,
-x2*L^7*M^19 - x4^2*A*B + x3*y5,
-y4*L^4*M^11 - x3^3*x4*A*B + x2*y5,
-x2*x3^3*L^3*M^8 - y5*B + x4*y4,
-x2^2*L^3*M^8 - x4*A*B^2 + x3*y4,
-x1*L^3*M^8 - x3^3*A*B^2 + x2*y4,
-y3*L*M^3 - x2^2*x3^2*A*B^2 + x1*y4,
-x1*x2^2*L^2*M^5 - y4*A*B^3 + x3*y3,
-x1^2*L^2*M^5 - x3^2*A^2*B^5 + x2*y3,
```

```
-x2^2*x3*A^2*B^5 - y2*L*M^3 + x1*y3
-y3*A*B^3 - x1^2*x2^2*L*M^2 + x3*y2,
-x3*A^3*B^8 - x1^3*L*M^2 + x2*y2,
-x2^2*A^3*B^8 - x0*L*M^2 + x1*y2,
-x1^3*x2*A^3*B^8 - y1*M + x0*y2,
-x2*A^7*B^19 - x0^2*L*M + x1*y1,
-y2*A^4*B^11 - x0*x1^3*L*M + x2*y1,
-y1*A^4*B^11 - x0^2*x1^3*L + x2*y0,
-y2*A*B^3*M - x1^3*x2^2 + x0*x3,
-y4*B*L*M^3 - x2^2*x3^3 + x1*x4,
```

These give each intermediate y_j multiplied by a little interval of x_i.

10.11 Bigger Magma calculation and the cross equations

```
> X := TypeIIPair([3,4,3,4,3]); Print(X);
        3       1       0       -3
        ----------      ----------
        4       2       4       2
        3       3       3       3
        4       2       4       2
        3       3       3       3
                3               3
                2               2
                2               2
        ----------      ----------
        0       -2      4       1
```

There are 35 Pfaffian equations, $35 = 2 + 3(k + l - 2)$ with $k = 5$, $l = 8$. Of these, the 8 tag equations around the big side appear in "big crosses"

$$\begin{array}{rcll}
x_5y_7 &=& y_8B &+\ x_4^3L^{19}M^{69}, \\
x_4y_8 &=& x_5^3A &+\ L^{30}M^{109}, \\[6pt]
x_3x_5 &=& x_4^4 &+\ BL^{11}M^{40}, \\
x_4y_6 &=& x_3^2L^8M^{29} &+\ x_5AB^2, \\[6pt]
x_4y_7 &=& x_5^2AB &+\ x_3L^{19}M^{69}, \\[6pt]
x_2x_4 &=& x_3^3 &+\ AB^3L^3M^{11}, \\
x_3y_6 &=& x_4^3AB^2 &+\ x_2L^8M^{29}, \\
x_3y_4 &=& x_4A^3B^8 &+\ x_2^3L^2M^7, \\[6pt]
x_1x_3 &=& x_2^4 &+\ A^4B^{11}LM^4, \\
x_2y_4 &=& x_3^2A^3B^8 &+\ x_1L^2M^7, \\
x_2y_3 &=& x_3A^7B^{19} &+\ x_1^2LM^3, \\[6pt]
x_0x_2 &=& x_1^3 &+\ A^{11}B^{30}M, \\
x_1y_3 &=& x_2^3A^7B^{19} &+\ x_0LM^3, \\[6pt]
x_1y_0 &=& A^{40}B^{109} &+\ x_0^4L, \\
x_0y_1 &=& x_1^2A^{29}B^{79} &+\ y_0M
\end{array} \tag{10.20}$$

(put $Y_1 = y_3$, $Y_2 = y_4$, $Y_3 = y_6$ to make the horizontal equation $x_iY_i = \cdots$).